ELECTROSPRAYED FIBER

WITH CONTROLLABLE PORE SIZE

FOR TISSUE REGENERATION

By

JONG KYU HONG

Bachelor of Engineering
Dongguk University
Seoul, Korea
1999

Master of Engineering
The University of Tokyo
Tokyo, Japan
2003

Submitted to the Faculty of the
Graduate College of the
Oklahoma State University
in partial fulfillment of
the requirements for
the Degree of
DOCTOR OF PHILOSOPHY
December, 2010

ELECTROSPRAYED FIBER

WITH CONTROLLABLE PORE SIZE

FOR TISSUE REGENERATION

Dissertation Approved:

Dr. Sudararajan V. Madihally

Dissertation Adviser

Dr. Khaled A. M. Gasem

Dr. Heather Fahlenkamp

Dr. Yu Jessie Mao

Outside Committee Member

Dr. Mark E. Payton

Dean of the Graduate College

ACKNOWLEDGMENTS

I am indebted to many persons whose help I benefited from during my candidacy for PhD at OSU. First of all, I sincerely appreciate my great advisor, Dr. Sudararajan V. Madihally for his guidance and special consideration. From reviewing literature, designing the innovative collector plate, developing the novel processes which produce a thin layer of fibers with large and controllable pore size, developing cell-glued 3D scaffold by using layer-by-layer assembly, disclosing several intellectual properties for patent while finishing this dissertation, he has been with me throughout entire process, and I will carry all I learned from him into my future.

I would like to express my gratitude to my committee members: Dr. Khaled A. M. Gasem, the chair of the committee and the head of school of chemical engineering, Dr Heather Fahlenkamp, and Dr. Yu Jessie Mao for their consideration and valuable suggestions. I also appreciate Dr. James Smay, Dr. Charlotte Ownby, and Mr. Curtis Andrew for their support on using SEM, confocal microscope, and H & E staining. Financial support was provided by the National Institutes of Health (1R21DK074858). I thank the laboratory members of Dr. Madihally's and Dr. Fahlenkamp's groups. I extend thanks to the staff of the school of chemical engineering, Edmon Low library, graduate school, and ISS for their help during my PhD.

I would like to share my appreciation for my previous supervisors and how they inspired me to make up this research independently: Professor Kazunori Kataoka at the

University of Tokyo in Tokyo, Japan; Dr. Young Ha Kim, Dr. Soo Hyun Kim, and Dr. Ki Dong Park at KIST in Seoul, Korea; Dr. Byung-sik Kim, Dr. Jung-Keug Park, Dr. Jong Choo Lee, Dr. Sang Kwon Park, and Dr. Eui Soo Lee at Dongguk University in Seoul, Korea.

I would like to extend my appreciation to my friends; Dr. Dooyoung Lee and his wife at the University of Pennsylvania who helped me feel very comfortable while visiting them just before starting these projects and inspired me very much. I appreciate to Dr. Jin Soo Kim, Dr. Hyunggi Lee and Dr. Dae Ho Um for their technical advising. I also appreciate Mr. Andrew Arterbery who shares his time with me in discussion about various topics which broaden my horizons. I would like to thank my other friends at the school of chemical engineering, at Colvin recreation center, in the Malaysian Drum Troupe, and in the Korean Catholic Community in Oklahoma State.

Also, I would like to express my appreciation to my family for their endless support: my two elder brothers, Dr. Jong Wook Hong and Mr. Jong Ho Hong; sister-in-laws, Dr. Mina Kim and Ms. Soo Hyun Kim; my nieces and nephews, Hyoju, Jaeyoung, Seunghae, and a new born child; and all of my extended family in the states and in Korea, especially, the families of Dr. Herald Joe and Dr. John Hong for their support during my PhD candidacy. Finally, I would like to express my sincere gratitude to my parents for their endless love and encouragement. My father (God rest his soul) and my mother are the basis of my life and my odyssey I have chosen to undergo during my whole life. Thanks to you all.

TABLE OF CONTENTS

Chapter Page

Chapter Page

LIST OF TABLES

LIST OF FIGURES

Figure Page

CHAPTER I

INTRODUCTION

Tissue engineering or regeneration is a multidisciplinary field to restore, maintain, and enhance tissue and organ function [1]. In tissue engineering, biodegradable scaffolds are used to support and guide cells to proliferate, organize and produce their own extracellular matrix (ECM). When tissue regeneration is performed outside the body, cells on scaffolds are grown in physiological conditions and implanted into the human body. Thus, tissue engineering is thought to consist of three key components: cell sources, scaffold, and cell-scaffold interaction. Along with cell sources and cell-scaffold interaction [2-3], a scaffold, is a critical component for tissue regeneration. Many groups have reported various methods [4-5] to fabricate scaffolds with various physical properties [6-7] using biomaterials [8]. Among them, electrospinning technology has recently emerged as a novel technique for tissue regeneration [9] because it is versatile and relatively economical to manufacture nanofibers mimicking natural ECM [10]. However, one significant drawback of electrospinning technology is inappropriate pore size of the three dimensional (3D) scaffolds for cells to grow inward.

Developing a novel process that allows formation of fibers with large and controllable pore size is, thus, necessary to overcome the current limitations of the electrospraying process when it is applied to tissue regeneration. To improve the quality of regenerated tissue, understanding the cell behavior on single fibers within the scaffold is important to design improved 3D scaffolds. Recent advances demonstrate that physical properties [6-7] of scaffolds such as pore size [2], topography [11] as well as chemical properties [8, 12] modulate cell behavior. However, it is difficult to study single cell behavior at this juncture on single electrosprayed fibers due to the small pore size of electrosprayed fibers. Thus, *I hypothesize* that the architecture of 3D scaffolds including pore size of scaffolds modulate cell behaviors such as cell infiltration, cell adhesion and cell colonization. *The goal of this dissertation* is to investigate the influence of the structure of 3D scaffolds on cell behaviors, especially, pore size affecting cell infiltration, cell attachment and cell colonization after the fabrication of electrosprayed fibers with large and controllable pore size using polycaprolactone (PCL) and gelatin (**Figure 1.1**). PCL was selected based on proven biodegradability, non-toxicity, and biocompatibility of PCL under the physiological conditions. Natural polymer gelatin (denatured collagen) was selected to improve the biological properties of PCL scaffolds. ***The specific aims of this dissertation*** are **1) to develop thin layer of PCL electrosprayed fibers with large pore size and evaluate its application in developing thick 3D scaffold, 2) to develop thin layers of PCL/gelatin electrosprayed fibers with controllable pore size and evaluate its utility to study single cell behavior in 3D configuration, and 3) to develop the hybrid PCL fiber with different molecular weight and evaluate its degradation under physiological condition.**

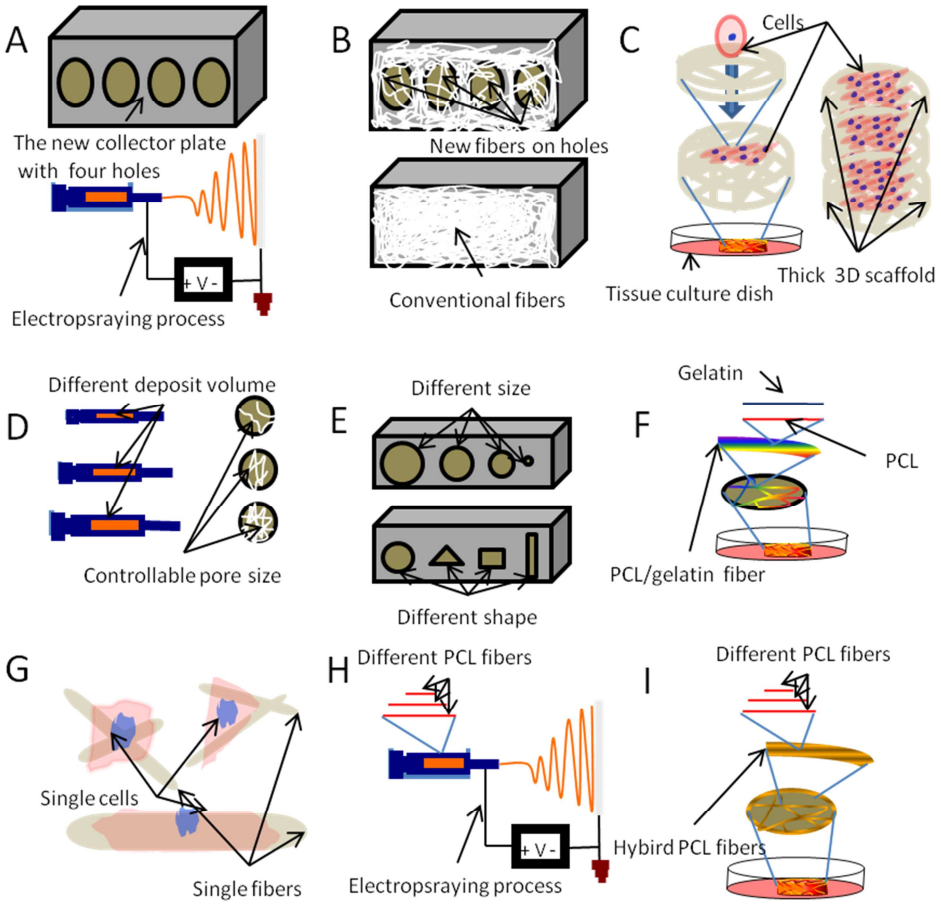

Figure 1.1. Schematics of the research scope. (**A**) The design of the innovative collector plate (with the void gaps) and development of electrospraying process to fabricate large pore size. (**B**) Comparison of the new and conventional fibers. (**C**) Evaluation of cell behavior and development of thick 3D scaffold using new PCL fibers and layer-by-layer assembly. (**D**) The development of controllable pore size by manipulating the deposit volume. (**E**) The effect of shape and size on the new fiber structure. (**F**) Gelatin distribution on single PCL/gelatin fiber and its stability test under physiological condition. (**G**) Single cell behavior study on single fibers. (**H**) The fabrication of electrosprayed PCL fibers of different molecular weight. (**I**) The degradation study of PCL fibers with hybrid molecular weights under physiological conditions.

The first specific aim is **to develop thin layers of PCL electrosprayed fibers with large pore size and evaluate its application in developing thick 3D scaffold** (**Figure 1A, 1B, and 1C**).

The current bottleneck of the electrospraying technology process for tissue regeneration is the lack of generating structural features necessary for building 3D tissues; the formed structures have very small pore sizes compared to size of human cells and do not allow cells to infiltrate into the layers below the surface. To solve this problem, I designed a novel collector plate which allows forming very thin layers with pore sizes suitable for cell infiltration and developed the new process of electrospraying using synthetic polymer polycaprolactone, (PCL) and natural polymer (gelatin) (**Figure 1A**). Thin samples could be handled without mechanically damaging the structure and could be transferred into cell culture plates. I evaluated physical (fiber diameter, shape factor, pore size of the fiber) and mechanical (load-extension curves) properties of the new fibers compared to conventional ones (**Figure 1B**). To show that this system can be utilized in tissue regeneration, I evaluated cell behavior (infiltration, adhesion, and spreading) using human foreskin fibroblast in 15% serum added media. Thin layers were stacked by layer-by-layer assembly to develop thick structures. Seven day cultures of fibroblasts show attachment and spreading of cells in every layer. Thirty day cell culture showed that cell-glued 3D scaffolds formed by layer-by-layer assembly and formed a tissue that could be tailored (**Figure 1C**).

The second specific aim is **to develop thin layers of PCL/gelatin electrosprayed fibers with controllable pore size and evaluate its utility to study single cell behavior in 3D configuration** (**Figure 1D, 1E, 1F, and 1G**).

Controlling the pore size in the fibers is important because pore size affects cell behavior such as infiltration and attachment. I designed the new process to control the pore size of fibers by manipulating the deposit volume of polymer solution (**Figure 1D**). By manipulating the deposit volume of polymer solution and the size of void in the new collector plate, the pore size (about 10 μm to 350 μm) of the fibers was controllable to meet the optimized pore size for cell behavior study. The evaluation of the shape and the size of the void in the new collector plate were also investigated since the electric field changes with the pattern of the void. Thus, different shapes (triangle, rectangle, and circle) of the void in the new collector plates were designed to evaluate the polymeric structure of the fibers. Then, I evaluated patterns of accumulated fibers, fiber diameter, shape factor, pore size of the fibers of the new fibers. These results showed that the shape of the void affected the alignment of the fibers and the different diameters of the void affect the pore size of the fibers (**Figure 1E**). I also developed 3D nanofibers made of PCL and gelatin using the solvent of hexafluoro-2-propanol (HFP). Distribution and stability of gelatin on single PCL/gelatin fibers was studied in two-week incubation under physiological condition using carboxyfluodiacetate-succinimidyl ester (CFDA-SE). These results showed that physical and chemical properties of nanofiber were sufficient to carry out single cell adhesion in serum free media (**Figure 1F**). Interaction of cells on single electrosprayed fibers was studied up to 24 hr using fibroblast in serum free media. These results showed that the cell shape on 3D nanofibers is dependent on the polymeric

structure of single fibers where cells were attached. Cell shapes were elliptical, triangular, and quadrangular on single fibers at nearby intersection of two single fibers, and on the intersection of two single fibers, respectively. The cell shape and size on 3D nanofibers are dependent on the polymeric structure of single fibers where cells were attached (**Figure 1G**).

The third specific aim is **to develop the hybrid PCL fiber with different molecular weight and evaluate its degradation under physiological condition** (**Figure 1H and 1I**).

PCL is a biocompatible material widely used in various biomedical applications. However, the long degradation periods under the physiological condition limit the broad use of PCL. Although several groups reported the degradation characteristics using membranes made of low molecular weight PCL, electrospraying process inhibits the fiber fabrication with low molecular weight due to the low viscosity of the solution. To overcome the limitation of the fabrication, I fabricated electrosprayed fiber with high, medium and low molecular weight PCL (**Figure 1H**). I used a novel collector plate to fabricate the large pore size, which also facilitates study of each fiber. I compared fiber characteristics and performed degradation characteristics for four weeks in physiological conditions. Comparison of fiber characteristics with different mixing ratio, and the acceleration of degradation of single PCL fiber by the mixture with low molecular weight were also demonstrated (**Figure 1I**).

Given the versatility of existing electrospinning technology for fabricating biomimic micro and nanosize fibers made of various biomaterials, these results will have

significant impact on regeneration of various tissues. The fabrication of fibers with large and controllable pore size overcomes the current issue of electrosprayed fibers when the fibers are applied to tissue regeneration. The thin layer of fibers with large pore size has significant potential to study single cell behaviors such as cell attachment and cell duplication, and construction of extracellular matrix in thick tissue development. Furthermore, the electrosprayed fiber with controllable pore size could be used in other fields such as sustainability, environmental engineering, and nanotechnology.

REFERENCES

1. Langer, R. and J. Vacanti, *Tissue engineering.* Science, 1993. **260**(5110): p. 920-926.
2. Baker, S.C., et al., *The relationship between the mechanical properties and cell behaviour on PLGA and PCL scaffolds for bladder tissue engineering.* Biomaterials, 2009. **30**(7): p. 1321-1328.
3. Lutolf, M.P. and J.A. Hubbell, *Synthetic biomaterials as instructive extracellular microenvironments for morphogenesis in tissue engineering.* Nat Biotech, 2005. **23**(1): p. 47-55.
4. Hollister, S.J., *Porous scaffold design for tissue engineering.* Nat Mater, 2005. **4**(7): p. 518-524.
5. Choi, N.W., et al., *Microfluidic scaffolds for tissue engineering.* Nat Mater, 2007. **6**(11): p. 908-915.

6. Moutos, F.T., L.E. Freed, and F. Guilak, *A biomimetic three-dimensional woven composite scaffold for functional tissue engineering of cartilage.* Nat Mater, 2007. **6**(2): p. 162-167.

7. Cushing, M.C. and K.S. Anseth, *MATERIALS SCIENCE: Hydrogel Cell Cultures.* Science, 2007. **316**(5828): p. 1133-1134.

8. Hubbell, J.A., *Biomaterials in Tissue Engineering.* Nat Biotech, 1995. **13**(6): p. 565-576.

9. Shin, H., S. Jo, and A.G. Mikos, *Biomimetic materials for tissue engineering.* Biomaterials, 2003. **24**(24): p. 4353-4364.

10. D. Li, Y.X., *Electrospinning of Nanofibers: Reinventing the Wheel?* Advanced Materials, 2004. **16**(14): p. 1151-1170.

11. Au, H.T.H., et al., *Interactive effects of surface topography and pulsatile electrical field stimulation on orientation and elongation of fibroblasts and cardiomyocytes.* Biomaterials, 2007. **28**(29): p. 4277-4293.

12. Zelzer, M., et al., *Investigation of cell-surface interactions using chemical gradients formed from plasma polymers.* Biomaterials, 2008. **29**(2): p. 172-184.

CHAPTER II

BACKGROUND

2.1. TISSUE ENGINEERING

Tissue engineering or regeneration is a multidisciplinary study to restore, maintain, and enhance tissue and organ function [1]. In the US, tissue and organ failure is a major problem [1], there are several treatment options: transplantation, surgical repair, artificial prostheses, mechanical devices, and drug therapy. By these methods, however, it is not possible to repair major damage of tissue and organs in a satisfactory way [2]. A potential alternative to conventional therapy is tissue engineering. The potential impact of tissue engineering is far broader in the future; the regeneration of organ and tissues in the 21st century is equivalent to the use of antibiotics in the 20th century [3]. Several engineered tissues have been approved by the Food and Drug Administration (FDA) [4]. Tissue engineering research and development are being chased by startup development businesses with an expenditure of more than $600 million per year. Budget of tissue engineering firms are growing at a compound annual rate of 16% since 1990s [5] and the investment exceeded $3.5 billion in 2002 [5]. Academic and corporate interests in tissue engineering continue to increase due to the medical and market potential [2].

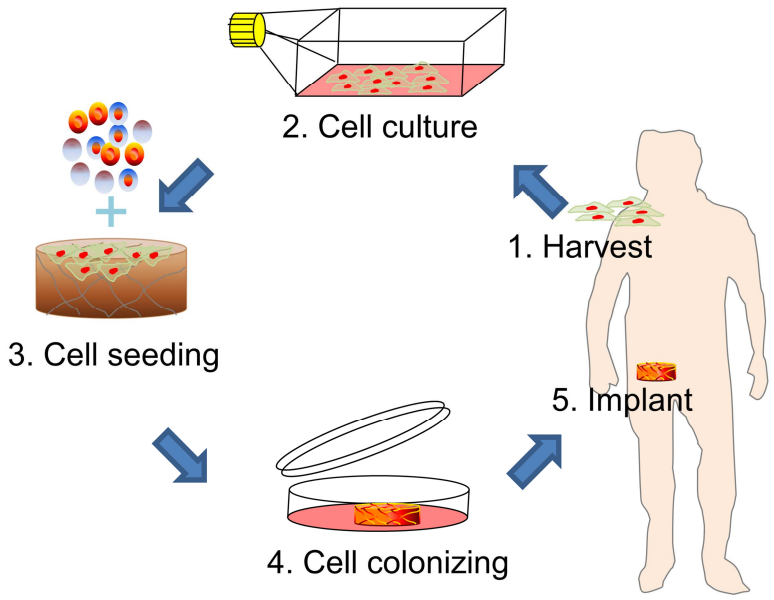

Figure 2.1. Schematic Procedure of Cell Culture. First, cells are harvested from the human body, then in vitro cell culture, cells are seeded onto a scaffold, a three dimensional matrix for growing cell with ingredients such as growth factors. Finally, the colonized cells in 3D scaffold is implanted into the human body to cure malfuctioning tissues or organs. There are three key elements (scaffold, cells, and scaffold-cell interations) of tissue engineering. Among three elements, scaffold, biomimetic matrix, is the most important because the strucure of 3D scaffold in micro and macroscale affects the cell behaviors such as cell adhesion, cell infiltration, cell coloniztion.

The goal of tissue engineering is to repair and restore tissue and organ functions using a combination of cells and scaffolds. The fundamental approach is to culture cells in 3D scaffolds. After in vitro cell culture, cells are seeded into 3D scaffold, which grow in physiological conditions. The scaffolds guide cell attachment and cell migration. Then, scaffolds allow attached cells to proliferate, organize and excrete their own ECM [6]. When scaffolds facilitate tissue and organ function properly, the scaffolds (cell growing matrix) are implanted into the human body (**Figure 2.1**). Thus, injured tissue and organs are addressed by implanting engineered tissues and organs, whereby organ replacement can be reduced [2]. To design and develop a method for tissue regeneration based on scaffolds, understanding three key elements (scaffolds, scaffold-cell interaction, and cells) are important to achieve better tissue regeneration.

2.1.1. Cell

First, cell sources in tissue engineering should be easily accessible, less immunologically responsible, and easily expandable without changing the physical trait and function, and without transmitting species-specific pathogens [7]. Several cell sources are categorized. Autologous [8] cells are harvested from the same individual to whom the regenerated tissue will be implanted. Allogenic [9] cells are obtained from the donor body of the same species. Xenogenic [10] cells are those isolated from individuals of another species. Syngenic [11] or isogenic cells come from genetically identical organisms, such as twins, clones. Primary [12] cells are harvested from an intact tissue. Secondary [13] cells are obtained from a cell bank which is manipulated to proliferate. Stem [14-17] cells are undifferentiated cells able to divide in culture and cause different

forms of specialized cells. Stem cells are grouped into adult [15] and embryonic [16] stem cells on the base of their sources. Adult stem cell is multipotent, for instance, a blood stem cell can develop into several types of blood cells. Most of the embryonic stem cells are pluripotent to be able to develop three germlayers (endoderm, mesoderm, and ectoderm).

2.1.2. Cell-scaffold interaction

Secondly, cells are naturally aware of their surroundings such as nearby signaling molecules [18-19]. Surrounding proteins affect complex stimulation of cell receptors, determining cell responses. These extrinsic factors cause a highly defined and specialized cell microenvironment essential to proper tissue development and function. Scaffold also guides the migration of cells into the implant site and stimulates their viability and proliferation. They also degrade in response to matrix remodeling enzymes excreted by the cells [20]. For instance, adhesion domains such as arginine-glycine-aspartate (RGD) has allowed the design of scaffold to modulate cell adhesion [21]. Also, growth factor related scaffold design has been reported [22-23]. For example, growth factor cooperated biomaterials increase the efficiency of cell seeding and cell proliferation, and facilitate rapid formation of dermal tissue [22].

Along with chemical stimulus, cell behaviors can also be affected by physical properties of scaffolds which are closely related to the architecture of scaffolds. The architectural features consist of pore size, porosity, fiber orientation, scaffold stiffness, and topography [24] (**Table 2.1**). Pore size influences cell binding, migration, depth of cellular in-growth, cell morphology and phenotypic expression [25]. Proper pore size

allows cells to spread into pores and join with surrounding cells. In an optimal range of pore size, cell ingrowths are moderated but out of optimum range, cells are hardly able to spread and to form networks. Optimum pore size depends on cell types and scaffold materials but the optimum range of pore size for most mature cell types is in the range of 100-150 um [26]. Pore size affects cell growth and scaffold properties as well. The elasticity of scaffold increases when the number of pores increases [27].

Porosity [28-29] regulates cell adhesion and migration. High porosity makes high surface area efficient for cell seeding, helpful for cell matrix interaction, and sufficient for extra cellular matrix regeneration. In addition, high porosity supports cell proliferation and higher porosity increases cell adhesion. Pore interconnectivity also enlarges overall surface area for cell attachment and enhances cell ingrowths. Fiber orientation [30] affects tissue regeneration. Despite similar proliferation, collagen is better synthesized by fibroblast on aligned nanofibers than on randomly arranged nanofibers; spindle-shaped fibroblasts or fibroblasts oriented in the same direction of aligned fibers is hypothesized to mimic in vivo condition quite well and to produce more ECM. Scaffold stiffness [29, 31] influences cell behaviors such as cell organization and cell viability. For instance, scaffold stiffness correlates with different degree of shrinkage in the cells. Reducing shrinkage results in spacious cell organization like normal cell morphology; scaffold shrinkage leads to cellular degeneration and shape deformation in the optimal range of scaffold stiffness.

Table 2.1. The influence of physical properties of scaffold on cell behaviors

Physical Properties	Cell Behaviors
Pore size	Cell ingrowths, cell morphology
Porosity	Cell adhesion, cell migration
Fiber orientation	ECM production
Scaffold stiffness	Cell viability, cell organization
Topography in microscale	Reshaping actin filaments
Single cell on single nanofibers	Novel issue for cell behaviors

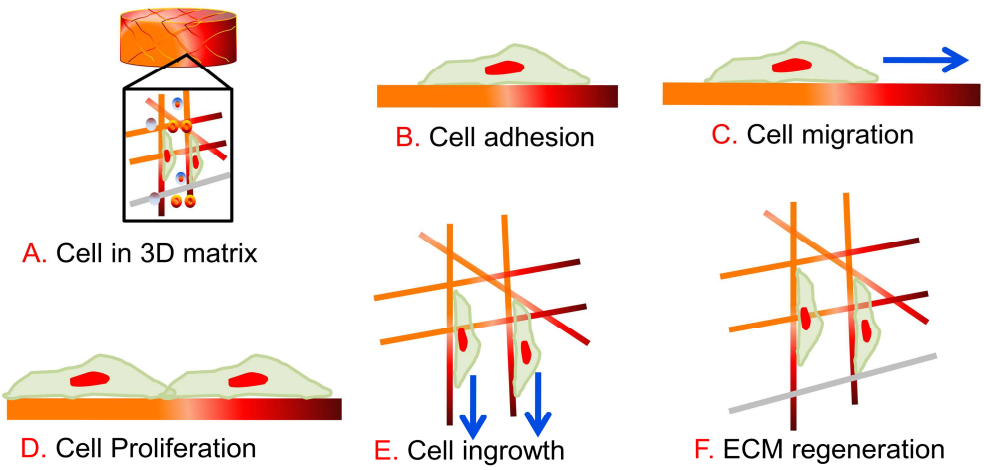

Figure 2.2. Cell behavior in nanofibers with controllable pore size in 3D scaffold. ECM statnds for extracelluar matrix.

Topography (surface landscape) [32] of scaffold affects cell behavior. Topographical reaction of cells to micrometer-range features such as grooves, and ridges has been well established for decades [33]. For instance, grooves prevent cells bending their cytoskeleton and reshaping its actin filaments to become accustomed to new topography. However, no one has studied the influence of fiber sizes in 3D scaffold with microscale or nanoscale architecture on cell behaviors [19]. Approaches with that level of detail regarding the cell behaviors such as cell attachment, cell migration, cell proliferation, cell infiltration, and ECM construction, influenced by physical properties such as nanofiber with controllable pore size in 3D scaffold can produce benefits such as better architectural design and more efficient fabrication process of micro or nanosize 3D scaffold (**Figure 2.2**).

2.1.3. Scaffold

Finally, a scaffold, into which cells are seeded, is an artificial structure supporting 3D tissue formation. The scaffold renders it possible for cells to influence their own microenvironments. Scaffold allows cell attachment and migration, enables diffusion of vital cell nutrients, and helps to retain cells. Further, chemical and mechanical properties of the scaffold influence cell viability and proliferation [34]. Appropriate pore size and porosity are essential to modulate cell seeding and diffusion. Biodegradability is essential because scaffolds are absorbed by the nearby tissue, which does not allow for surgical removal from the body. The surface of scaffold is suitable for cell attachment and migration. The mechanical properties of scaffold are harmonious with the tissue at implant site.

The development of chemistry, cell biology, and materials science are modulating fabrication of smart biomaterials that are only getting smarter [35]. However, more than 2000 years ago, Chinese, Aztecs, and the Romans used biomaterials. It is only in the past few decades that biomaterials begin to be broadly in medical application [36]. Biopolymers [37] are broadly grouped into two categories: synthetic and natural polymers. Synthetic polymers such as polycaprolactone (PCL) [38] have the benefit of tailoring its mechanical properties such as microstructure. Natural biomaterials such as gelatin [39] have cell signals to modulate cell behavior such as cell adhesion. However, synthetic biomaterials are short of cell signal to manipulate cell behavior and natural biomaterials lack tailorability of mechanical properties [40]. ***In this dissertation***, PCL and gelatin were mainly used for scaffold fabrication because both are very economical. PCL is biodegradable polyester synthesized by ring opening polymerization of ε-caprolactone. PCL with melting point 60°C is degraded by hydrolysis of its ester linkages in physiological conditions and is therefore used as an implant in the body. PCL is a Food and Drug Administration (FDA) approved material used in the human body. PCL [41] has been investigated as a scaffold. Gelatin [38] is a protein derived from denaturing of the collagen of skin and bones. The melting point of gelatin depends on its grade and concentration. Mechanical properties of gelatin are related to thermal history.

Several processes have been reported to fabricate scaffold with proper mechanical properties of pore size and porosity (**Table 2.2**). Solvent casting & particulate leaching (SCPL), Emulsification/freeze-drying [42], computer assisted design and manufacturing (CAD/CAM) technologies [43], phase separation [44-45], nanofiber self assembly (NSA) [46], textile technologies [47]. Among them, electrospinning (the process of fabricating synthetic fibers in nanometer to micrometer size with non-woven structure using electrostatic forces) has been issued for 3D scaffold in the field of tissue engineering since non-woven meshes are similar to ECM in scale [48]. Electrospinning [48-49] is also versatile and relatively economical technology which is suitable for producing porous scaffolds [50]. Many groups are studying nanofibers with electrospinning technology using different synthetic and natural biomaterials along with different cells to prove the possibility for 3D scaffold [49, 51]**.** One significant drawback of electrospinning technology is, however, inadequate pore size for cells to grow inward into three dimensional (3D) scaffolds. Manmade structures have tiny pores compared to human cells, and do not allow cells to infiltrate into the layers below the surface. According to a US patent licensed in 2008 [52], the pore sizes are less than 10 micrometer while human cells are typically greater than 10 micrometer in size. Hence, cell growth is restricted to the surface only. The reduced pore size is primarily due to multiple layers of fibers deposited to obtain thicker structures that withstand mechanical handling in other steps. For example, fibers have to be peeled-off from the collector plate and transferred to the tissue culture condition which could damage the structure.

Table 2.2. Fabrication Methods of scaffold for tissue regeneration

METHOD	MICROSCALE FIBER	NANOSCALE FIBER
Solvent Casting/ Particular Leaching	**x**	
Emulsification/Freeze-drying	**x**	
Computer Aid Design/ Computer Aid Manufacturing	**x**	
Phase Separation		**x**
Nanofibers Self Assembly		**x**
Textile Technology	**x**	**x**

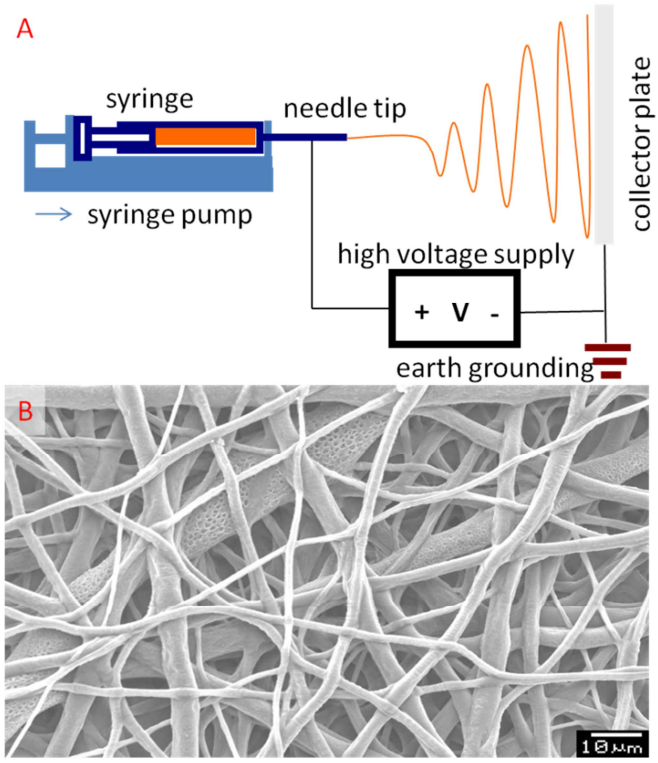

Figure 2.3. Conventional electrospray setup. (**A**) schematic showing conventional setup (**B**) micrograph of a polymeric structure obtained using conventional technique.

Table 2.3. History of electrospinning

YEAR	EVENT
1897	Electrospinning Phenomena
1902	US Patents with electrospinning
1939	Solving incomplete solvent evaporation
1969	Solution and process parameter study
1971	Usage of melt polymer
1978	Tissue engineering
1981	Era of nanotechnology

The electrospray apparatus (**Figure 2.3**) consists of a syringe pump, syringe and needle tip, high voltage power supply, earth grounding and a collector. When a collector is spun to orient the fibers, it is referred to as electrospinning. When high voltage is applied in the system, the polymer solution flies from needle tip to collector [53-54]. During the flight of the solution, the solvent evaporates and the polymer forms non-woven fibers on the collector. Most soluble polymers with high molecular weight can be electrosprayed or electrospun [55]. Nanofibers can be made of natural polymers, polymer blends, nanoparticle permeated polymers, and ceramics [55]. Different morphologies (beaded, smooth, core-shell, and porous fibers) have been reported [55]. Since the technology allows the possibility of tailoring the mechanical properties and biological properties, there has been a significant effort to adapt the technology for use in tissue regeneration, drug delivery, and biomedical devices [54]. One significant drawback of the electrospinning technology involved in tissue engineering is, however, inadequate pore size for cells to grow inward into three dimensional (3D) scaffolds. In this chapter, I review the existing electrospinning technology and address our strategy to fabricate new fibers with large pore size and apply the thin layer of eletrosprayed fibers to single cell behavior study and thick 3D scaffold development.

2.2. ELECTROSPINNING

2.2.1. History of electrospinning

Electrospinning (electrostatic spinning) [54, 56], a process of fabricating micro and nanosize fibers with non-woven structure, has been known of over 100 years (**Table 2.3**). Electrospinning was first observed in 1897 [57] and was first patented in the US in

1902 [58]. In 1934 when Formhals patented a process and apparatus using electric charges to spin synthetic fibers, electrospining virtually became a valid technique to produce small sized fibers [59]. Formhals designed a movable thread-collecting device that allowed for the collection of fibers in a stretched state. Using this apparatus, Formhals spun cellulose acetate in acetone/alcohol solution and collected aligned fibers. In 1939, Formhals also developed a new process by increasing the distance between collector sites to improve the problem of incomplete solvent evaporation [60]. Researchers post Formhals focused on better understanding of the electrospinning process. In 1969, Taylor reported about the jet form process in which he examined how the droplet behavior of polymer solution at the edge of a capillary in an electric field [61]. Taylor found that when the surface tension was balanced by electrostatic forces, the pendant droplet developed in to a cone from the apex of which the fiber jet was emitted. This is one reason why electrospinning can generate much smaller fibers than the diameter of the capillary. Further, Taylor determined that 49.3 degrees with respect to the axis of the cone at the cone apex is the proper angle to balance the surface tension with the electrostatic forces by examining viscous fluids. After Taylor's work, interest shifted to exploring the effect of individual processing parameters on the structural properties of electrosprayed fibers. In 1971, Baumgarten investigated the relationship between parameters (solution viscosity, flow rate, applied voltage etc.) and the properties of fibers (fiber diameter). Baumgarten found that fiber diameters initially decreased when electric field increased, reached the minimum, and started to increase when further increasing the applied electric field [62]. In 1978, polyurethane meshes were first applied to tissue engineering for development of vascular prosthesis. In 1981, Larrondo and

Mandley also examined the effect of melt processing of the polymer on diameters of electrospun fibers [63-64]. They found that melting temperature is inversely related to the fiber diameters, which were bigger than those fabricated from polymer solution. Since 1980s, Electrospinning has regained attentions due to the era of nanoscience and nanotechnology [65]. Over 200 universities and research institutes are studying the electrospinning process and it has a potential to application in various fields such as tissue engineering [55].

A search performed in Science Direct on March 1, 2010 indicates the dramatic increase in electrospinning and its application. In 2009 alone, more than 600 journal articles were published on various aspects of electrospinning process and fiber fabrication (**Figure 2.4**). Articles were published by such journals as Polymer, Biomaterials, Materials Letters, Acta Biomaterialia, Carbohydradrate Polymers, European Polymer Journal, Journal of Membrane Science, Sensors and Actuators B: Chemical, Journal of Colloid and interface Science, and Synthetic Metals. These articles can be grouped into two categories: one category is research into various material related researches and their fundamental characteristics, mainly published in journals such as Polymer, Materials Letters, and Carbohydrate Polymers etc. Major emphasis is placed on the relationship between the electrospinning parameters and distribution of fiber sizes. The other category is related to utilizing electrospinning technology in various applications, particularly biomedical applications and journals include Biomaterials, Acta Biomaterialia. An example is the possibility of forming electrosprayed fibers using biomaterials, modifying the fiber characteristics to suit the requirements of scaffold properties for tissue regeneration (**Figure 2.5**), and evaluating the effect on cellular

interactions. Only a brief summary into the developments related to the effect of various parameters on fiber size is provided while referring the readers to numerous recent reviews related to this topic (see **Appendix A** for more details).

2.2.2. Controlling Fiber size in electrospinning

Fiber characteristics depend on a number of parameters which can be broadly grouped into two categories: processing parameters and solution parameters [54]. Processing parameters include applied voltage, polymer solution flow rate, and capillary-collector distance and solution parameters include solvent volatability, molecular weight of the polymer, polymer concentration, solution viscosity, and solution conductivity. Along with process and solution parameters, environmental (also referred as ambient in some articles) parameters such as temperature and humidity also affect the fiber characteristics. Many of these parameters have been extensively discussed in relevance to biodegradable polymers [54, 66]. Only a brief summary is provided below.

When applied voltage is increased, the fiber diameter initially decreases and then increases. The fiber diameter also increases with increased flow rate of the polymer solution and with increased polymer concentration. However, fiber diameter decreases as distance between capillary and collector plate is increased or with increase in solution conductivity. In general, the process parameters affect fiber sizes but the exact relationship is unique to each polymer-solvent system. The processing environment also affects the morphology of fibers. Thus, under the optimized solvent and environmental conditions, the fiber size is controllable by manipulating the process parameters such as the distance between a nozzle and collector plate [54, 66].

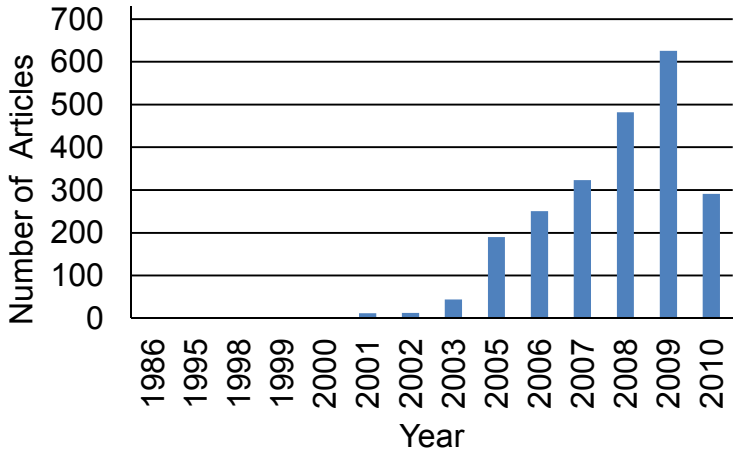

Figure 2.4. Number of articles about electrospinning by Science Direct on March 1, 2010.

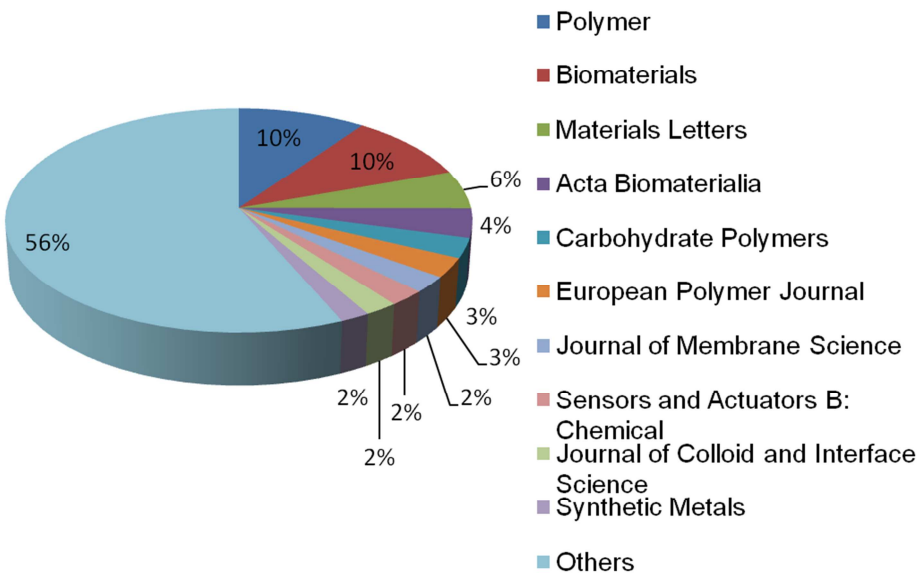

Figure 2.5. Distribution of journals publishing the article about electrospinning in 2009.

2.2.3. Materials for electrospinning

Electrosprayed fibers are fabricated using various materials (polymers [54], ceramics [67], and metals [67]) to apply to many research fields such as energy, and environmental engineering but for tissue regeneration the fibers are usually made of biomaterials (synthetic and natural polymers) that are used in medical devices or in contact with biological systems (**Table 2.4**). These materials are biodegradable; nontoxic, and biocompatible. Thus, scaffolds are chemically degradable under the physiological conditions, are not toxic while *in vivo* and *in vitro* cell culture, and have an ability to perform with an appropriate host response in a specific application.

Many of these materials are also biodegradable. Hence, scaffolds are chemically degradable under the physiological conditions, non-toxic during *in vivo* and *in vitro* cell colonization, and have an ability to perform with an appropriate host response in a specific application. Both synthetic polymers and natural polymers like Polycaprolactone (PCL) [100, 101] , poly (glycolic acid), poly (lactic acid) [102-108], amorphous 50:50 poly-lactide-co-glycolide (PLGA), methacrylic terpolymers (such as methyl methacrylate) [109], gelatin (denatured collagen) [110], alginates [111], chitosan [112], glycosaminoglycans [113-119] fibrin [120] and silk [121] have been explored in the formation of electrospun fibers [122, 123]. PGA was used to develop a synthetic absorbable suture. PLA products including tissue screws, tacks, and suture anchors, as well as systems for meniscus and cartilage repair are commonly used. Synthetic polyesters degrade by hydrolysis [124] and their degradation rates and mechanical properties can be altered via polymerization techniques [125-127] and processing conditions [128-131]. However, these polymers show poor regulation on cellular activity

[132]. Alternatively, block copolymers of poly(ethylene oxide) and poly(butylene terephthalate) have been developed. These materials are subjected to both hydrolysis (via ester bonds) and oxidation (via ether bonds). Although a number of other materials generated using polymer chemistry, synthetic polymers do not possess a surface chemistry which is familiar to cells. Despite significant efforts to improve these limitations via co-polymerization [133] and grafting RGD peptides (necessary for cell adhesion) [134, 135], recreating all the biological responses needs significant investigation.

On the contrary, ECM components play a significant role in tissue remodeling under pathological conditions and their role in diverse molecular mechanisms have been extensively studied in clinical samples [136, 137]. However, the problem in using natural polymers is processing into different forms without chemical modifications. For example, gelatin can be processed into 3D porous structure using electrospinning, however, it is not stable at physiological conditions. The 3D porous structure looses mechanical stability in few minutes without a stabilization reaction using a cross linker. Cross-linking reduces biological activity of gelatin in addition to introducing complexities related to toxicity of the cross-linker and calcification due to preferential chelation. Since each polymer system has a weakness in biological regulation or mechanical requirement, blending synthetic polymers with natural polymers has been explored [138-141]. Using this concept, extensive work on generating scaffolds from blends of natural and synthetic polymers [142-145] and other crystalline components has been performed [146]. Selecting suitable solvents, different polymers have been blended to control the mechanical and biological nature of the porous scaffold [147-149].

Table 2.4. Materials for electrospinning

SYNTHETIC POLYMER	NATURAL POLYMER	METALS/CERAMICS
Polycaprolactone	Gelatin	Cobalt acetate/poly(vinyl acetate)
Poly(d,l-lactic-co-glycolic acid)	Collagen	Magnesium titanate/poly(vinyl acetate)
Poly(ethylene-co-vinyl alcohol)	Fibrinogen	Nickel acetate/poly(vinyl acetate)
Poly(l-lactide-co-ε-caprolactone)	Silk Fibroin	Palladium acetate/polycarbonate
Poly glycolic acid	Chitin	Zinc acetate/poly(vinyl acetate)
Polyurethane	Chitosan	Vanadium sol/poly(vinyl acetate)

2.2.4. Nozzle configuration in electrospinning

A variety of nozzle configurations have been explored to engineer the physical and chemical properties of electrosprayed fibers (**Figure 2.6**). The most common configuration is the single ejection system. In this system, polymer solution ejects from a single needle tip and flies from the needle tip to the collector plate when the high voltage is applied to the electrospraying system. Also, several dual ejection systems exist such as coaxial [68], sequential [69], and simultaneous [69] configuration. In the coaxial system (**Figure 2.6A**), two different polymer solutions flow throughout two different needles with a big needle outside a smaller needle to fabricate core-shell fibers. Another dual configuration is simultaneous system. In this system, two separated polymer solutions, ejected from two different needle tips side by side, fly together to a collector plate simultaneously. Thus, hybrid structure of the fiber can be fabricated to control the mechanical, chemical, and biological properties of the fiber structure. Simultaneous deposition allows intermeshing of two polymers and controlling the micro-architecture at the nanoscale. In simultaneous deposition, the aluminum connector is used to couple the tips (**Figure 2.6B**). The other one is the sequential eject system. In this system, two different polymer solutions are deposited on a collector plate on top of one another and fabricate layer-by-layer of electrosprayed fibers. Thus, the multilayer allows the fiber to improve the structural characteristics: physically, chemically, and biologically (**Figure 2.6C**).

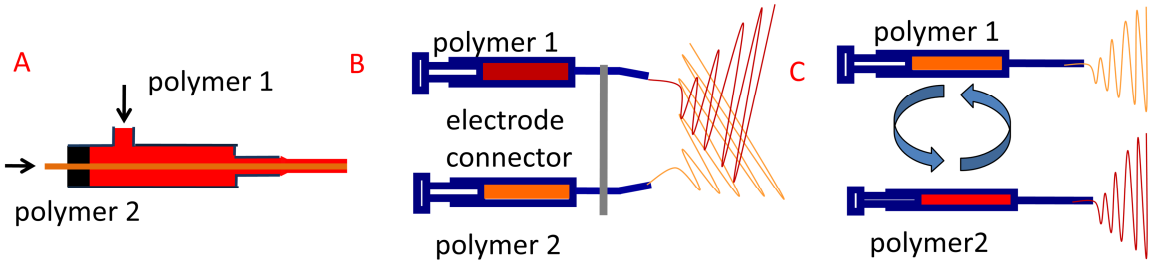

Figure 2.6. Nozzle configuration. (**A**) Coaxial, (**B**) simultaneous, (**C**) sequential ejects to fabricate multilayered, mixed fibers and core-shell structure of fibers, respectively.

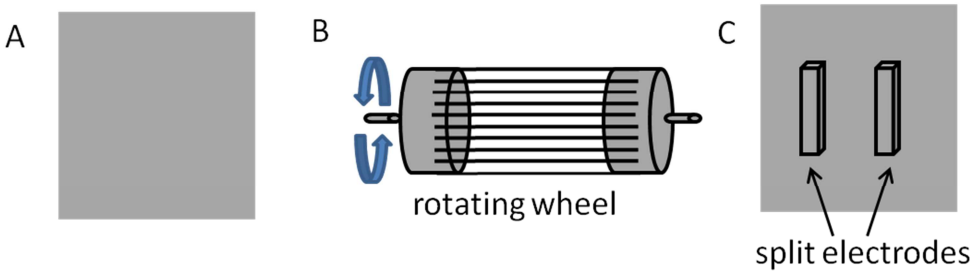

Figure 2.7. Collector plate. (**A**) Plane (**B**) Rotating and (**C**) Split collector plate.

2.2.5. Collector Plate

Collector plates in electrospraying process have a role not only in the fiber collector but also in a conductive substrate such as aluminum foil. The general shape of the collector plate was a square wrapped with aluminum foil. The fibers deposited on the general collector plate [70] as a random mass due to the bending instability of the highly charged jet. When collector plates such as rotating rod and rotating wheel were spun, the electrospraying process is called electrospinning (electrospraying + spinning). The rotating collector type [71] and their rotation speed determine the fiber alignment. Also, several split electrodes [72] have been used to fabricate aligned fibers using two conductive materials divided by a gap where aligned fibers are deposited (**Figure 2.7**).

2.3. OVERCOMING THE CURRENT DRAWBACK OF ELECTSPRAYING FOR TISSUE REGENERATION IN THIS STUDY

Electrospraying process is versatile for manufacturing of nano and microsize fibers similar to ECM. However, the big drawback of this process is that the pore size of the fibers is too small to allow cells to infiltrate into the pores of the fibers in the 3D scaffold. Thus, the aim of this study is to fabricate new fibers with large and controllable pore size by designing an innovative collector plate and the new process. Using the new fibers, the cell attachment on single fibers and other cell behaviors such as cell growing, cell colonization on and between the fibers were evaluated. Finally cell glued three dimensional scaffold was developed as a model of stable thick 3D scaffold.

2.4. REFERENCES

1. Langer, R. and J. Vacanti, *Tissue engineering.* Science, 1993. **260**(5110): p. 920-926.
2. *Tissue engineering*, in *Nature Biotechnology*. 2000. p. IT56-IT58.
3. Davenport, R.J., *What Controls Organ Regeneration?* Science, 2005. **309**(5731): p. 84.
4. Kirsner, R.S., *The use of Apligraf in acute wounds.* The Journal Of Dermatology, 1998. **25**(12): p. 805-811.
5. Lysaght, M.J. and J. Reyes, *The Growth of Tissue Engineering.* Tissue Engineering, 2001. **7**(5): p. 485-493.
6. Griffith, L.G. and G. Naughton, *Tissue Engineering--Current Challenges and Expanding Opportunities.* Science, 2002. **295**(5557): p. 1009-1014.
7. Shieh, S.-J. and J.P. Vacanti, *State-of-the-art tissue engineering: From tissue engineering to organ building.* Surgery, 2005. **137**(1): p. 1-7.
8. Larouche, D., et al., *Regeneration of Skin and Cornea by Tissue Engineering*. Stem Cells in Regenerative Medicine. 2009. 233-256.
9. Price, R., Das-Gupta, Victoria, Harris, Paul, Leigh, Irene, Navsaria, Harshad, *The Role of Allogenic Fibroblasts in an Acute Wound Healing Model.* Plastic & Reconstructive Surgery, 2004. **113(6)**: p. 1719-1729.
10. Yang, K.C., et al., *Chitosan/Gelatin Hydrogel Prolonged the Function of Insulinoma/Agarose Microspheres In Vivo During Xenogenic Transplantation.* Transplantation Proceedings, 2008. **40**(10): p. 3623-3626.

11. Zimmermann, W.-H., et al., *Cardiac Grafting of Engineered Heart Tissue in Syngenic Rats.* Circulation, 2002. **106**(90121): p. I-151-157.

12. De Bartolo, L., et al., *Human hepatocyte functions in a crossed hollow fiber membrane bioreactor.* Biomaterials. In Press, Corrected Proof.

13. Lee, W., et al., *Multi-layered culture of human skin fibroblasts and keratinocytes through three-dimensional freeform fabrication.* Biomaterials, 2009. **30**(8): p. 1587-1595.

14. Park, J.-K., et al., *Development of bioartificial liver system and potential of stem cells as hepatocyte source.* Journal of Biotechnology, 2008. **136**(Supplement 1): p. S115-S115.

15. Chen, F.H., K.T. Rousche, and R.S. Tuan, *Technology Insight: adult stem cells in cartilage regeneration and tissue engineering.* Nat Clin Pract Rheum, 2006. **2**(7): p. 373-382.

16. Shen, G., et al., *Tissue engineering of blood vessels with endothelial cells differentiated from mouse embryonic stem cells.* Cell Res, 2003. **13**(5): p. 335-341.

17. Bianco, P. and P.G. Robey, *Stem cells in tissue engineering.* Nature, 2001. **414**(6859): p. 118-121.

18. Hollister, S.J., *Porous scaffold design for tissue engineering.* Nat Mater, 2005. **4**(7): p. 518-524.

19. Stevens, M.M. and J.H. George, *Exploring and Engineering the Cell Surface Interface.* Science, 2005. **310**(5751): p. 1135-1138.

20. Hubbell, J.A., *Bioactive biomaterials.* Current Opinion in Biotechnology, 1999. **10**(2): p. 123-129.

21. Kurihara, H. and T. Nagamune, *Cell adhesion ability of artificial extracellular matrix proteins containing a long repetitive Arg-Gly-Asp sequence.* Journal of Bioscience and Bioengineering, 2005. **100**(1): p. 82-87.

22. Gu, Z., et al., *Synthesis and characterization of PLGA-gelatin complex with growth factor incorporation as potential matrix.* Journal of Alloys and Compounds, 2009. **474**(1-2): p. 450-454.

23. Wenk, E., et al., *Microporous silk fibroin scaffolds embedding PLGA microparticles for controlled growth factor delivery in tissue engineering.* Biomaterials, 2009. **30**(13): p. 2571-2581.

24. Lawrence, B.J. and S.V. Madihally, *Cell colonization in degradable 3D porous matrices.* Cell adhesion & Migration, 2008. **2(1)**: p. 1-8.

25. O'Brien, F.J., et al., *The effect of pore size on cell adhesion in collagen-GAG scaffolds.* Biomaterials, 2005. **26**(4): p. 433-441.

26. I V Yannas, E.L., D P Orgill, E M Skrabut, and G F Murphy, *Synthesis and characterization of a model extracellular matrix that induces partial regeneration of adult mammalian skin.* Proceedings of the National Academy of Sciences of the United States of America, 1989. **86(3)**.

27. Doi K, N.Y., Matsuda T . *Novel compliant and tissue-permeable microporous polyurethane vascular prosthesis fabricated using an excimer laser ablation technique.* Journal of biomedical materials research, 1996. **31(1)**.

28. Namba, R.M., et al., *Development of porous PEG hydrogels that enable efficient, uniform cell-seeding and permit early neural process extension.* Acta Biomaterialia. In Press, Accepted Manuscript.

29. Byrne, D.P., et al., *Simulation of tissue differentiation in a scaffold as a function of porosity, Young's modulus and dissolution rate: Application of mechanobiological models in tissue engineering.* Biomaterials, 2007. **28**(36): p. 5544-5554.

30. Sun, S., I. Titushkin, and M. Cho, *Regulation of mesenchymal stem cell adhesion and orientation in 3D collagen scaffold by electrical stimulus.* Bioelectrochemistry, 2006. **69**(2): p. 133-141.

31. Levy-Mishali, M., J. Zoldan, and S. Levenberg, *Effect of Scaffold Stiffness on Myoblast Differentiation.* Tissue Engineering Part A, 2009. **15**(4): p. 935-944.

32. Au, H.T.H., et al., *Interactive effects of surface topography and pulsatile electrical field stimulation on orientation and elongation of fibroblasts and cardiomyocytes.* Biomaterials, 2007. **28**(29): p. 4277-4293.

33. Curtis, A. and C. Wilkinson, *New depths in cell behaviour: reactions of cells to nanotopography.* Biochemical Society Symposium, 1999. **65**: p. 15-26.

34. Thomson R. C., W.M.C., Yaszemski M. J., Mikos A. G., *Biodegradable polymer scaffolds to regenerate organs.* Advances in polymer science, 1995. **122**: p. 245-274.

35. Anderson, D.G., J.A. Burdick, and R. Langer, *MATERIALS SCIENCE: Smart Biomaterials.* Science, 2004. **305**(5692): p. 1923-1924.

36. Langer, R. and D.A. Tirrell, *Designing materials for biology and medicine.* Nature, 2004. **428**(6982): p. 487-492.

37. Hench, L.L. and J.M. Polak, *Third-Generation Biomedical Materials.* Science, 2002. **295**(5557): p. 1014-1017.

38. Ghasemi-Mobarakeh, L., et al., *Electrospun poly(ε-caprolactone)/gelatin nanofibrous scaffolds for nerve tissue engineering.* Biomaterials, 2008. **29**(34): p. 4532-4539.

39. Lien, S.-M., L.-Y. Ko, and T.-J. Huang, *Effect of pore size on ECM secretion and cell growth in gelatin scaffold for articular cartilage tissue engineering.* Acta Biomaterialia, 2009. **5**(2): p. 670-679.

40. Xue, L. and H.P. Greisler, *Biomaterials in the development and future of vascular grafts.* Journal Of Vascular Surgery: Official Publication, The Society For Vascular Surgery & International Society For Cardiovascular Surgery, North American Chapter, 2003. **37**(2): p. 472-480.

41. Gercek, I., R.S. Tigli, and M. Gumusderelioglu, *A novel scaffold based on formation and agglomeration of PCL microbeads by freeze-drying.* Journal of Biomedical Materials Research. Part A, 2008. **86**(4): p. 1012-1022.

42. Liu, X., Y. Won, and P.X. Ma, *Porogen-induced surface modification of nano-fibrous poly(l-lactic acid) scaffolds for tissue engineering.* Biomaterials, 2006. **27**(21): p. 3980-3987.

43. Sun, W. and P. Lal, *Recent development on computer aided tissue engineering -- a review.* Computer Methods and Programs in Biomedicine, 2002. **67**(2): p. 85-103.

44. Liu, X., et al., *Biomimetic nanofibrous gelatin/apatite composite scaffolds for bone tissue engineering.* Biomaterials. In Press, Corrected Proof.

45. Ruiyun Zhang, P.X.M., *Synthetic nano-fibrillar extracellular matrices with predesigned macroporous architectures.* Journal of biomedical materials research, 2000. **52**(2): p. 430-438.

46. Zhang, S. and X. Zhao, *Design of molecular biological materials using peptide motifs.* Journal of Materials Chemistry, 2004. **14**(14): p. 2082-2086.

47. Blaker, J.J., S.N. Nazhat, and A.R. Boccaccini, *Development and characterisation of silver-doped bioactive glass-coated sutures for tissue engineering and wound healing applications.* Biomaterials, 2004. **25**(7-8): p. 1319-1329.

48. Pengcheng Zhao, H.J., Hui Pan, Kangjie Zhu, Weiliam Chen,, *Biodegradable fibrous scaffolds composed of gelatin coated poly(ε-caprolactone) prepared by coaxial electrospinning.* Journal of Biomedical Materials Research Part A, 2007. **83A**(2): p. 372-382.

49. Vasita, R. and D.S. Katti, *Nanofibers and their applications in tissue engineering.* International Journal Of Nanomedicine, 2006. **1**(1): p. 15-30.

50. D. Li, Y.X., *Electrospinning of Nanofibers: Reinventing the Wheel?* Advanced Materials, 2004. **16**(14): p. 1151-1170.

51. Shin, H., S. Jo, and A.G. Mikos, *Biomimetic materials for tissue engineering.* Biomaterials, 2003. **24**(24): p. 4353-4364.

52. *Fibrous 3-dimensional scaffold via electrospinning for tissue regeneration and method for preparing the same.* USPTO, 2008. 0233162.

53. Anthony L. Andrady, D.S.E., *Electrospinning in a controlled gaseous environment description/claims.* US Patent, 2008. 0063741.

54. Sill, T.J. and H.A. von Recum, *Electrospinning: Applications in drug delivery and tissue engineering.* Biomaterials, 2008. **29**(13): p. 1989-2006.

55. Ramakrishna, S., et al., *Electrospun nanofibers: solving global issues.* Materials Today, 2006. **9**(3): p. 40-50.

56. Bhardwaj, N. and S.C. Kundu, *Electrospinning: A fascinating fiber fabrication technique.* Biotechnology Advances. In Press, Corrected Proof.

57. Zeleny, J., *The Electrical Discharge from Liquid Points, and a Hydrostatic Method of Measuring the Electric Intensity at Their Surfaces.* Physical Review, 1914. **3**(2): p. 69.

58. Morton, W.J., *Method of dispersing fluids* US Patent, 1902. 705691.

59. Formhals A, i., *Process and apparatus for preparing artificial threads.* . US Patent 1934(No. 1,975): p. 504.

60. Formhals A, *Method and apparatus for spinning.* US Patent 1939(No. 2,169, 962).

61. Taylor, G., *Electrically Driven Jets.* Proceedings of the Royal Society of London. A. Mathematical and Physical Sciences, 1969. **313**(1515): p. 453-475.

62. Baumgarten, P.K., *Electrostatic spinning of acrylic microfibers.* Journal of Colloid and Interface Science, 1971. **36**(1): p. 71-79.

63. Larrondo, L. and R.S.J. Manley, *Electrostatic fiber spinning from polymer melts. I. Experimental observations on fiber formation and properties.* Journal of Polymer Science: Polymer Physics Edition, 1981. **19**(6): p. 909-920.

64. Larrondo, L. and R.S.J. Manley, *Electrostatic fiber spinning from polymer melts. II. Examination of the flow field in an electrically driven jet.* Journal of Polymer Science: Polymer Physics Edition, 1981. **19**(6): p. 921-932.

65. Huang, Z.-M., et al., *A review on polymer nanofibers by electrospinning and their applications in nanocomposites.* Composites Science and Technology, 2003. **63**(15): p. 2223-2253.

66. Bhardwaj, N. and S.C. Kundu, *Electrospinning: A fascinating fiber fabrication technique.* Biotechnology Advances. **28**(3): p. 325-347.

67. Chronakis, I.S., *Novel nanocomposites and nanoceramics based on polymer nanofibers using electrospinning process--A review.* Journal of Materials Processing Technology, 2005. **167**(2-3): p. 283-293.

68. Zhang, Y., et al., *Preparation of Core−Shell Structured PCL-r-Gelatin Bi-Component Nanofibers by Coaxial Electrospinning.* Chemistry of Materials, 2004. **16**(18): p. 3406-3409.

69. Kidoaki, S., I.K. Kwon, and T. Matsuda, *Mesoscopic spatial designs of nano- and microfiber meshes for tissue-engineering matrix and scaffold based on newly devised multilayering and mixing electrospinning techniques.* Biomaterials, 2005. **26**(1): p. 37-46.

70. Frenot, A. and I.S. Chronakis, *Polymer nanofibers assembled by electrospinning.* Current Opinion in Colloid & Interface Science, 2003. **8**(1): p. 64-75.

71. Xu, S., et al., *Electrospinning of native cellulose from nonvolatile solvent system.* Polymer, 2008. **49**(12): p. 2911-2917.

72. Wang, H., et al., *Fabrication of aligned ferrite nanofibers by magnetic-field-assisted electrospinning coupled with oxygen plasma treatment.* Materials Research Bulletin, 2009. **44**(8): p. 1676-1680.

73. Xie, J., et al., *The differentiation of embryonic stem cells seeded on electrospun nanofibers into neural lineages.* Biomaterials, 2009. **30**(3): p. 354-362.

74. Yang, F., J.G.C. Wolke, and J.A. Jansen, *Biomimetic calcium phosphate coating on electrospun poly(ε-caprolactone) scaffolds for bone tissue engineering.* Chemical Engineering Journal, 2008. **137**(1): p. 154-161.

75. Wong, S.-C., A. Baji, and S. Leng, *Effect of fiber diameter on tensile properties of electrospun poly([var epsilon]-caprolactone).* Polymer, 2008. **49**(21): p. 4713-4722.

76. Tillman, B.W., et al., *The in vivo stability of electrospun polycaprolactone-collagen scaffolds in vascular reconstruction.* Biomaterials, 2009. **30**(4): p. 583-588.

77. Zhuo, H., J. Hu, and S. Chen, *Electrospun polyurethane nanofibres having shape memory effect.* Materials Letters, 2008. **62**(14): p. 2074-2076.

78. Paneva, D., et al., *Novel electrospun poly([epsilon]-caprolactone)-based bicomponent nanofibers possessing surface enriched in tertiary amino groups.* European Polymer Journal, 2008. **44**(3): p. 566-578.

79. Lee, S.J., et al., *The use of thermal treatments to enhance the mechanical properties of electrospun poly(ε-caprolactone) scaffolds.* Biomaterials, 2008. **29**(10): p. 1422-1430.

80. Chew, S.Y., et al., *The effect of the alignment of electrospun fibrous scaffolds on Schwann cell maturation.* Biomaterials, 2008. **29**(6): p. 653-661.

81. Wu, Y., L.A. Carnell, and R.L. Clark, *Control of electrospun mat width through the use of parallel auxiliary electrodes.* Polymer, 2007. **48**(19): p. 5653-5661.

82. Van Royen, P., et al., *Characterisation of the surface composition in electrospun nanowebs with static secondary ion mass spectrometry (S-SIMS).* Talanta, 2007. **71**(4): p. 1464-1469.

83. Li, W.-J., et al., *Engineering controllable anisotropy in electrospun biodegradable nanofibrous scaffolds for musculoskeletal tissue engineering.* Journal of Biomechanics, 2007. **40**(8): p. 1686-1693.

84. Kang, X., et al., *Adipogenesis of murine embryonic stem cells in a three-dimensional culture system using electrospun polymer scaffolds.* Biomaterials, 2007. **28**(3): p. 450-458.

85. Ayodeji, O., et al., *Carbon dioxide impregnation of electrospun polycaprolactone fibers.* The Journal of Supercritical Fluids, 2007. **41**(1): p. 173-178.

86. Van Royen, P., et al., *Characterisation of electrospun nanowebs with static secondary ion mass spectrometry (S-SIMS).* Applied Surface Science, 2006. **252**(19): p. 6992-6995.

87. Luong-Van, E., et al., *Controlled release of heparin from poly(ε-caprolactone) electrospun fibers.* Biomaterials, 2006. **27**(9): p. 2042-2050.

88. Puppi, D., et al., *Electrospun Polymeric Meshes for Application in Tissue Engineering.* Biomedicine & Pharmacotherapy, 2008. **62**(8): p. 489-490.

89. Marras, S.I., et al., *Biodegradable polymer nanocomposites: The role of nanoclays on the thermomechanical characteristics and the electrospun fibrous structure.* Acta Biomaterialia, 2008. **4**(3): p. 756-765.

90. Lee, J., et al., *The effect of gelatin incorporation into electrospun poly(l-lactide-co-ε-caprolactone) fibers on mechanical properties and cytocompatibility.* Biomaterials, 2008. **29**(12): p. 1872-1879.

91. Jeon, H.J., et al., *Preparation of poly(ε-caprolactone)-based polyurethane nanofibers containing silver nanoparticles.* Applied Surface Science, 2008. **254**(18): p. 5886-5890.

92. Heydarkhan-Hagvall, S., et al., *Three-dimensional electrospun ECM-based hybrid scaffolds for cardiovascular tissue engineering.* Biomaterials, 2008. **29**(19): p. 2907-2914.

93. Erisken, C., D.M. Kalyon, and H. Wang, *Functionally graded electrospun polycaprolactone and β-tricalcium phosphate nanocomposites for tissue engineering applications.* Biomaterials, 2008. **29**(30): p. 4065-4073.

94. Choi, J.S., et al., *The influence of electrospun aligned poly(ε-caprolactone)/collagen nanofiber meshes on the formation of self-aligned skeletal muscle myotubes.* Biomaterials, 2008. **29**(19): p. 2899-2906.

95. Baker, B.M., et al., *The potential to improve cell infiltration in composite fiber-aligned electrospun scaffolds by the selective removal of sacrificial fibers.* Biomaterials, 2008. **29**(15): p. 2348-2358.

96. Schnell, E., et al., *Guidance of glial cell migration and axonal growth on electrospun nanofibers of poly-ε-caprolactone and a collagen/poly ε-caprolactone blend.* Biomaterials, 2007. **28**(19): p. 3012-3025.

97. Lin, K., et al., *Reducing electrospun nanofiber diameter and variability using cationic amphiphiles.* Polymer, 2007. **48**(21): p. 6384-6394.

98. Kim, T.G., D.S. Lee, and T.G. Park, *Controlled protein release from electrospun biodegradable fiber mesh composed of poly(ε-caprolactone) and poly(ethylene oxide).* International Journal of Pharmaceutics, 2007. **338**(1-2): p. 276-283.

99. Chong, E.J., et al., *Evaluation of electrospun PCL/gelatin nanofibrous scaffold for wound healing and layered dermal reconstitution.* Acta Biomaterialia, 2007. **3**(3): p. 321-330.

100. Hutmacher DW, Schantz T, Zein I, Ng KW, Teoh SH, Tan KC. *Mechanical properties and cell cultural response of polycaprolactone scaffolds designed and fabricated via fused deposition modeling.* J Biomed Mater Res., 2001. **55**: p. 203-16.

101. Lowry KJ, Hamson KR, Bear L, Peng YB, Calaluce R, Evans ML, et al. *Polycaprolactone/glass bioabsorbable implant in a rabbit humerus fracture model.* J Biomed Mater Res., 1997. **36**: p. 536-41.

102. Lavik E, Teng YD, Snyder E, Langer R. *Seeding neural stem cells on scaffolds of PGA, PLA, and their copolymers.* Methods Mol Biol., 2002. **198**: p. 89-97.

103. Nakamura T, Hitomi S, Watanabe S, Shimizu Y, Jamshidi K, Hyon SH, et al. *Bioabsorption of polylactides with different molecular properties.* J Biomed Mater Res., 1989. **23**: p.1115-30.

104. Mooney DJ, Mazzoni CL, Breuer C, McNamara K, Hern D, Vacanti JP, et al. *Stabilized polyglycolic acid fibre-based tubes for tissue engineering.* Biomaterials, 1996. **17**: p. 115-24.

105. Gao J, Niklason L, Langer R. *Surface hydrolysis of poly(glycolic acid) meshes increases the seeding density of vascular smooth muscle cells.* J Biomed Mater Res., 1998. **42**: p. 417-24.

106. Marra KG, Szem JW, Kumta PN, DiMilla PA, Weiss LE. *In vitro analysis of biodegradable polymer blend/hydroxyapatite composites for bone tissue engineering.* J Biomed Mater Res., 1999. **47**: p. 324-35.

107. Engelberg I, Kohn J. *Physico-mechanical properties of degradable polymers used in medical applications: a comparative study.* Biomaterials, 1991. **12**: p. 292-304.

108. Ozawa T, Mickle DA, Weisel RD, Koyama N, Wong H, Ozawa S, et al. *Histologic changes of nonbiodegradable and biodegradable biomaterials used to repair right ventricular heart defects in rats.* J Thorac Cardiovasc Surg., 2002. **124**: p. 1157-64.

109. Heath DE, Cooper SL. *Interaction of endothelial cells with methacrylic terpolymer biomaterials.* J Biomed Mater Res B Appl Biomater., 2010. **92**: p. 289-97.

110. Mao JS, liu HF, Yin YJ, Yao KD. *The properties of chitosan-gelatin membranes and scaffolds modified with hyaluronic acid by different methods.* Biomaterials, 2003. **24**: p. 1621-9.

111. Dar A, Shachar M, Leor J, Cohen S. *Optimization of cardiac cell seeding and distribution in 3D porous alginate scaffolds.* Biotechnol Bioeng., 2002. **80**: p. 305-12.

112. Madihally SV, Matthew HW. *Porous chitosan scaffolds for tissue engineering.* Biomaterials, 1999. **20**: p. 1133-42.

113. Rothenburger M, Vischer P, Volker W, Glasmacher B, Berendes E, Scheld HH, et al. *In vitro modelling of tissue using isolated vascular cells on a synthetic collagen matrix as a substitute for heart valves.* Thorac Cardiovasc Surg., 2001. **49**: p. 204-9.

114. Yannas IV. *Models of organ regeneration processes induced by templates.* Ann N Y Acad Sci., 1997. **831**: p. 280-93.

115. Zaleskas JM, Kinner B, Freyman TM, Yannas IV, Gibson LJ, Spector M. *Growth factor regulation of smooth muscle actin expression and contraction of human articular chondrocytes and meniscal cells in a collagen-GAG matrix.* Exp Cell Res., 2001. **270**: p. 21-31.

116. Spilker MH, Asano K, Yannas IV, Spector M. *Contraction of collagen-glycosaminoglycan matrices by peripheral nerve cells in vitro.* Biomaterials, 2001. **22**: p. 1085-93.

117. Kessler PD, Byrne BJ. *Myoblast cell grafting into heart muscle: cellular biology and potential applications.* Annu Rev Physiol., 1999. **61**: p. 219-42.

118. Taylor PM, Allen SP, Dreger SA, Yacoub MH. *Human cardiac valve interstitial cells in collagen sponge: a biological three-dimensional matrix for tissue engineering.* J Heart Valve Dis., 2002. **11**: p. 298-306; discussion -7.

119. Pieper JS, Hafmans T, van Wachem PB, van Luyn MJ, Brouwer LA, Veerkamp JH, et al. *Loading of collagen-heparan sulfate matrices with bFGF promotes angiogenesis and tissue generation in rats.* J Biomed Mater Res., 2002. **62**: p. 185-94.

120. Bensai, d W, Triffitt JT, Blanchat C, Oudina K, Sedel L, et al. *A biodegradable fibrin scaffold for mesenchymal stem cell transplantation.* Biomaterials, 2003. **24**: p. 2497-502.

121. McClure MJ, Sell SA, Ayres CE, Simpson DG, Bowlin GL. *Electrospinning-aligned and random polydioxanone-polycaprolactone-silk fibroin-blended scaffolds: geometry for a vascular matrix.* Biomed Mater., 2009. **4**: 055010.

122. Lee KY, Jeong L, Kang YO, Lee SJ, Park WH. *Electrospinning of polysaccharides for regenerative medicine.* Adv Drug Deliv Rev., 2009. **61**: p. 1020-32.

123. Jang JH, Castano O, Kim HW. *Electrospun materials as potential platforms for bone tissue engineering.* Adv Drug Deliv Rev., 2009. **61**: p. 1065-83.

124. Kulkarni RK, Moore EG, Hegyeli AF, Leonard F. *Biodegradable poly(lactic acid) polymers.* J Biomed Mater Res., 1971 **5**: p. 169-81.

125. Saito N, Okada T, Toba S, Miyamoto S, Takaoka K. *New synthetic absorbable polymers as BMP carriers: plastic properties of poly-D,L-lactic acid-polyethylene glycol block copolymers.* J Biomed Mater Res., 1999. **47**: p. 104-10.

126. Park IK, Yang J, Jeong HJ, Bom HS, Harada I, Akaike T, et al. *Galactosylated chitosan as a synthetic extracellular matrix for hepatocytes attachment.* Biomaterials, 2003. **24**: p. 2331-7.

127. Ho KL, Witte MN, Bird ET. *8-ply small intestinal submucosa tension-free sling: spectrum of postoperative inflammation.* J Urol., 2004. **171**: p. 268-71.

128. Pistner H, Bendix DR, Muhling J, Reuther JF. *Poly(L-lactide): a long-term degradation study in vivo.* Part III. Analytical characterization. Biomaterials, 1993. **14**: p. 291-8.

129. Kranz H, Ubrich N, Maincent P, Bodmeier R. *Physicomechanical properties of biodegradable poly(D,L-lactide) and poly(D,L-lactide-co-glycolide) films in the dry and wet states.* J Pharm Sci., 2000. **89**: p. 1558-66.

130. Yoon JJ, Park TG. *Degradation behaviors of biodegradable macroporous scaffolds prepared by gas foaming of effervescent salts.* J Biomed Mater Res., 2001. **55**: p. 401-8.

131. Lu L, Peter SJ, Lyman MD, Lai HL, Leite SM, Tamada JA, et al. *In vitro and in vivo degradation of porous poly(DL-lactic-co-glycolic acid) foams.* Biomaterials, 2000. **21**: p. 1837-45.

132. Massia SP, Hubbell JA. *Covalently attached GRGD on polymer surfaces promotes biospecific adhesion of mammalian cells.* Ann N Y Acad Sci., 1990. **589**: p. 261-70.

133. Park A, Wu B, Griffith LG. *Integration of surface modification and 3D fabrication techniques to prepare patterned poly(L-lactide) substrates allowing regionally selective cell adhesion.* J Biomater Sci Polym Ed., 1998. **9**: p. 89-110. 1998.

134. Eid K, Chen E, Griffith L, Glowacki J. *Effect of RGD coating on osteocompatibility of PLGA-polymer disks in a rat tibial wound.* J Biomed Mater Res., 2001. **57**: p. 224-31.

135. Fussell GW, Cooper SL. *Synthesis and characterization of acrylic terpolymers with RGD peptides for biomedical applications.* Biomaterials, 2004. **25**: p. 2971-8.

136. Lindahl U, Kusche-Gullberg M, Kjellen L. *Regulated diversity of heparan sulfate.* J Biol Chem., 1998. **273**: p. 24979-82.

137. Babu M, Diegelmann R, Oliver N. *Fibronectin is overproduced by keloid fibroblasts during abnormal wound healing.* Mol Cell Biol., 1989. **9**: p. 1642-50.

138. Lu H, Ko Y-G, Kawazoe N, Chen G. *Cartilage tissue engineering using funnel-like collagen sponges prepared with embossing ice particulate templates.* Biomaterials.In Press, Corrected Proof.

139. Zhang X, Thomas V, Xu Y, Bellis SL, Vohra YK. *An in vitro regenerated functional human endothelium on a nanofibrous electrospun scaffold.* Biomaterials, 2010. **31**: p. 4376-81.

140. Ghasemi-Mobarakeh L, Prabhakaran MP, Morshed M, Nasr-Esfahani M-H, Ramakrishna S. *Electrospun poly(ε-caprolactone)/gelatin nanofibrous scaffolds for nerve tissue engineering.* Biomaterials, 2008. **29**: p. 4532-9.

141. Zhang YZ, Feng Y, Huang ZM, Ramakrishna S, Lim CT. *Fabrication of porous electrospun nanofibres.* Nanotechnology, 2006. **17**.

142. Linh NT, Min YK, Song HY, Lee BT. *Fabrication of polyvinyl alcohol/gelatin nanofiber composites and evaluation of their material properties.* J Biomed Mater Res B Appl Biomater., 2010. 95: p. 184-91.

143. Tigli RS, Kazaroglu NM, Mav ISB, Gumusderel IOM. *Cellular Behavior on Epidermal Growth Factor (EGF)-Immobilized PCL/Gelatin Nanofibrous Scaffolds.* J Biomater Sci Polym Ed., 2010.

144. Lee H, Kim G. *Biocomposites electrospun with poly(epsilon-caprolactone) and silk fibroin powder for biomedical applications.* J Biomater Sci Polym Ed., 2010. **21**: p. 1687-99.

145. Choi JS, Lee SJ, Christ GJ, Atala A, Yoo JJ. *The influence of electrospun aligned poly(epsilon-caprolactone)/collagen nanofiber meshes on the formation of self-aligned skeletal muscle myotubes.* Biomaterials, 2008. **29**: p. 2899-906.

146. Sheikh FA, Barakat NA, Kanjwal MA, Nirmala R, Lee JH, Kim H, et al. *Electrospun titanium dioxide nanofibers containing hydroxyapatite and silver nanoparticles as future implant materials.* J Mater Sci Mater Med., 2010. **21**: p. 2551-9. 2010.

147. Stankus JJ, Freytes DO, Badylak SF, Wagner WR. *Hybrid nanofibrous scaffolds from electrospinning of a synthetic biodegradable elastomer and urinary bladder matrix.* J Biomater Sci Polym Ed., 2008. **19**: p. 635-52.

148. Gupta D, Venugopal J, Mitra S, Giri Dev VR, Ramakrishna S. *Nanostructured biocomposite substrates by electrospinning and electrospraying for the mineralization of osteoblasts.* Biomaterials, 2009. **30**: p. 2085-94.

149. Zhang Y, Venugopal JR, El-Turki A, Ramakrishna S, Su B, Lim CT. *Electrospun biomimetic nanocomposite nanofibers of hydroxyapatite/chitosan for bone tissue engineering.* Biomaterials, 2008. **29**: p. 4314-22.

CHAPTER III

THREE-DIMENSIOMNAL SCAFFOLD OF ELECTROSPRAYED FIBERS WITH LARGE PORE SIZE FOR TISSUE REGENERATUION

3.1. INTRODUCTION

The electrospinning technique has recently emerged as a novel technique for tissue regeneration because it allows fabrication of nano and micro size fibers, which are very similar to the characteristic of a natural extracellular environment. A major problem in electrospinning technology is the lack of generating structural features necessary for building three-dimensional (3D) tissues [1, 2]. The pore sizes are less than 10 μm, while human cells are typically greater than 10 μm in size [3]. Hence, cell growth is restricted to the surface only. The reduced pore size is primarily due to multiple layers of fibers deposited to obtain thicker structures that withstand mechanical handling in subsequent steps.

Addressing the cell seeding problem by depositing both the polymer as well as cells simultaneously is a recent advancement [4]. However, this approach is not practical as cells will be exposed to a) toxic organic solvents used in the process, b) high shear rates induced by the flow of fluids through narrow nozzles, and c) sub-optimal environmental conditions during manufacturing. These factors affect cell viability and tissue growth. Due to reduced pore size and restricted cell infiltration, it is not possible to regenerate tissues of a thickness suitable for clinical transplantation.

In this study, I introduce an innovative electrospraying technique with a novel collector plate which allows the formation of very thin layers of micro- and nanofibers. Due to reduced thickness, pore size (~60 μm) of the formed layers is suitable for mammalian cell infiltration. I performed the fibroblast cell culture of multiple layers using layer-by-layer assembly: place one layer of thin fibers, seed cells and repeat. I show the 3D scaffolds of thin layers of electrosprayed fibers in which human fibroblasts are growing not only horizontally but also vertically due to large pore sizes of electrosprayed fibers. The implications of the 3D scaffold with layer-by-layer technique will expand to other cells, fibers, tissues and organs, and becomes a phenotype of 3D scaffolds in tissue regeneration.

3.2. MATERIALS AND METHOD

3.2.1. Materials

Polycaprolactone (PCL, Mn=80,000) and Gelatin Type A were purchased from Sigma (St, Louis, MO) and PCL (M_w=43,000-50,000) was obtained from Polysciences (Warrington, PA). Chloroform, methanol, and acetic acid were purchased from Pharmco

(Brookfield, CT). For cell culture study, Human foreskin fibroblast (HFF-1) was obtained from American Type Culture Collection (ATCC, Walkersville, MD). Dulbecco's modified Eagle Medium (DMEM), glucose and amphotericin B were obtained from Sigma (St, Louis, MO). Fetal bovine serum (FBS), Alexa Fluor 546 and 4',6-diamidino-2-phenylindole (DAPI) were purchased from Invitrogen (Carlsbad, CA). TrypLE Express, penicillin-streptomycin, and L-glutamine were obtained from Gibco (Grand Island, NY) and sodium bicarbonate was purchased from EMD (Gibbstown, NJ).

3.2.2. Fabrication of the thin layer of electrosprayed fibers

Electrospraying apparatus consisted of a syringe pump (74900 series, Cole-Parmer Instrument Company, Vernon Hills, IL), BD 10 mL syringe (Luer-Lok Tip; Becton Dickinson and Company, Franklin Lakes, NJ), needle tip, high voltage power supply (ES30P-5W/DAM, Gamma high Voltage Research, Ormond Beach, FL), earth grounding, and a collector plate (**Figure 3.1A**). The novel collector had four holes (diameter, 1.9 cm and depth 1.2 cm) in a wooden frame (3 cm × 10 cm × 2 cm) wrapped with aluminum foil (**Figure 3.1E**).

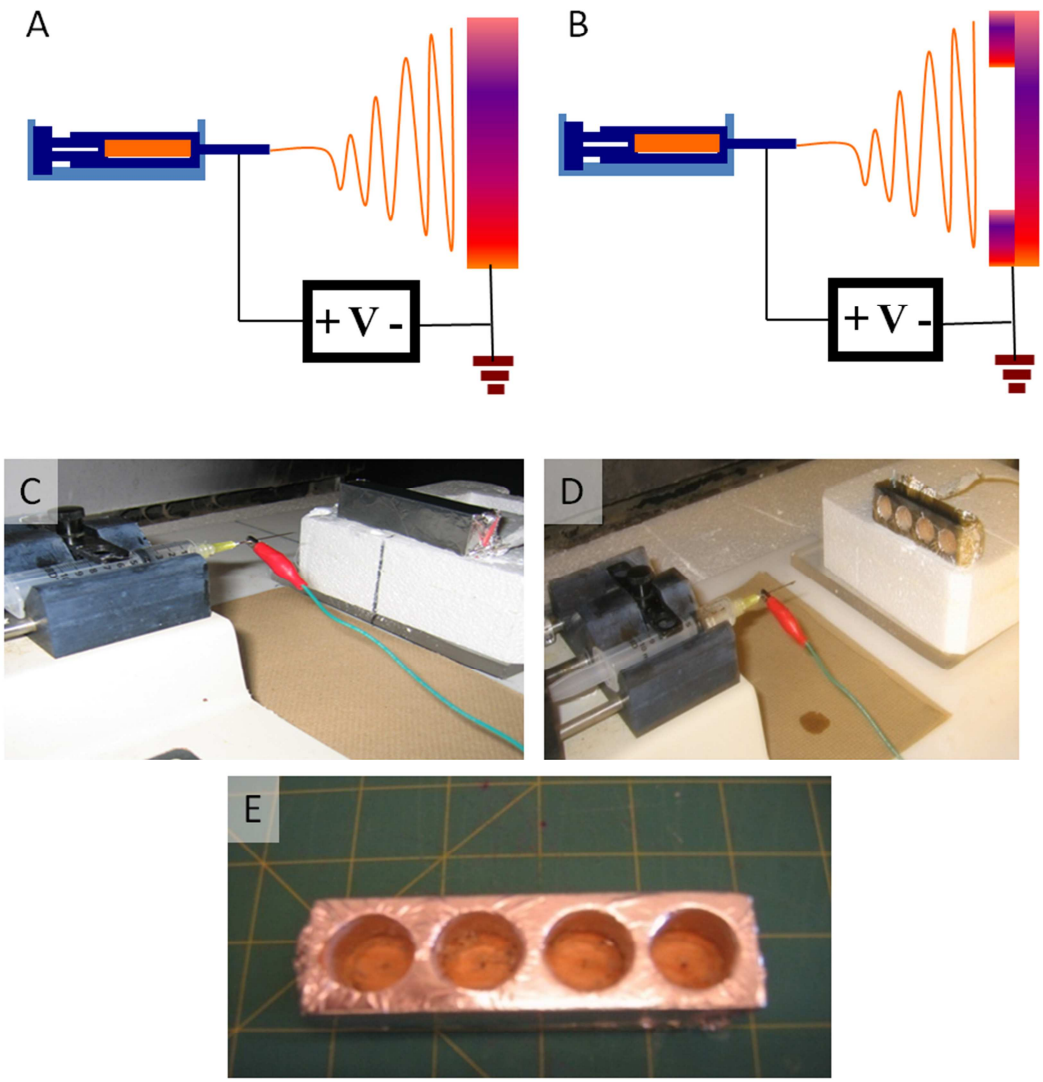

Figure 3.1. Novel electrospray setup. (**A**) Schematic representation of conventional electrospray setup. (**B**) Schematic representation of novel electrospray setup. (**C**) Photograph of conventional electrospray setup and (**D**) Photograph of novel electrospray setup. (**E**) Photograph of the novel collector.

The conventional collector plate of the same size as the novel collector without a hole was wrapped with aluminum foil. Electrosprayed fibers were fabricated at 40 mL/hr and 20 kV. For micro-sized fibers, 20% (wt/v) PCL (M_w=43,000-50,000) dissolved in a mixture solvent of chloroform and methanol (mixing ratio 9 to 1), was sprayed using a 14G needle. The distance of the collector plate was 12 cm from the tip of the needle. For nano-sized fibers, 10% (wt/v) PCL dissolved in a mixture solvent of chloroform and methanol (mixing ratio 9 to 1) was sprayed using a 26 G needle. The distance of the collector plate was 15 cm from the tip of the needle. Deposit volume of the solution was 0.75 mL. Gelatin fibers were formed using 20% (wt/v) gelatin dissolved in acetic acid and distilled water (mixing ratio 7 to 3). Flow rate, needle size, high voltage supply and distance between the needle tip and the collector were 10 ml/hr, 20 G, 10 kV, and 8 cm.

For simultaneous and sequential deposit, 20 w/v% PCL (Mn=80,000) was prepared with a solvent mixture of chloroform and methanol (mixing ratio 9 to 1). In the simultaneous and the sequential processes, fibers were formed in the same condition described for gelatin fiber formation using the novel collector.

3.2.3. Microstructure characterization

Samples were analyzed using JEOL 6360 (Jeol USA Inc., Peabody, MA) at an accelerated voltage of 9 to 20 kV similar to our previous publications [5]. In brief, samples were attached to an aluminum stub using a conductive graphite glue (Ted Pella Inc., Redding, CA) and sputter-coated with gold for 1 minute before SEM study.

Along with the obtained SEM images, fiber diameters, pore size and shape factors of pores ($4\pi\times$area/perimeter^2, when the number is closer to 1, the cell shape is closer to a

circle) were quantified using Sigma Scan Pro (SPSS Science, Chicago, IL). More than 35 points of fibers and pores were analyzed.

For simultaneous and sequential deposit, 20 w/v% PCL (Mn=80,000) was prepared with a solvent mixture of chloroform and methanol (mixing ratio 9 to 1). In the simultaneous and the sequential processes, fibers were formed the same conditions described for gelatin fiber formation using the novel collector.

3.2.4. Mechanical test

Micro size fibers were fabricated using a collector plate (10 cm × 3.5 cm × 2 cm) with a rectangular hole (5 cm × 1 cm × 1 cm) had an additional flat surface area or peripheral area of a rectangular hole, resulting in two rectangular holes (one with a flat surface and the other without). Fibers accumulated on the flat surface were used as samples for conventional fibers while the fibers collected in the hole were used as samples for novel fibers. Tensile testing was performed at room temperature with dry conditions by the method previously described [6]. In brief, 25 mm (width) × 10 mm (length) rectangular strips were cut from novel and conventional sample and strained to break at a constant crosshead speed of 10 mm/min using INSTRON 5542 (INSTRON, Canton, MA).

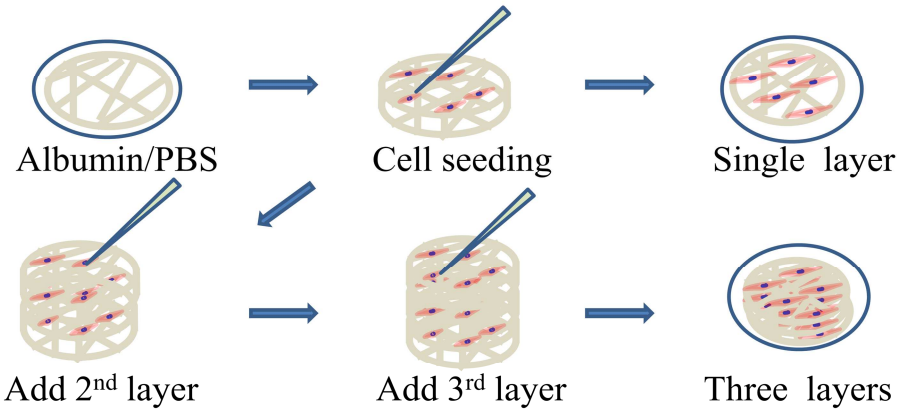

Figure 3.2. Schematic of the process of cell seeding.

3.2.5. Cell culture

HFF-1 was cultured in DMEM supplemented with 4 mM L-glutamine, 4.5 g/L glucose, 1.5 g/L sodium bicarbonate, 100 U/mL penicillin-streptomycin, 2.5 mg/mL amphotericin B, and 15 % FBS. The cells were maintained in a CO_2 incubator at 37 ℃. The media was changed every 2 days. Before cell seeding, cells were detached with 2% TrypLE Express, centrifuged, and suspended in serum-added media.

Microsize fibers were fabricated using 20 w/v% of PCL (Mw=43000) in chloroform/methanol (ratio 9 to 1) and the novel collector. Flow rate, needle size, high voltage supply and distance between the needle tip and the collector were 10 ml/hr, 20 G, 10 kV, and 8 cm. The deposit volume was 0.75 mL. Fibers on the aluminum frame were sterilized using UV light for 4 hours, immersed in ethanol for 4 hours, and rinsed by PBS three times. The thin layers were soaked in 15 % serum added media for 4 hours. The cell culture plates were treated with albumin to minimize cell adhesion to the tissue culture plastic surface prior to insertion of a thin layer of fibers (**Figure 3.2**). Then, 30,000 cells in 100 μL were seeded onto 5 points of fibers in a single layer of the aluminum frame.

For three layer cultures, the cell culture in the single layer was repeated three times by using layer-by-layer technique: place one layer of the sample, seed cells on five points of the sample and repeat the process of sample loading and cell seeding two more times. Ten minutes after cell-seeding, 2 and 3 mL of media were added into 6 well plates for single and three layers, respectively.

3.2.6. Evaluating of cell distribution and organization

At 1, 4 and 7 days after cell culture; the sample was fixed with 3.7 %

formaldehyde, rinsed with PBS, and immersed in ethanol at -20°C. Then, the sample was stained with 2 mL of Alexa phalloidin (0.66 μM) for cytoskeletal actin and counterstained with 2 mL of DAPI (30 nmol) for nuclei of cells, respectively [7]. The samples were first observed under an inverted fluorescent microscope (Nikon TE2000, Melville, NY). Digital micrographs were collected using a CCD camera. The data was treated using Corel Paint Shop Pro Photo X2 to modulate the brightness, contrast, and clarification.

Also, 3D images of cells on fibers in the single and three layers were collected using a confocal microscope (Leica TCS SP II, Heidelberg, Germany). Image stacks of both single and three layers along the z-axis were collected at a step size of 1.282 μm for single-layer cultures and 4.271 μm for three-layer cultures. The observed thickness of the z-axis for single and three layers were 30.77 and 89.70 μm, respectively. At each step, the two fluorescent signals of nuclei and skeletal actin and one light signal of fibers were collected. Then, fluorescent and light signals of cells on fibers in the single layer at 15.36 μm in z-axis were overlapped. To obtain 3D hologram, fluorescence signals of cells at each step were merged in the three-layers.

Samples were also analyzed using SEM to evaluate the distribution of fibers and cells. For this purpose, samples were dried using ethanol and analyzed similar to the fibers described above.

3.2.7. Histology assay

30 days after cell culture, the samples formed using single and three layers of fibers were tailored using a tweezer and scissors. The aluminum frames of the samples

were completely removed. Random parts of the samples were fixed in 3.7 % formaldehyde, dried through an ethanol gradient, and embedded in paraffin. The samples were cut into 4 μm and stained with hematoxylin and eosin (H & E) for histology analysis [8].

3.3. RESULTS

3.3.1. Fabrication of the thin layer of highly porous fibers

Conventional electrospray setup consists of a syringe pump, syringe and a needle of appropriate size, high voltage power supply, earth grounding, and a stationary collector plate (**Figure 3.1A**). The collector plate is a flat conducting plate where the polymer fibers accumulate. After certain elution volume, the fibers are removed and used in the needed application. To remove the material, larger volumes are deposited which leads to fibrous structures with limited pore size. I questioned whether the fibers could be accumulated by creating a hole in the collector plate. For this purpose, different size holes were created in wood, plastic or glass, and wrapped around with a conductive aluminum foil (**Figure 3.1B**), which can be autoclaved when sterilization is necessary. The collector plate was designed with the intention of using it as a support structure during transport and subsequent handling. Experiments performed under the same conditions as the traditional collector plate showed the presence of fibers in the holed area, suggesting the possibility of forming thin layers. Different shapes such as a circle, hexagon and rectangle with varying sizes (up to 10 cm) were tested. These results showed the possibility of obtaining thin layers. Since the aluminum foil could be simply peeled off from the core structure, it is also easy for the thin layer to be handled without

mechanical damage from external stress.

Absence of the continuous conducting medium could alter the electrical field. Hence, I questioned how the distribution of fibers would be altered and whether the formed fibers would have different architecture. Similar to other reports, fibers generated on the conventional plate showed multiple layers of fibers (**Figure 3.3A**) under scanning electron microscopy. However, few layers of fibers were observed in the open area of the new collector plate, (**Figure 3.3B**) while multiple layers were observed on the sheet. Many fiber morphologies appeared smooth and similar between the two conditions, except in case of a large fiber; in the conventional plate (**Figure 3.3A**), many fibers showed pores on their surface. To test whether nanosize fibers could be obtained using the new collector plate, processing parameters were optimized by manipulating the flow rate of the solution, the strength of voltage, and the distance between the needle tip and the collector. The conventional collector plate showed multilayered nanofibers (**Figure 3.3C**). Similar nanofibers were collected on the new collector plate with a single layer (**Figure 3.3D**), suggesting the applicability of this collector plate to other conditions.

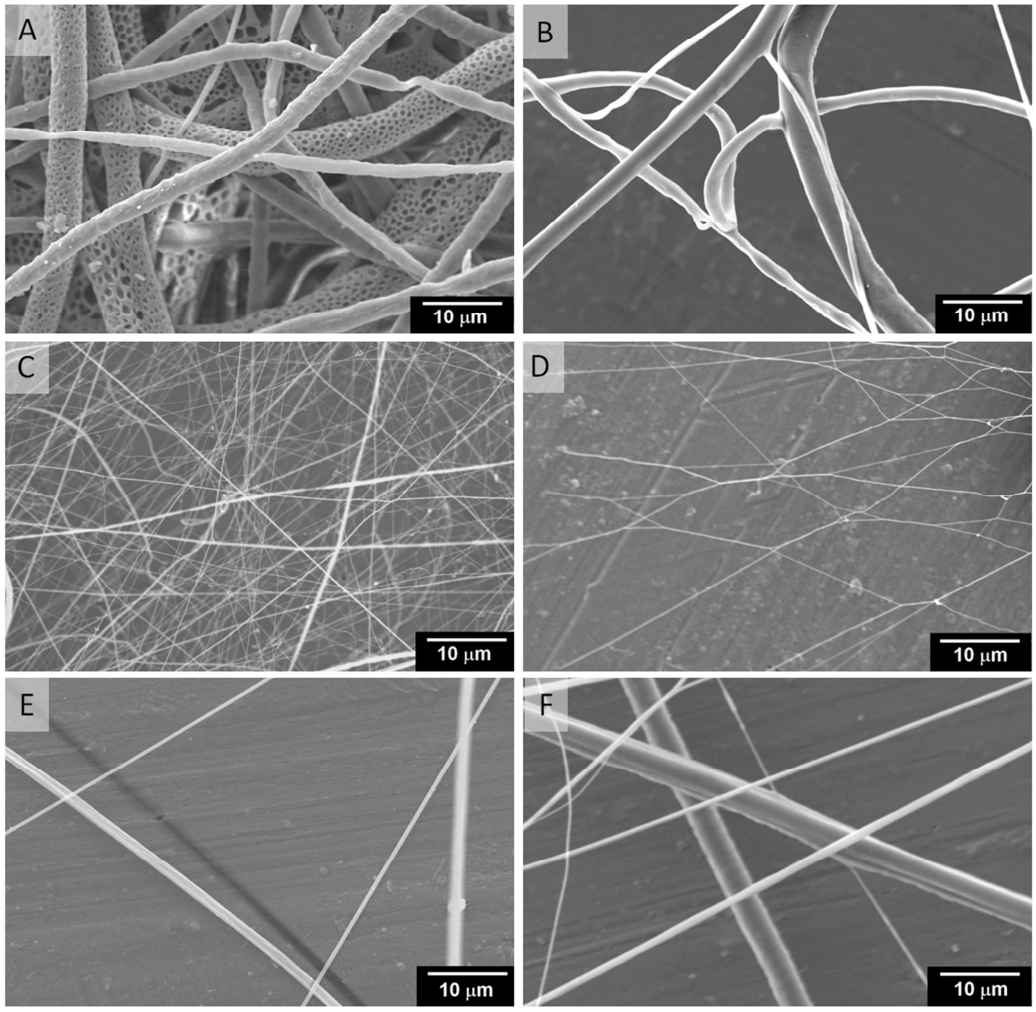

Figure 3.3. Morphology of fibers using novel and conventional collectors. Microfibers made of PCL (Mw=43000) with (**A**) conventional collector and (**B**) novel collector at the same condition. Nanofibers made of PCL (Mw=43000) with (**C**) conventional collector and (**D**) novel collector under the same conditions. (**E**) Fibers made of Gelatin Type A using the novel collector. (**F**) Hybrid fibers made of microsize PCL (M_n=80000) fibers and naonsize Gelatin Type A fibers in sequential process using the novel collector.

To test whether the new collector plate is applicable to other polymeric systems, forming fibers using naturally derived gelatin was tested. These results showed that the gelatin fibers accumulated similar to the PCL fibers (**Figure 3.3E**). Others have also used sequential (exchanging the syringes containing two different polymeric solutions in sequence) and simultaneous (using two syringes containing two different polymeric solutions at the same time) process of electrospraying to deposit two different polymers for controlling the micro-architecture [9-12]. To test this possibility, PCL and gelatin were deposited sequentially or simultaneously. These results showed (**Figure 3.3F**) that thin layers of fibers of different polymers can be collected on the novel collector plate.

To understand the effect of hydration on the fibers, formed fibers were observed under light microscopy before and after hydration. Upon hydration in phosphate buffered saline (PBS), the PCL fiber structure remained the same. However, gelatin fibers completely dissolved in PBS as they were not stabilized by any cross-linker. When composite structures were hydrated, PCL fibers still remained intact even after thirty or more days. However, the fibers made of PCL and gelatin were entangled and collapsed within 15 minutes because gelatin dissolved in PBS. Thus, one could easily comprehend the alterations in fibrous architecture using these thin layers.

3.3.2. Fiber characterization

To understand fiber size and pore size, fibers were generated under the same condition of solution (concentration of solution) and process parameters (flow rate, needle size, distance between the needle tip and the collector, and high voltage supply) using the novel and the conventional collector plates. Quantification of scanning electron

micrographs showed that the new collector plate does not affect the fiber size nor the shape of the pores in the scaffolds (**Figure 3.4A**). Even when nanofibers were formed under other conditions, no significant difference was obtained. Thus, this new collector plate can be easily adapted to various other polymers in conjunction with the intended application. Controlling fiber sizes is also possible using appropriate solvents and the distance of the collector plate. This suggests that the technology is versatile and can be easily integrated into existing technologies. The shape factor (**Figure 3.4B**) of pores formed due to random distribution of fibers were similar in both cases.

Pore size (**Figure 3.4C**) of the scaffold formed with the new collector plate showed significant increase due to the decreased density of fibers deposited in the open area. However, under the same conditions of solution and process parameters, the diameter of fibers generated by the novel and conventional fibers were quite similar. The pore size of fiber produced with the novel collector is much greater than those produced with the conventional one.

Collected fibrous structures under the same conditions for the same time were tested under tensile loading in the dry state at room temperature. Load-extension curves (**Figure 3.4D**) showed that the extension of novel fibers was twice as long as that of conventional fibers; novel fibers showed 250 % strain where as the conventional fibers showed 100% strain. However, the load carrying capacity of the fibrous structures were nearly half that of conventional fibers. These differences could be attributed to the decreased density of fibers in the novel collector plate; due to free space between the fibers on the sample, thin layers can stretch but cannot carry as much of a load.

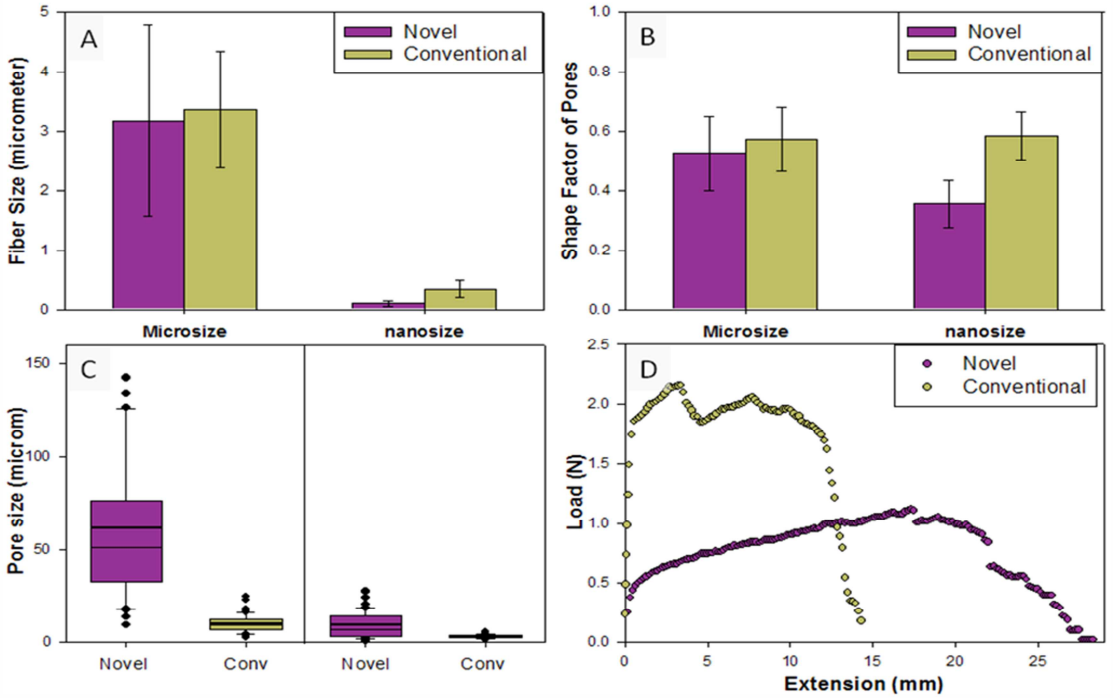

Figure 3.4. Comparison of fibrous layer characteristics. (**A**) Fiber diameters and the error bars correspond to the standard deviation (n = 50). (**B**) Shape factor and the error bars correspond to the standard deviation (n = 50). (**C**) Box plot showing the distribution of pore size with 10th, 25th, 50th, 75th, and 90th percentiles and the mean value (thick line within each box). Values that were outside 95th and 5th percentiles were treated as outliers. (**D**) The load–extension behavior.

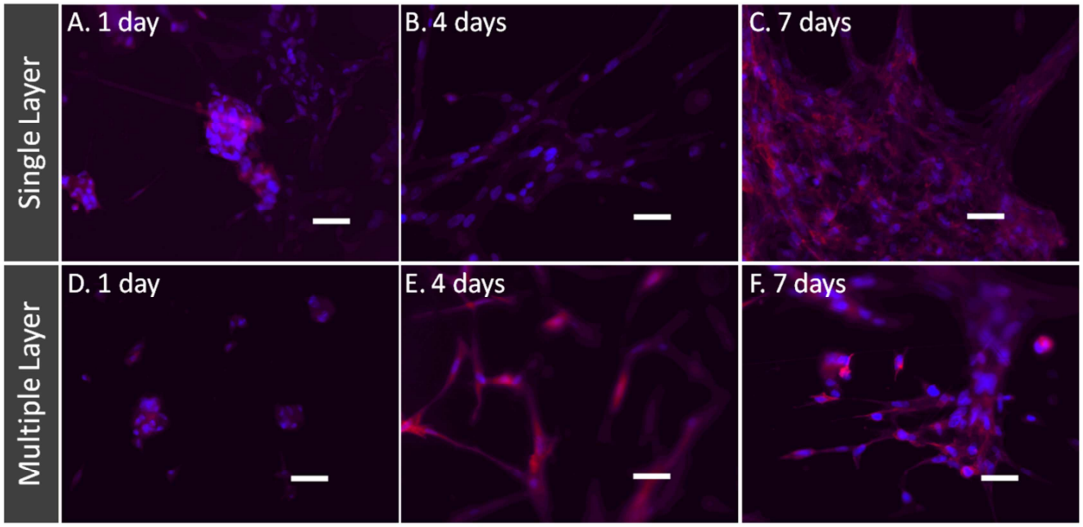

Figure 3.5. Cell colonization in single and three layers of the fibers. (**A-C**) Fluorescent micrographs of cells on single layer of fibers. (**D-F**) Fluorescent micrographs of cells on three layers of fibers. The samples were stained with Alexa phalloidin for cytoskeletal actin (red) and counterstained with DAPI for nuclei (blue) of cells. Scale bar corresponds to 50 µm.

3.3.3. Developing 3D colonized cells

To test whether cells can be cultured on these thin layers, formed porous structures along with the aluminum foil were inserted onto albumin-coated (to minimize cell adhesion to the tissue culture plastic) seeded with HFF-1 cells. For evaluating layer-by-layer assembly, the process of inserting the thin layer and seeding cells was done three times (**Figure 3.2**). Entire assembly was cultured for 7 days in serum containing medium with the routine monitored by light microscopy. An increase in the number of cells was observed on fibers in single and three layers. Further, many cells in both single and three layers appeared in clusters at the initial time point, but showed spreading and a spindle shape. By day 7, a number of pores were covered with the regenerated components. To assess the cellular components, they were stained for cytoskeletal actin and counterstained for nucleus using DAPI. To avoid background fluorescent signal pollution from cells on the surface of the cell culture dish, the samples were moved into new dishes after staining and washing. Fluorescent images (**Figure 3.5**) in single or three layers showed a qualitative improvement in the cells up to 7 days. Moreover, cells were individually distributed and surrounded by matrix elements, suggesting that the cells are functional. In addition, some cells were focused in the plane of view and others were unfocused, as they were attached in different layers of fibers.

To better understand the distribution of cells in three-dimensions, confocal microscopic analysis was performed using a step size of 1.2821 μm. Reconstructed confocal images of three layers showed the presence of cells in every layer in 89.7 μm thickness of three layer culture (**Figure 3.6**). In a single layer culture, more cells appeared as they are distributed in a narrow thickness. To assess the distribution of cells in relation to fibers, light microscopy image on the same plane was overlayed with fluorescent images. An obtained micrograph showed that cells were surrounded by fibers and attached to the fibers, particularly in pores which were not too large relative to the size of cells. Note that **Figure 3.6H** is a 3D image which can be better visualized using a 3D-spectacle. This suggested that cells are distributed continously in three-dimensions.

Samples were also evaluated using SEM to understand distribution of cells within the fibers. These results revealed (**Figure 3.7A**) that the cells on all fibers attached to the fibers and were entangled by the fibers. Cells attached and spread throughout the matrix. In some locations, cells showed numerous lamellapodia and filapodia with anchorage points to the fibers (**Figure 3.7B**), probably via the adhesion of serum proteins to the polymeric matrix. However, in many locations individual cells could not be be identified, probably due to the presence of secreted matrix elements. Cells grew through fibers and the thickness of fibers increased. Cell clusters were observed both vertically and horizontally, covering several fibers. This suggests that cells grew due to a thin layer of electrosprayed fibers with large pore sizes.

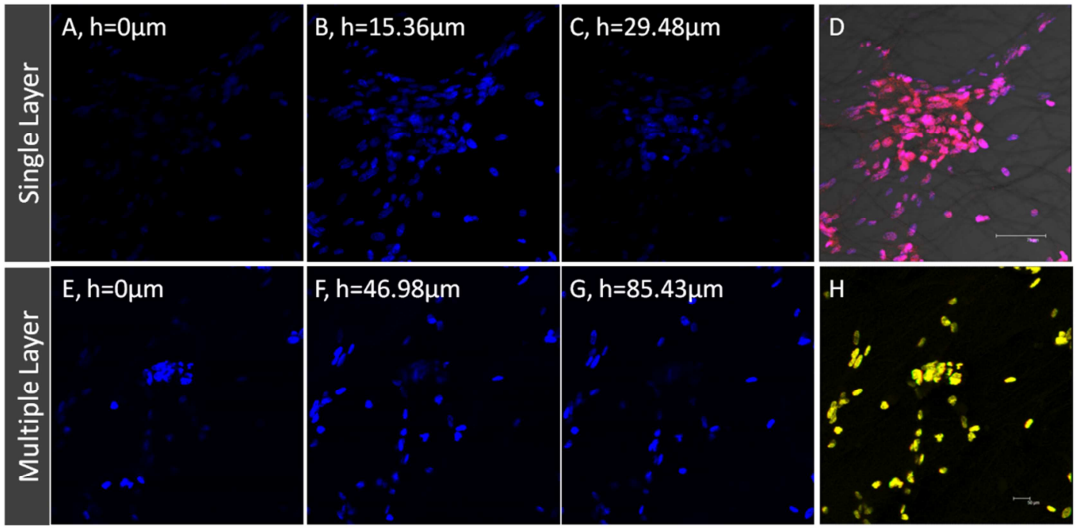

Figure 3.6. Cell distribution on different heights of the fibrous assembly at day 7. (**A-C**) The nuclei of cells on fibers at different heights in single layer. (**D**) Overlayed image of fluorescence and light signals from cells and electrosprayed fibers in the single layer at 15.36 µm. (**E-G**) The nuclei of cells on fibers at different heights in the three layers. (**E**) Compilation of images in different planes showing distribution of cells in three-layers, best seen using 3D spectacles.

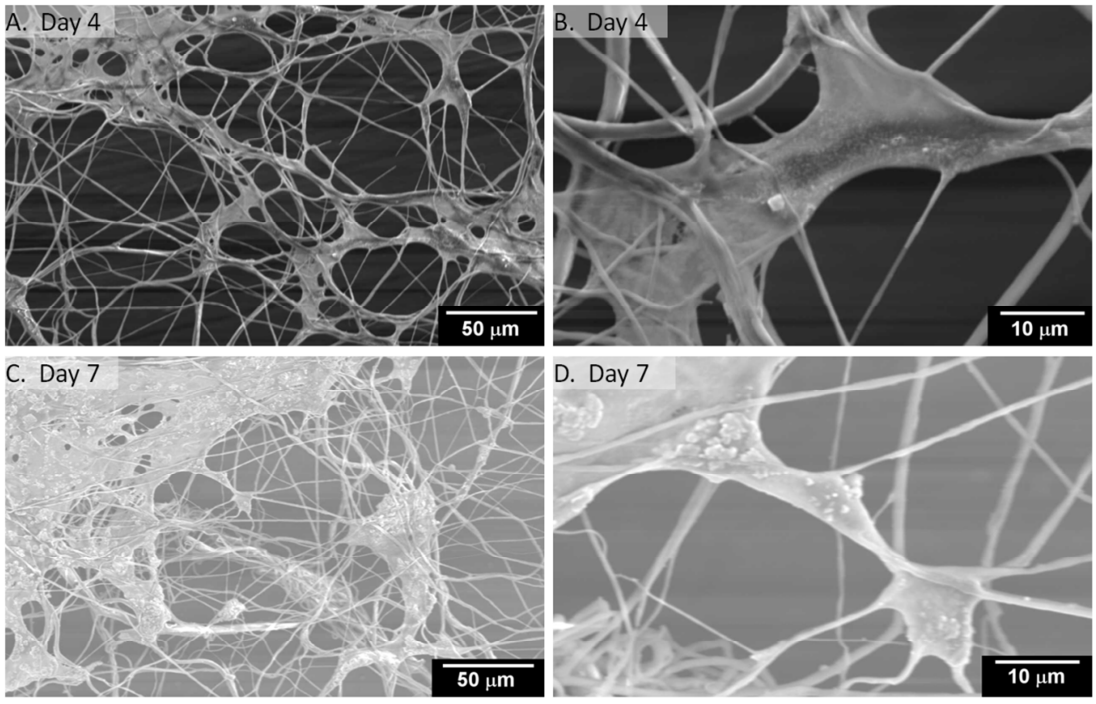

Figure 3.7. Morphology of cells in single layer of fibers by SEM.

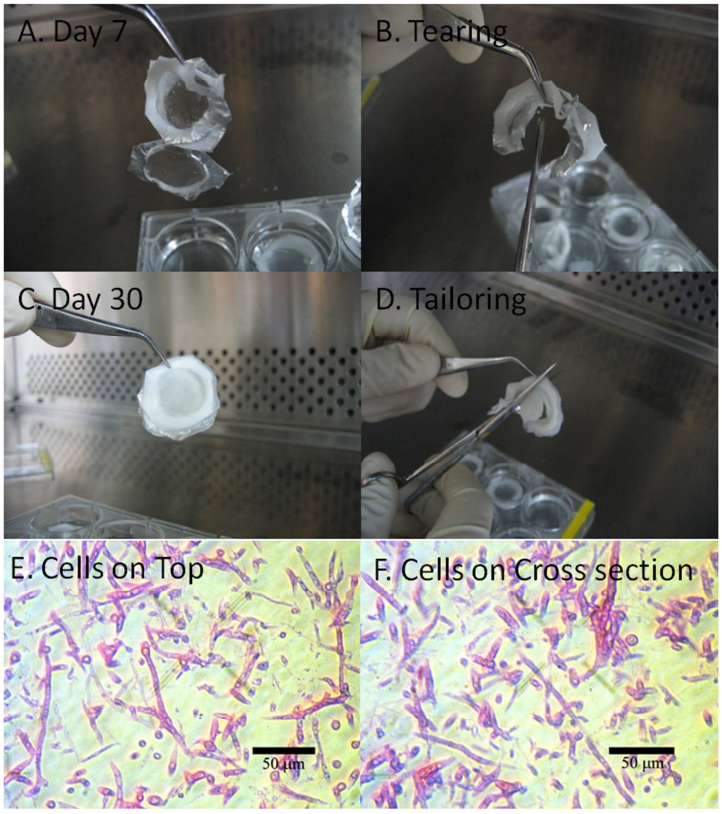

Figure 3.8. Cell glued 3D scaffolds. (**A**) Three layers of fibers after cell culture of 7 days (**B**) Collapsing three layers while cutting after cell culture for 7 days (**C**) Cell glued three layers of fibers after cell culture of 30 days (**D**) Tailoring tissue-like materials after cell culture of 30 days. (**E-F**) Cell morphology after cell culture for 30 days using top area and cross section of three layers stained with H & E for nuclei (red) and cytoplasm (dark pink).

3.3.4. Cell-glued 3D scaffold

To confirm whether three layers of fibers were attached after a 7 day cell culture, the sample was lifted by a tweezer but the bottom layer of the sample was detached from the sample (**Figure 3.8A**). Moreover, the sample disappeared while cutting with scissors because the complexity of the fibers and cells was still weak mainly due to the fragile structure of fibers (**Figure 3.8B**). When cell cultures were continued up to 30 days, three layers merged into a single structure, probably due to the regeneration of matrix elements and cell growth (**Figure 3.8C**). Moreover, the shape of the 3D scaffold was stable and tailorable without the deformation of the scaffold while and after the scaffold was cut by scissors (**Figure 3.8D**).

The samples were cut into small random pieces for further analyses by SEM and histology. The dry thickness of the 3-layered assembly was 280 μm using SEM (not shown here). Clustered cells existed on the top and side of the 3D scaffold. HFF-1 cells were distributed throughout the scaffold not only vertically but also horizontally and this distribution supports the complex structure of cells and fibers without any mechanical damage even after cutting into the small pieces for H & E staining (**Figure 3.8E** and **3.8F**). Cells grew on the surface of fibers. HFF-1s wrapped around a single fiber and elongated along the fiber. These cells attached to adjacent cells growing on another nearby fiber not only vertically but also horizontally. The cells were distributed throughout in all dimensions of the scaffold without any distinguishable layers between cells and fibers. This complex structure of fibers and cells in three layers glued three layers into one 3D scaffold after 30 days, to tailor the shape of the scaffold, and to cut into small pieces without any mechanical damage. Thus, the cells glued 3D scaffold was

fabricated using the thin layer of PCL fibers, and HFF-1 in 15 % serum added media after 30 day cell culture as a phenotype of 3D scaffold using electrosprayed fibers with large pore size.

3.4. DISCUSSION

Biodegradable scaffolds are used to support and guide the in-growth of cells and the scaffolding material eventually disappears leaving only the necessary healthy tissue in a topologically required form. This study demonstrated the possibility of i) developing very thin layers of fibers from different polymers, ii) handling them in tissue culture conditions, and iii) building multiple layers of cells and fibers. Cells attach and distribute in 3D synthetic polymer PCL. Since the technology is simple, the novel collector could be associated with existing techniques of electrospinning for a number of other biomaterials. The thin layer of electrosprayed fibers is easy to handle without mechanical damage due to the support of an aluminum frame. Even when fibers were handled for the morphology study, the polymeric structures of the fibers remained intact, suggesting their ability to endure outside stress. Without directly grabbing the fragile fibers, the aluminum foil provides a hard frame for the thin layers of the fibers to be picked up with tweezers and preventing the fibers from being destroyed.

The pore size of fibers produced with the new collector plate are larger than those produced with conventional collectors due to the decreased density of fibers. However, the diameter of fibers under the same conditions are similar and can be manipulated by controlling solution (concentration of polymer solutions, solvent) and process parameters (flow rate, needle tip, distance between tip and collector, and high voltage supply). Thus,

the larger pore size of fibers were generated while the diameter of fibers were controlled by using the collector. In other words, the innovative technique of the collector is easy to combine with the existing technology of electropraying or electrospinning.

This study opens a new window of opportunity to understand a number of cellular interactions in 3D environment, mimicking physiological conditions. For example, a single layer can be visualized in a regular light microscope and the presence of fibers creates a rough architecture similar to a physiological environment. Thus, a single layer can also be used in cell culture to study the interactions in single cells in 3D space. Traditional tissue culture conditions can be converted into 3D cultures without significant effort. Thin layers can be placed serially to develop thick 3D structures by adapting layer-by-layer assembly. One could build tissues to the required thickness layer-by-layer.

SEM images of cells cultured on fibrous scaffolds fabricated using electrospinning showed that the cells can grow and proliferate within the fibrous scaffold. The cells were growing on fibers and were intertwined with the fibers. The novel collector overcame barriers of electrosprayed and electrospun fibers. The majority of fibers made by the existing technology showed that the pore sizes between the fibers were not proper for cells to infiltrate into the pore between and among fibers. It was demonstrated that HFF-1 cells grew and proliferated when cultured onto scaffolds made of thin layers of fibers fabricated by electrospraying using a novel collector. In addition, the single layer of electrospun fibers was expanded up to three layers. Further, the layer-by-layer assembly also helps solve problems associated with the uniform seeding of cells into the porous structure, typically observed in many scaffolds synthesized by subtractive techniques such as porogen-leaching and freeze drying. Moreover, cells in the 3D

scaffold grew and became distributed throughout the sample, not only horizontally but also vertically, suggesting that diffusion of media was sufficient for cells to functionalize in the three layers. Thus, two core techniques of a thin layer of electrosprayed fibers with large pore sizes and layer-by-layer assembly, are a synergistic effect on overcoming current barriers such as thicker tissue regeneration.

In this study, PCL was used to demonstrate the concept of cell colonization on thin layers, which does not have a cell binding domain. Much of the cell adhesion is due to the interaction with the serum proteins, as cells were cultured in 15% serum containing media. To better understand the cellular interactions with fibers, changes in adsorption of serum protein needs to be measured [13]. The cell glued 3D scaffolds demonstrated that cells in three layers were functional and well distributed in the sample. However, a thicker 3D scaffold study using four or more layers needs to clarify the limitation of media diffusion. When the limitation becomes clear, a new reactor design needs to allow cells to functionalize in thicker 3D scaffolds. Not only that, analysis of cellular activity needs to be extended to include other types and functionality; assembly and maturation of matrix elements in tissue regeneration plays a significant role in determining the biomechanics and the quality of the regenerated tissue. In addition, evaluating alteration in cellular activity after immobilizing proteins containing cell adhesion domains could provide more information on the importance of fiber thickness and roughness. Recent advances in tissue regeneration, 3D matrix physical properties such as hydrophilicity, stiffness [14], porosity [15], pore size and void fraction can affect cell morphology, attachment and function. Also, cellular activity is influenced by scaffold stiffness [16-18]. Cells show reduced spreading and disassembly of actin even when soluble adhesive

ligands are present in weak gels [19-20]. Maximum tractional force generated by a cell could be as much as 10-15 % of substrate modulus [19]. Further, the rigidity of the scaffolds may affect the formation of ECM which can affect cellular activity [21]. Bulk tensile properties were evaluated. However, to understand the influence of scaffold stiffness, properties of individual fibers need to be analyzed using techniques such as nanoindentation. In addition, the influence of fiber curvature on cell colonization also needs to be analyzed.

This study focused on using thin layers of electrosprayed fibers in tissue regeneration. This technique could also be used in numerous other applications such as chemical and biochemical protection in defense and security, solar cells and fuel cells in sustainability, membranes and filters in environmental engineering and biotechnology [22].

3.5. CONCLUSION

In summary, the novel collector plate allows the formation of thin layers of electrosprayed fibers with large pore sizes. The thin layer of electrosprayed fibers can be easily handled without mechanical damage because of the supporting structure. This collector is also versatile enough to be associated with existing techniques of electrospinning to manipulate mechanical and biological properties of novel fibers. This methodology overcame the major barrier of the electrospinning technique and its application for tissue regeneration. The novel fibers allow a single cell study on single fibers in a single layer, and in multilayer by using a layer-by-layer technique. Furthermore, Cell glued 3D scaffold of the thin layer of electrosprayed fibers with large

pore sizes will expand its implications on other cells, fibers, tissues and organs.

3.6. REFERENCES

1. Sill, T.J. and H.A. von Recum, *Electrospinning: Applications in drug delivery and tissue engineering.* Biomaterials, 2008. **29**(13): p. 1989-2006.
2. Nisbet, D.R., et al., *Review Paper: A Review of the Cellular Response on Electrospun Nanofibers for Tissue Engineering.* J Biomater Appl, 2008: p. 0885328208099086.
3. *Fibrous 3-dimensional scaffold via electrospinning for tissue regeneration and method for preparing the same.* USPTO, 2008. 0233162.
4. Stankus, J.J., et al., *Fabrication of cell microintegrated blood vessel constructs through electrohydrodynamic atomization.* Biomaterials, 2007. **28**(17): p. 2738-2746.
5. Mondalek, F.G., et al., *The incorporation of poly(lactic-co-glycolic) acid nanoparticles into porcine small intestinal submucosa biomaterials.* Biomaterials, 2008. **29**(9): p. 1159-66.
6. Sarasam, A. and S.V. Madihally, *Characterization of chitosan-polycaprolactone blends for tissue engineering applications.* Biomaterials, 2005. **26**(27): p. 5500-8.
7. Pok, S.W., K.N. Wallace, and S.V. Madihally, *In vitro characterization of polycaprolactone matrices generated in aqueous media.* Acta Biomater, 2010. **6**(3): p. 1061-8.
8. Madibally, S.V., et al., *Influence of insulin therapy on burn wound healing in rats.* J Surg Res, 2003. **109**(2): p. 92-100.

9. Gupta, P. and G.L. Wilkes, *Some investigations on the fiber formation by utilizing a side-by-side bicomponent electrospinning approach.* Polymer, 2003. **44**(20): p. 6353-6359.

10. Hellmann, C., et al., *High Precision Deposition Electrospinning of nanofibers and nanofiber nonwovens.* Polymer, 2009. **50**(5): p. 1197-1205.

11. Kidoaki, S., I.K. Kwon, and T. Matsuda, *Mesoscopic spatial designs of nano- and microfiber meshes for tissue-engineering matrix and scaffold based on newly devised multilayering and mixing electrospinning techniques.* Biomaterials, 2005. **26**(1): p. 37-46.

12. Varesano, A., R.A. Carletto, and G. Mazzuchetti, *Experimental investigations on the multi-jet electrospinning process.* Journal of Materials Processing Technology, 2009. **209**(11): p. 5178-5185.

13. Tillman, J., A. Ullm, and S.V. Madihally, *Three-dimensional cell colonization in a sulfate rich environment.* Biomaterials, 2006. **27**(32): p. 5618-26.

14. Balgude, A.P., et al., *Agarose gel stiffness determines rate of DRG neurite extension in 3D cultures.* Biomaterials, 2001. **22**(10): p. 1077-84.

15. Dar, A., et al., *Optimization of cardiac cell seeding and distribution in 3D porous alginate scaffolds.* Biotechnol Bioeng, 2002. **80**(3): p. 305-12.

16. Zaleskas, J.M., et al., *Growth factor regulation of smooth muscle actin expression and contraction of human articular chondrocytes and meniscal cells in a collagen-GAG matrix.* Exp Cell Res, 2001. **270**(1): p. 21-31.

17. Lee, C.R., A.J. Grodzinsky, and M. Spector, *The effects of cross-linking of collagen-glycosaminoglycan scaffolds on compressive stiffness, chondrocyte-*

mediated contraction, proliferation and biosynthesis. Biomaterials, 2001. **22**(23): p. 3145-54.

18. Sieminski, A.L., R.P. Hebbel, and K.J. Gooch, *The relative magnitudes of endothelial force generation and matrix stiffness modulate capillary morphogenesis in vitro.* Exp Cell Res, 2004. **297**(2): p. 574-84.
19. Lo, C.M., et al., *Cell movement is guided by the rigidity of the substrate.* Biophys J, 2000. **79**(1): p. 144-52.
20. Pelham, R.J., Jr. and Y. Wang, *Cell locomotion and focal adhesions are regulated by substrate flexibility.* Proc Natl Acad Sci U S A, 1997. **94**(25): p. 13661-5.
21. Wozniak, M.A., et al., *Focal adhesion regulation of cell behavior.* Biochim Biophys Acta, 2004. **1692**(2-3): p. 103-19.
22. Ramakrishna, S., et al., *Electrospun nanofibers: solving global issues.* Materials Today, 2006. **9**(3): p. 40-50.

CHAPTER IV

REGULATING PORE SIZE IN NANOFIBROUS SCAFFOLDS:

EFFECT ON CELLULAR SHAPE

4.1. INTRODUCTION

Cell-matrix interactions are essential to many biological phenomena in medical science and engineering. For example, the medical device-tissue response affects the performance of implantable devices. Also, cell-matrix interactions are important for design of scaffold in tissue engineering [1-6]. The cell response to various topographical features such as grooves, ridges, stops, pores, wells and nodes in micro- or nanoscale have been studied in various cells such as fibroblasts, neuronal cells, macrophages, epithelial cells, endothelial cells, smooth muscle cells and stem cells [7]. Cellular responses to these topographies vary from cell attachment and migration to production of new tissue and differentiation. These cell-substrate interactions have been studied in micron range but the recent researches have reported that mammalian cells do respond to nanoscale features [8]. However, *in vitro* single cell responses to 3D nanofiber mimicking *in vivo* extracellular environment has not yet been understood due to the technological limitations of forming 3D structures [9-10].

Electrospinning has recently emerged as a technique for tissue regeneration due to the possibility of fabricating nano and microfibers mimicking *in vivo* condition. However, reduced pore size of electrosprayed fibers restricts mammalian cells from infiltrating into the sub-layers and accessing the 3D space [11-17]. To overcome this barrier, I developed a novel electrospraying process for use in tissue regeneration, as described in the previous chapter [18]. New technology allowed formation of nanofibers with pore sizes suitable for mammalian cells to infiltrate the 3D scaffold. Thirty day cell culture study confirmed that human fibroblasts in serum containing media on a synthetic biomaterial, polycaprolactone (PCL) colonized multiple layers of fibers, merging into one stable 3D scaffold [18]. However, for understanding the cellular interactions on single fibers, one has to mimic *in vivo* extracellular environment. For this purpose, forming fibers with controllable pore size and with substrates containing cell binding is necessary. Further, cells have to be cultured in a medium that does not contain animal derived serum [19]. Due to biodegradability, non-toxicity, and biocompatibility of PCL under the physiological conditions, PCL has been applied to fabrication of many medical devices [20-21], or scaffolds for tissue regeneration of *in vivo* [22] and *in vitro* [22-23] cell culture using serum added media mainly because of the lack of cell binding domain such as RGD in PCL scaffold. To improve physiological properties of scaffolds, natural polymers such as collagen [24], or gelatin (denatured collagen) [25] are blended. Cross linking natural polymers to synthetic polymers using bifunctional compounds such as glutaraldehyde has also been used to address the instability issues. Since cross linkers cause toxicity, common solvents such as Hexafluoro-2-propanol (HFP) have been used to dissolve PCL and gelatin together. Fibers have been formed using conventional

electrospinning without any cross linkage [26] and then fibers have been analyzed by Fourier transform infrared spectroscopy (FTIR) [26] and differential scanning calorimetry (DSC) [27]. However, these conventional analyses were similar to PCL and gelatin in two dimensional samples, without showing any detail in single fibers.

In this study, I address the influence of the shape change of the void in the new collector plate and the fabrication of innovative electrosprayed fibers with controllable pore size by manipulating the diameter of the void in the new collector plate and the deposit volume of polymer solution of PCL and gelatin with the new collector plate. Distribution and stability of gelatin on single PCL/gelatin fibers was studied in two-week incubation under physiological condition study using a molecular probe or carboxyfluorescein diacetate-succinimidyl ester (CFDA-SE). Interaction of cells on single electrosprayed fibers was studied up to 24 hr. These results show that the cell shape is determined by where the cells attach on the 3D nanofibers.

4.2. MATERIALS AND METHOD

4.2.1. Materials

Polycaprolactone (PCL, Mn=80,000), gelatin type A, and hexafluoro-2-propanol (HFP) were purchased from Sigma-Aldrich (St. Louis, MO). For cell culture study, Human foreskin fibroblast (HFF-1) was obtained from American Type Culture Collection (ATCC, Walkersville, MD). Fibroblast growth media (FGM), L-Glutamine, Insulin, and human fibroblast growth Factor were obtained from Lonza (Walkersville, MD). TrypLE Express was purchased from Gibco (Grand Island, NY) and CFDA-SE was obtained from Invitrogen (Carlsbad, CA).

4.2.2. Fabrication of electrosprayed fiber with different collector plate

Electrospraying apparatus consisted of a syringe pump (74900 series, Cole-Parmer Instrument Company, Vernon Hills, IL), BD 10 mL syringe (Luer-Lok Tip; Becton Dickinson and Company, Franklin Lakes, NJ), needle tip, high voltage power supply (ES30P-5W/DAM, Gamma high Voltage Research, Ormond Beach, FL), earth grounding, and different shape and size of collector plate. The condition of fabrication was different for different studies (**Table 4.1**).

4.2.3. Shape and size effect of the void in the collector plate

For shape effect study, 22 w/v % PCL was dissolved in a mixture solvent of chloroform and methanol (mixing ratio 9 to 1). Flow rate, needle size, high voltage supply and distance between the needle tip and the collector were 10 mL/hr, 20 G, 10 kV, and 9 cm with the novel collector plate. Shapes of the void in the collector plate were circle (diameter, 1.5 cm) and triangle (the length of each side, 1.5 cm) in a wooden frame (3 cm × 10 cm × 2 cm), and rectangle (the size of rectangle, 5 cm x 1 cm) in a wooden frame (3.5 cm ×10 cm × 2 cm) and the depth of all the voids was 1.2 cm.

The polymer solution with concentration of 10 wt/v % was prepared by dissolving PCL in HFP and stirred for 24 hr at room temperature. Flow rate, needle size, high voltage supply and distance between the needle tip and the collector were 2 μL/hr, 24 G, 12 kV, and 9 cm with the novel collector plate (diameter, 0.9, 1.4, or 1.9 cm and depth 1.2 cm) in a wooden frame (3 cm × 10 cm × 2 cm) wrapped with aluminum foil to the influence of the void size.

Table 4.1. Fabrication condition of PCL fiber

Modification of process	Polymer	Concentration (w/v %)	Solvent	Flow rate	Needle	High voltage	Distance
Effect of different shape of the void in the new collector plate	PCL	22 %	CF/MeOH (ratio 9:1)	10 ml/hr	20 G	10 kV	9 cm
Effect of different size of void in the new collector plate	PCL	10 %	HFP	2 µL/hr	24 G	12 kV	9 cm
Effect of the deposit volume of the polymer solution	PCL/gelatin (ratio 7:3)	10 %	HFP	1 µL/hr	24 G	13 kV	8 cm

4.2.4. Deposit volume effect of electrosprayed PCL/gelatin fibers

The polymer solution with concentration of 10 wt/v % was prepared by dissolving PCL and gelatin with a weight ratio of 70:30 in HFP and stirred for 24 hr at room temperature. The solution was electrosprayed from a 10 mL syringe with a needle gauge of 24 G and mass flow rate of 1 μL/hr. A high voltage of 13 kV was applied to the needle tip using high voltage power supply when solution was ejected using a syringe pump. The distance between the needle tip and collector plate was 8 cm. For the collection of conventional fibers, a conventional collector plate (3 cm × 10 cm × 2 cm) wrapped with aluminum foil was used, whereas, the novel collector, with four holes (diameter, 1.9 cm and depth 1.2 cm) a wooden frame (3 cm × 10 cm × 2 cm) wrapped with aluminum foil, was used for collecting novel fibers or electrosprayed fibers with controllable large pore sizes. The deposit volumes were 0.3, 0.6 or 0.9 μL for both conventional and novel fibers.

4.2.5. Microstructure characterization

Samples were analyzed using JEOL 6360 (Jeol USA Inc., Peabody, MA) at an accelerated voltage of 9 to 30 kV similar to our previous publications [28]. In brief, samples were attached to an aluminum stub using a conductive graphite glue (Ted Pella Inc., Redding, CA) and sputter-coated with gold for 40 seconds before SEM analysis. Using the digital micrographs, fiber diameters, pore sizes and shape factors of pores ($4\pi \times \text{area}/\text{perimeter}^2$) were quantified using Sigma Scan Pro (SPSS Science, Chicago, IL). More than 50 points of fibers and pores were analyzed for each condition.

4.2.6. Gelatin distribution test on single fibers using CFDA-SE

Two electrosprayed fibers made of 10 wt/v % PCL/gelatin 70:30 or 10 wt/v % PCL were fabricated using HFP after 24 hr dissolving. Both fibers were soaked into Krebs Henseleit Buffer solution (pH 7.4). CFDA-SE was added into the solution and incubated for 30 min at 37°C. The samples were analyzed using inverted microscope (Nikon TE2000, Melville, NY).

4.2.7. Stability test of PCL/gelatin fiber

PCL/gelatin electrosprayed fibers on aluminum frame were fabricated using 10% PCL/gelatin 70:30 solution dissolved for 1 day. The fibers were placed in 6-well plate containing 5 ml of Krebs Henseleit buffer solution (pH 7.4) in each well and were incubated in 5 % CO_2 incubator at 37 °C for 3 and 14 days. After each degradation time, the samples were stained with CFDA-SE at 37 °C for 30 min and observed using an inverted light and fluorescent microscope.

4.2.8. Cell culture study

New fibers on aluminum frame (deposit volume 0.6 μL) were used for cell adhesion test. The samples were exposed to UV radiation for 2 hr and washed with PBS for 20 min. Each sample was placed onto 6 well plates treated by albumin. Before cell seeding, HFF-1 cells were stained using CFDA-SE and 30,000 cells in 100 μL were seeded onto 5 points of each samples. The cells on the samples were cultured in 5 % CO_2 incubator at 37 °C using 2ml FGM media supplemented with L-glutamine, insulin and human fibroblast growth factor for 3, 8, and 24 hr. Cells cultured on tissue culture plastic

surface for an extended period of time were used as a control while assessing surface area and shape factor.

4.2.9. Cell morphology study

The samples were fixed using 3.7 % formaldehyde and then single cells were first observed under an inverted light and fluorescent microscope (Nikon TE2000, Melville, NY). Digital micrographs were collected using CCD camera. The shape and area of cells on the samples were quantified using Sigma Scan Pro. More than 50 cells were analyzed. Also, the images of single cells were collected using a confocal microscope (Leica TCS SP II, Heidelberg, Germany). In addition, the samples were dried using ethanol, sputtered using gold, and analyzed using SEM.

4.2.10. Statistical analysis

Statistical analysis was carried out using single-factor analysis of variance (ANOVA). A value of $p \leq 0.05$ was considered statistically significant.

4.3. RESULTS

4.3.1. Effect of shape of the void in the collector plate

It is well understood that pore size within the scaffold influences cellular activity. The pore diameter must be controllable for cells to infiltrate into the pore and attach to the fibers in 3D scaffold. Also, scaffold pore size and shape are important to the distribution of ligands presented to cells [29]. To understand how pore size is affected, I tested collector plates with three different shapes of the void. Analysis of distribution of

fibers showed (**Figure 4.1**) that the pattern of the distribution depends on the shape of the void region. For the circular void in the collector plate, the fibers were randomly deposited throughout the entire void of the collector plate (**Figure 4.1A, 4.1D,** and **4.1G**). For the triangular void, the fibers aligned perpendicular to the bisector of the vertices at the edge of the vertices. However, the fibers at the middle of the void were randomly deposited unlike the fiber at the vertices (**Figure 4.1B, 4.1E,** and **4.1H**). For the rectangular void, the fibers aligned from one short side to the other side perpendicular to the long sides of the rectangle in large scale. However, the fibers were randomly deposited in the entire void when 22 w/v% PCL solution in the mixture of chloroform and methanol (9:1) was used (**Figure 4**.**1C**, **4.1F**, and **4.1I**). I then evaluated the patterns of the fibers in the aluminum frame (electrodes) of the new fibers. Unlike the distribution in the voids, the density of the fibers was high in the aluminum frame and they were deposited randomly on the aluminum frame (**Figure 4.1D**, **4.1E**, and **4.1F**).

I also tested the pattern of PCL nanofibers under the different conditions by manipulating process parameters (voltage, distance between the needle tip and the new collector plates, and injection rate). Furthermore, I used different polymers such as different molecular weight of PCL, natural polymer (gelatin), and the mixture of PCL and gelatin. The fibers on the voids and on the aluminum frame of the new collector plate were randomly oriented in the same pattern, suggesting that the fiber orientation was independent of the diameter of the circular void and the polymer composition. Likewise, the size and the morphology of the single fibers was not affected by the geometrical patterns of the voids in the collector plate. Solution and process parameters of electrospinning mainly govern the size of the fibers.

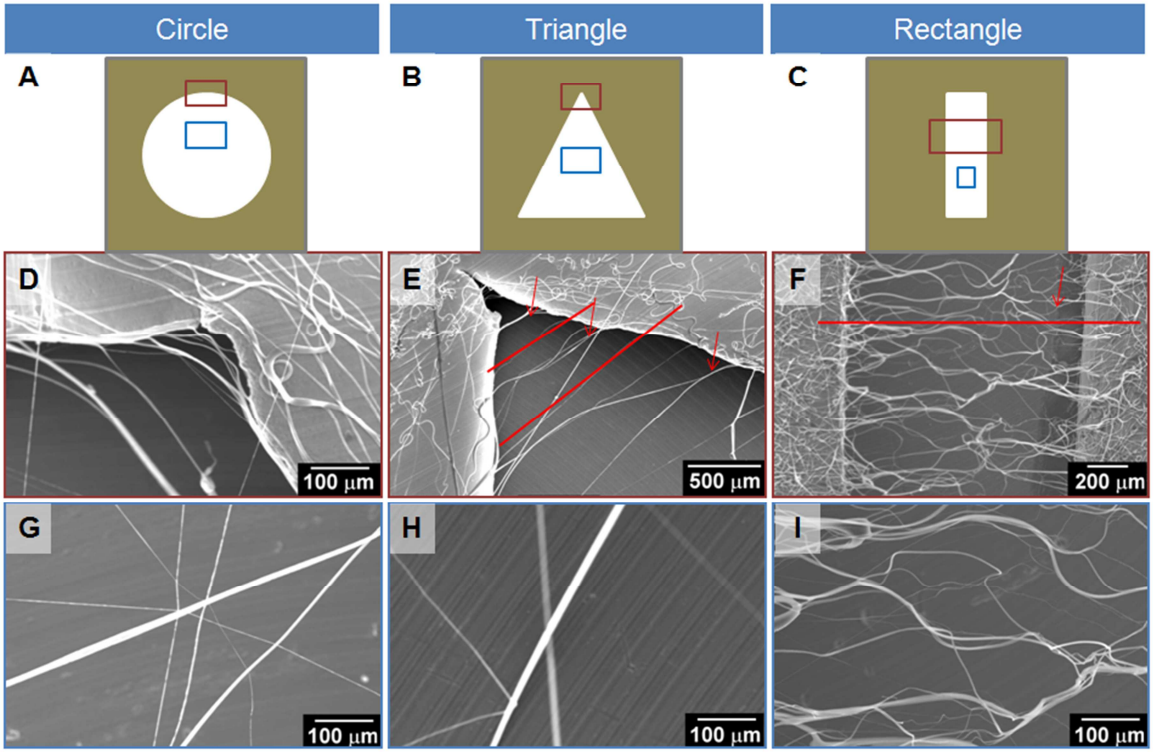

Figure 4.1. Schematics of the different shapes of the void in the collector plates and polymeric structure of electrosprayed fibers. The polymeric structure of the fibers with (**A**) circular, (**B**) triangular and (**C**) rectangular shape of the void in the new collector plate. (**D-I**) scanning electron micrographs of electrosprayed nanofibers made of PCL in HFP with different shapes of the vold.

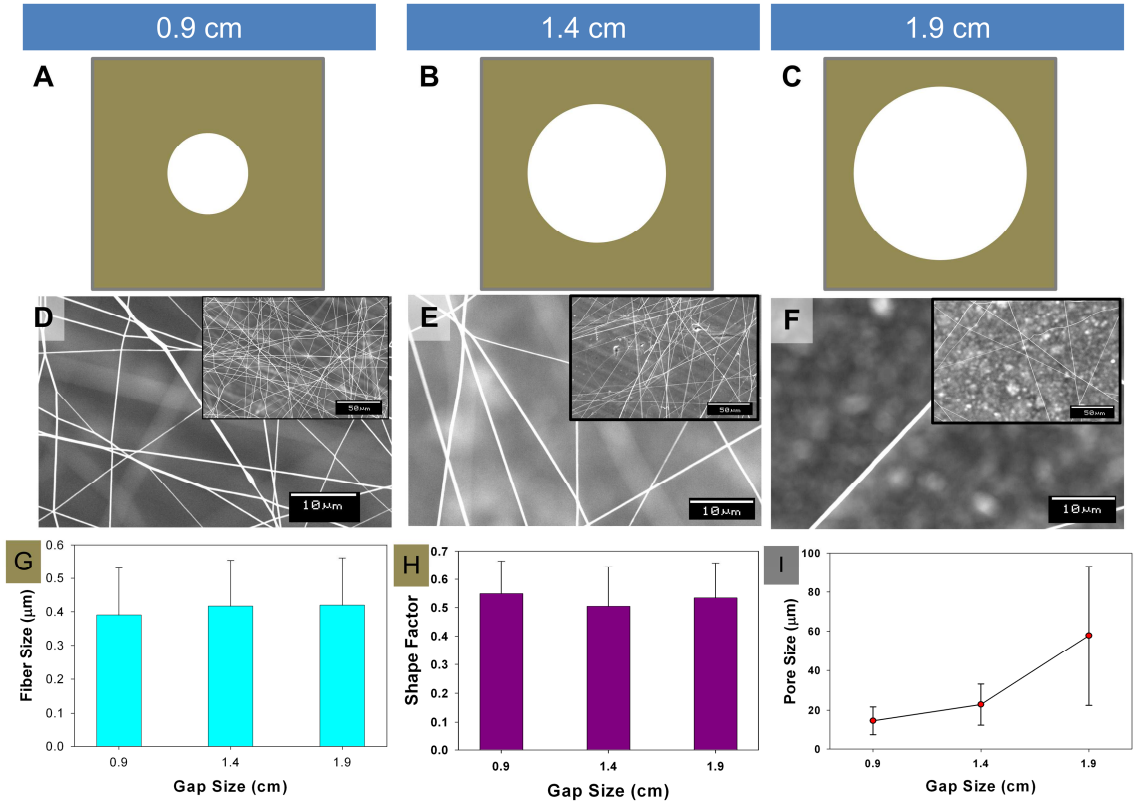

Figure 4.2. Schematics of the void size and polymeric structure of electrosprayed fibers. (**A-C**) The Schematic of the void size in the new collector plates and (**D-F**) scanning electron micrographs of electrosprayed nanofibers made of PCL in HFP increasing the void size of the collector plate from 0.9 via 1.4 to 1.9 cm. Inset in (**D-F**) are micrographs with low magnification showing pore size distribution. **(G)** Fiber diameters. **(H)** Shape factor. **(I)** Pore size. The error bars correspond to the standard deviation (n = 50).

4.3.2. Effect of different sizes of the void in the collector plate.

I tested the effect of the void sizes in collector plate on the pore size of formed structures (**Figure 4.2**). When the void size was increased from 0.9 cm via 1.4 cm to 1.9 cm (**Figure 4.2A-4.2C**), the fiber diameter and shape factors of the pores in structures (**Figure 4.2D-4.2F**) did not change, however, the pore sizes increased (**Figure 4.2D-4.2F**). To better understand the effect of void size on pore size, micrographs were quantified for fiber diameters, shape factors, and pore sizes of the fibers, and standard deviations **Figure 4.2G-4.2I**. The fiber diameters made of PCL in HFP were estimated to about 400 nm and the shape factors of the pores in structures were about 0.50 when the void size increased from 0.9 via 1.4 to 1.9 cm. However, the average pore sizes of the fibers were increased from 14.71, 22.83, and 57.77 μm, respectively while increasing the void size from 0.9, via 1.4 and 1.9 cm, respectively; these pore sizes in the structures were statistically significant. Also, the pore size distribution increased when the void size increased since fewer layers of fibers deposited in the void of the new collector plate.

4.3.3. Effect of deposition volume on pore size.

The pore size is also controllable by manipulating the deposit volume of the polymer solution. This process is simple since the pore sizes are controllable in the same size and shape of the void of the collector plates, reducing the effort to prepare different collector plates with different sizes and shapes of voids. Further, it is convenient to perform cell culture under the same surface area i.e., with the same void size but with different pore size. The fibers generated by the conventional collector plate without any void (**Figure 4.3**) showed multiple layers of fibers similar to other reports [11]. Even as

increasing deposit volume from 0.3 via 0.6 to 0.9 μL, physical properties (shape factors, fiber diameters, and pore sizes of fibers) of the conventional fibers appear similar to each other (**Figure 4.3D-4.3E**). The diameter of fibers and shape factor of pores fabricated by the new collector plate appear similar to those of conventional ones. However, the pore sizes of the structures decreased with increase in deposit volume of the PCL/gelatin solution (**Figure 4.3A-4.3C**). To better understand the effect, micrographs (**Figure 4.3A** to **4.3F**) were assessed for fiber diameters, pore shape factors, pore size distributions in the structures (**Figure 4.3G-4.3I**). For both conventional and new collector plates, the average fiber diameters were 700 nm and the shape factors of the pores were 0.55. Also, the pore sizes of all structures formed using conventional collector plates were similar (~5 μm). However, the pore sizes of structures formed using the collector plates were significantly different when the deposit volumes were changed. As the deposit volume increased from 0.3 via 0.6 to 0.9 μL, the average pore sizes decreased from 339, 129, and 51μm, respectively; these pore sizes of the new fibers were statistically significant. Also, the distribution of the pore sizes reduced with the increase in deposit volumes. Since multiple layers of fibers deposited among the void of the new collector plate when the deposit volumes were increased, the pore sizes decreased. Required optimum pore size for many cells in 3D scaffold is reported to be between 50 μm and 150 μm [30-33]. Thus, the structures with 129 μm average pore size (**Figure 4.3B)** were used for further study of the gelatin distribution, the fiber stability and single cell morphology.

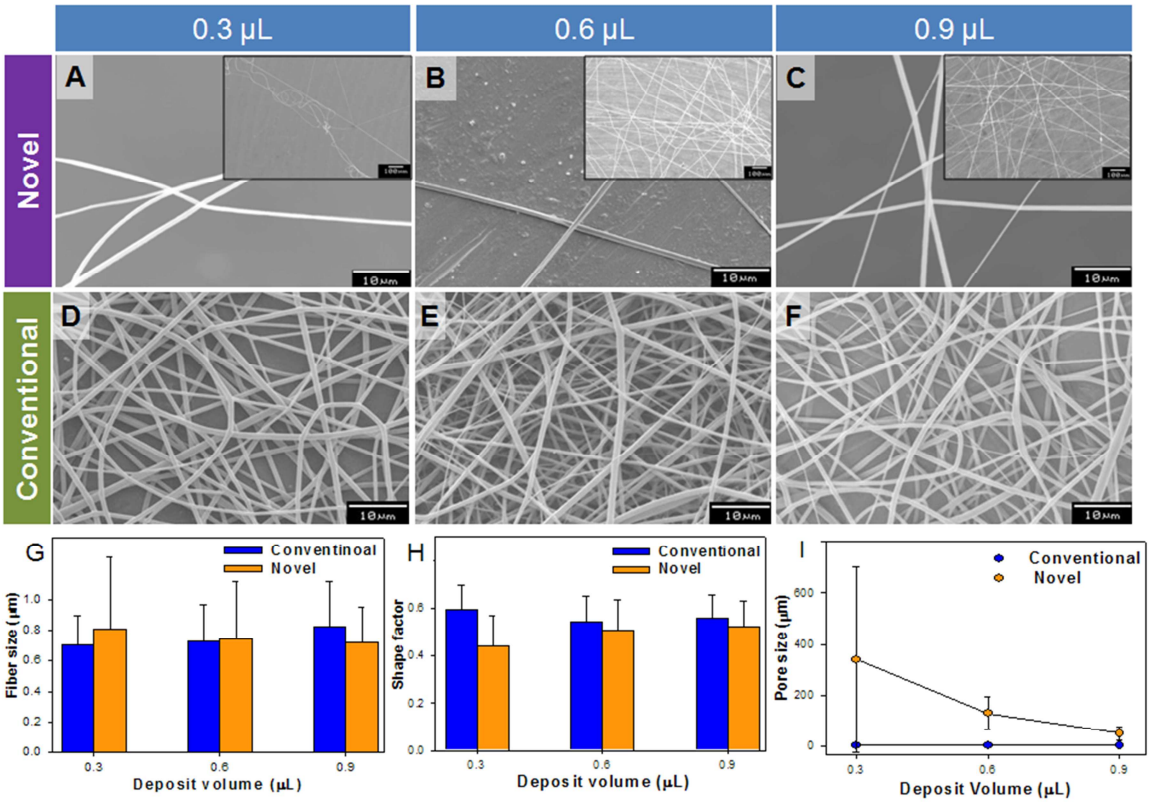

Figure 4.3. Polymeric structure of electrosprayed fibers with different deposit volume. Scanning electron micrographs of (**A-C**) novel and (**D-F**) conventional electrosprayed nanofibers made of PCL/gelatin 70:30 increasing the deposit volume of the PCL/gelatin solution from 0.3 via 0.6 to 0.9 µL. Inset in (**A-C**) are micrographs with low magnification showing pore size distribution. **(G)** Fiber diameters. **(H)** Shape factor. **(I)** Pore size. The error bars correspond to the standard deviation (n = 50).

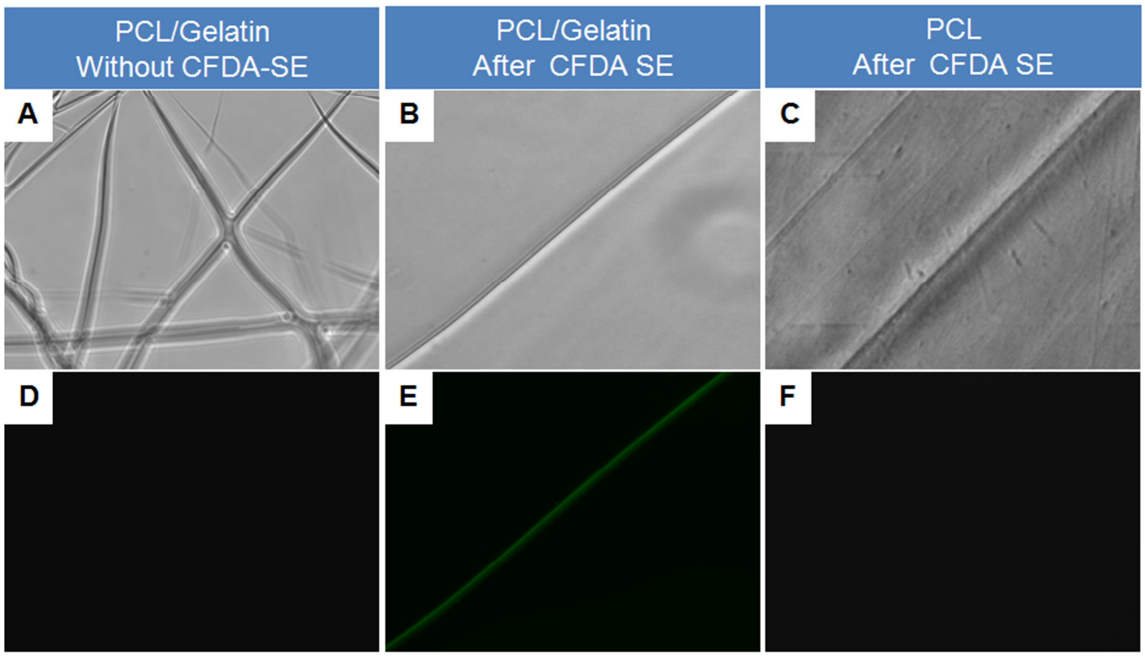

Figure 4.4. Distribution of gelatin in the fiber. Novel fibers made of PCL/gelatin 70:30 (**A** and **D**) before and (**B** and **E**) after CFDA-SE staining. (**C** and **F**) Novel fibers made of PCL after CFDA-SE staining. The images (**Figure A-C**, and **Figure D-F**) were collected by light and fluorescent microscopes, respectively.

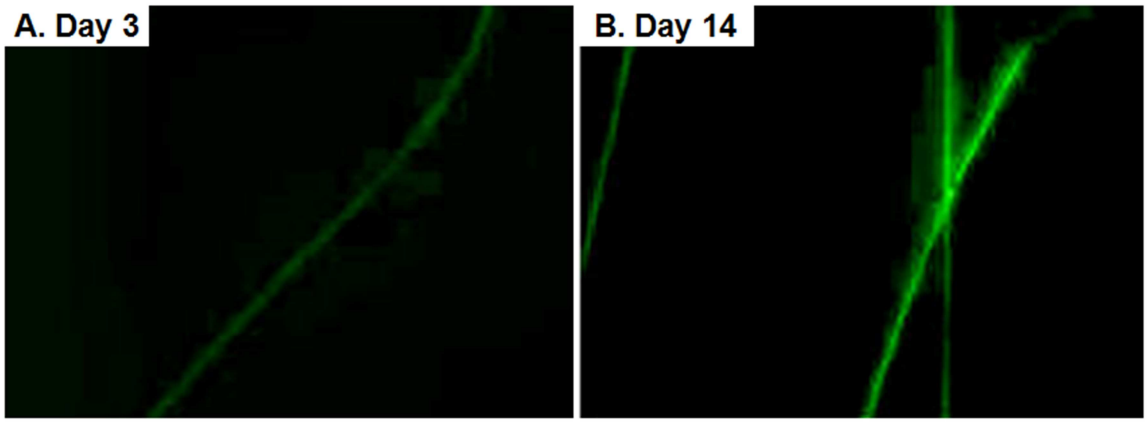

Figure 4.5. **Stability of gelatin in the nanofibers.** The images of PCL/gelatin 70:30 fibers after incubation under the physiological conditions after staining CFDA at day (**A**) 3 and (**B**) 14.

4.3.4. Gelatin distribution on PCL/gelatin fibers after CFDA-SE staining.

Fibers have been formed using conventional electrospinning without any cross linkage and presence of both polymers have been confirmed by Fourier Transform Infrared Spectroscopy (FTIR) [26] and differential scanning calorimetry (DSC) [27]. However, conventional analyses methods such as FTIR and thermograms do not show the local distribution of gelatin within nanofibers [26-27]. To understand *in situ* distribution of gelatin in single nanofibers, it was stained with a fluorescent marker, CFDA-SE; the amino groups in gelatin covalently bond with activated CFDA in CFDA-SE. Light microscope images show the fibers made of PCL/gelatin before or after CFDA-SE staining (**Figure 4.4A** and **4.4B**) and the fiber made of PCL after CFDA-SE staining (**Figure 4.4C**). All the fibers were observable under a light microscope. However, only the fibers made of PCL/gelatin were detected in fluorescent microscope after CFDA-SE staining (**Figure 4.4E**). The green fiber architecture exactly matched the grey fiber of PCL/gelatin fibers, suggesting that gelatin was uniformly distributed in single fibers made of PCL/gelatin (**Figure 4.4B** and **4.4E**). However, the PCL/gelatin fibers before CFDA-SE staining were not observed under fluorescent microscope due to the absence of CFDA-SE staining (**Figure 4.4D**). Also, PCL fibers were not detected even after CFDA-SE staining because PCL lacks amino groups in the structure (**Figure 4.4F**).

4.3.5. Stability of PCL/gelatin fiber containing electrosprayed fibers.

Understanding the stability of the blended PCL-gelatin fibers in physiological conditions is critical for further use in single cell study and tissue regeneration.

Polymeric blends could be unstable under physiological conditions in which protein may dissolve prematurely to form gel or polypeptide may degrade resulting in loss of biological activity. The fibers were kept in Krebs Henseleit buffer solution (pH 7.4) in a CO_2 incubator at 37°C for 2 weeks. After two weeks of incubation, the PCL/gelatin fibers were stable and showed the presence of both components. Compared to **Figure 4.4E**, the green fibers at day 3 (**Figure 4.5A)** and 14 (**Figure 4.5B)** were moderately dispersed, suggesting some preferential swelling of gelatin in PCL/gelatin fibers. However, the fibers on the aluminum frame were still stable. Entire set could be handled without any mechanical damage (**Figure 4.5A** and **Figure 4.5B**).

4.3.6. Cell - electrosprayed nanofiber interaction.

The PCL/gelatin fiber with average pore size (129 μm) was used for *in vitro* cell culture study in serum free media. The nanofibers made of PCL/gelatin 70:30 after 1 day dissolving in HFP were utilized as they met necessary requirements (described above) for cell behavior study. The cell behavior was studied for up to 24 hr, mainly to avoid indirect effects due to *de novo* deposited matrix elements. The cell morphology using inverted light and fluorescent microscope on single fiber after 3, 8 and 24 hr of cell seeding in serum free media showed that the cell shapes on fibers depend on cell location, unlike unique spindle shape on tissue culture plastic surface. Since intracellular CFDA-SE fluorescence was detectable in these cells suggests they are viable. SEM images and confocal microscopy images showed the different single cell morphologies dependent on the distribution of fibers. When the cell attached on the single fiber, the shape of cell appeared elliptical (**Figure 4.6A**, **4.6D**, and **4.6G**), with cells hugging the fiber all

around. Even though the cell size was at least 30 times bigger than that of the fiber size, single cell attached to the single nanofiber and hugged around the 3D nanofiber; the diameter of a single cell was more than 20 μm when it was suspended in media but the diameter of single fiber was about 700 nm. The cell shape was triangular when the cell attached nearby the intersection of two fibers (**Figure 4.6B**, **4.6E**, and **4.6H**). Cells attached from corners of the fiber intersection to among two fibers were triangular. Also, the cell shape was quadrangular when the cell attached on the intersection of two single fibers (**Figure 4.6C**, **4.6F**, and **4.6I**). The single cell on the intersection elongated out toward the four directions of the two single fibers.

Using the micrographs, cell shapes and spread were quantified. The cell morphology did not change significantly when tested after 24 hr cell culture. Thus, *in vitro* single cell attachment on 3D nanofibers is dependent on the configuration of fibers, not the period of *in vitro* cell culture within 24 hr. Compared to the shape factor (~0.25) and cell area (~5000 μm^2) on tissue culture plates (TCP), the cell area on the 3D electrosprayed fibers were similar. On the other hand, the cell shapes on the 3D scaffold were broad ranging from 0.2 to 0.8. These changes in shape were primarily due to the 3D configuration of fibers where cells attached. To understand any correlation between shape factor changes to cell surface area, shape factor was divided into three groups after 3 hr incubation: i) <0.4, ii) 0.4- 0.6 and iii) >0.6 (**Figure 4.6J**). Cell surface areas corresponding to those three groups were plotted and there was no correlation between the shape factor changes to the cell surface area (**Figure 4.6K**).

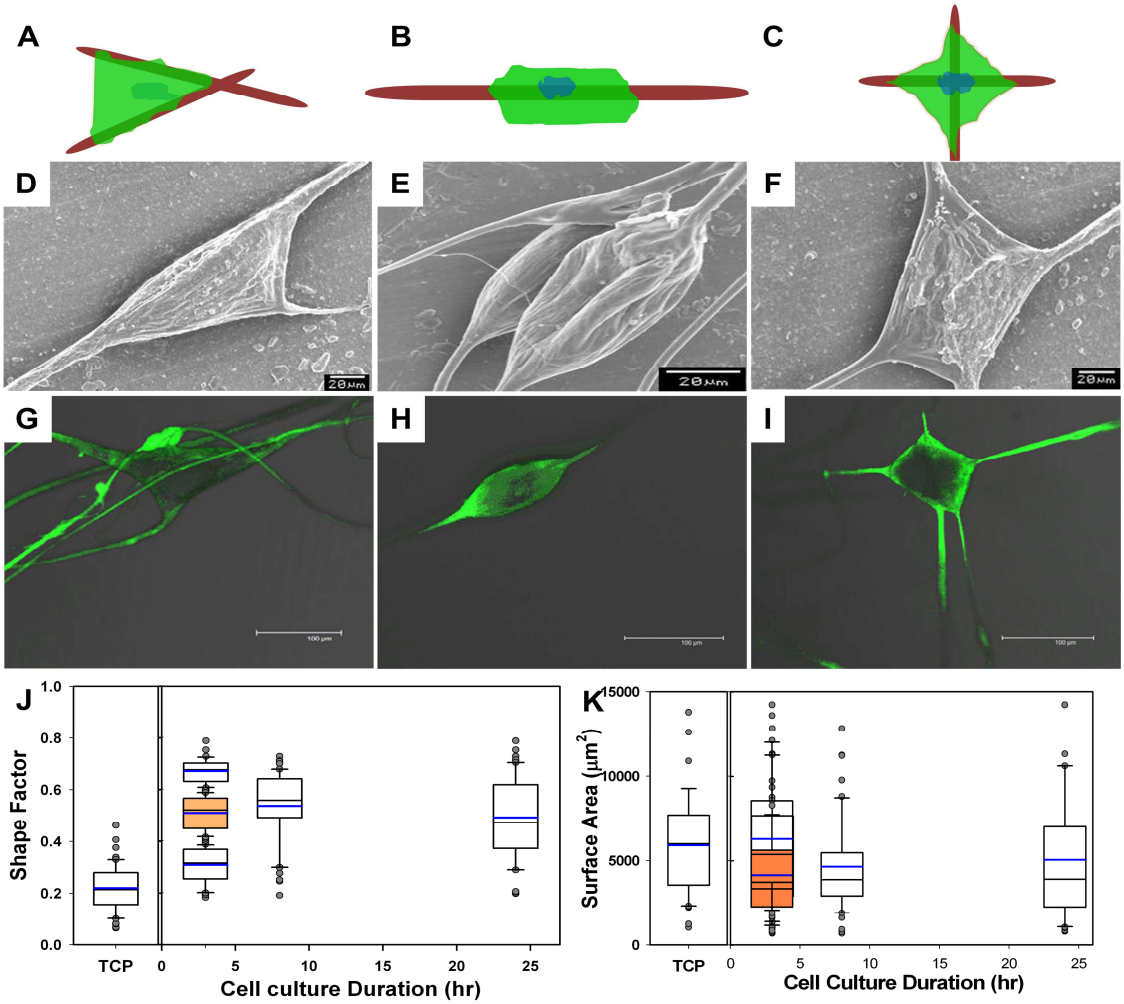

Figure 4.6. Cell morphology on single fibers. (**A-C**) Schematics of cell shape on different configuration of single fibers. (**D-F**) Scanning electron micrographs of single cells on fibers in thin layer of electrosprayed fibers. (**G-I**) Confocal fluorescent micrographs of single cells on fibers in thin layer of electrosprayed fibers (scale bar corresponds to 100 μm). Box plot showing the distribution of (**J**) shape factor and (**K**) area of single cell attached in single fibers with 10^{th}, 25^{th}, 50^{th}, 75^{th}, and 90^{th} percentiles and the mean value (blue thick line within each box). Values that were outside 95^{th} and 5^{th} percentiles were treated as outliers (n = 50). TCP stands for traditional 2D culture plate.

4.4. DISCUSSION

This study addressed the primary drawback of electrospraying technology of small pore size, inhibiting access to 3D space throughout the entire fibrous structure. Accessing the entire 3D porous space is critical to various applications to determine the successful implementation of the technology. In particular, pore size plays a significant role in cell colonization because pore size affects cell binding, migration, depth of cellular in-growth, cell morphology and phenotypic expression [34]. Many mature cell types including fibroblasts are unable to completely colonize scaffolds with the pore sizes >300 μm due to the difficulty in bridging large distances [33, 35-38]. An "optimum pore size range" for supporting cell in-growth for a majority of the mature cell types (except osteoblasts and osteocytes) is in the range of 50 -150 μm [33].

I studied the effect of size and shape of the void in the new collector plate. The pore size increased when the void size was decreased. The fibers aligned when deposited at the edge of the triangular void in the collector plate. These trends are similar to the fiber patterns in gold/quartz collector plates [39]. The diameter of the single fiber was the same since the fiber size is dependent on the solution and process parameters, independent of the geometrical patterns of the new collector plates. When insulated area (such as void in quartz) is introduced into the collector plate, the insulated area changes the structure of the electric field, resulting in geometrical change of the fiber patterns [39-40]. When a specific shape of the insulated void is introduced into a conductive collector plate, the distribution of the electric field is more complex [39] like the circular void, suggesting the need for further studies dealing with the electrofields in the void of the collector plate. The geometric patterns of the voids partially affect the alignment of the

fibers (the vertices of the triangular void). In general; the size and shape of the voids in the collector plates allow the randomly oriented fibers in the void and the density of the fibers on a void is lower than on the aluminum frame.

The fiber sizes are dependent on the solution and process parameters of electrospraying, as demonstrated in a number of studies. Thus, it was easy to control the fiber sizes by i) manipulating process parameter and ii) selecting appropriate polymer-solvent system. I generated fibers with controllable pore sizes by manipulating the deposit volume of polymer solution; the average pore sizes were about 50, 130, and 300 μm. This new process is simple but versatile because it is easy to control the pore size of fibers i) without any extra apparatus except the new collector plate and ii) without altering the solution and process parameters.

Along with physical properties such as pore size of fibers, the chemical properties of electrosprayed fibers are also important to achieve a desirable outcome. In this regard, I fabricated the nanofibers using the mixture of synthetic and natural polymers (PCL and gelatin). Gelatin has RGD like binding sites to allow single cells to attach to the surface of the 3D single fiber in serum free media [41]. Gelatin distribution test with CFDA-SE showed uniform distribution throughout the entire fiber. This functionality of the fiber is very similar to that of extracellular matrix (ECM). However, gelatin dissolves in aqueous media under the physiological condition. Thus, I fabricated the fiber with the mixture of PCL/gelatin because PCL is a synthetic polymer with good mechanical properties. The stability test of PCL/gelatin fiber showed no significant difference in distribution and morphology for two weeks under the physiological condition. Thus, I confirmed the chemical function and stable structure of the 3D scaffold of electrosprayed fibers with

controllable pore size to demonstrate the *in vitro* single cell study on 3D single nanofibers similar to *in vivo* ECM [45].

Cells are cultured outside the body using tissue culture plastic-ware made of polystyrene or other polymers but processed to promote cell adhesion. Much of the investigation into cellular interactions depends on 2D cell culture systems that do not recreate the structure or function of scaffolds similar to *in vivo* environment. Existing 3D models are not adapted in many laboratories due to significant difficulties in 3D cultures relative to the 2D culture including problems with uniform cell seeding and inability to replicate the *in vivo* circumstance for cell and tissue inside animals or humans. For example, microfabrication has been studied to create architecturally complex scaffolds and to overcome some limitation of 2D scaffold [4, 42]. However, these complex structures are expensive to form and do not provide 3D circumstance to single cells because the cell morphology study showed that single cell behaves like cells on 2D scaffold because microfabrication limits the creation of 3D scaffold similar to ECM [43].

In vitro cell adhesion study on 3D nanofibers with controllable pore size is critical to understand the *in vitro* cell behaviors similar to *in vivo* cell behavior on ECM mainly consisting of collagen fibers to act as a supporting framework of tissues and cells. The size and shape of collagen fibers are various, depending on the tissues and organs. The shape is cord or tape with a width of 1 – 20 μm and the collagen fibrils (unit can be observed by electron microscopy) are cylindrical with a diameter ranging from 10 to over 500 nm where cells attach and hug [44]. Our *in vitro* cell study also showed that single cells were attaching to the nanofibers and hugging a single nanofiber. The cell shapes were different when they lodged in one or two single electrosprayed fibers. Cell shapes

were elliptical, triangular, and quadrangular on single fiber, nearby intersection of two single fibers, and on the intersection of two single fibers, respectively. However, shape did not regulate the cell spreading area. Cell adhesion study could be visualized in inverted light and fluorescent microscope because the novel fibers allowed the light to pass through the large pore sizes. Thus, these new 3D structures with controllable pore size open a new window to *in vitro* cell behavior study on 3D nanofiber mimicking 3D ECM inside mammalian environments. These 3D structures overcome the current drawbacks of conventional electrosprayed fibers with narrow fiber sizes and the current cell behavior model using the microfabrication method where cells act on modified 2D plates, not 3D space like our 3D single cell behavior model with the new fiber. Furthermore, our *in vitro* 3D cell behavior model has implications for other cell culture studies such as cell migration study, shorter and longer cell adhesion study, cell proliferation study, cell organization, *de novo* synthesis and assembly of ECM. One could make fibers using various natural and synthetic biomaterials and modified morphology such as porosity, stiffness, microscale topography, and fiber orientation. Single layer of fibers has a potential for long-term cell culture study. The aluminum frame also plays an important role in both fiber fabrication and cell culture study. The aluminum foil works as electrodes while the fiber fabricates and acts as a frame during the cell culture study. Mainly due to the frame, the fiber was stable without any mechanical damage even after cell culture.

This study focused on using thin layers of fibers in tissue regeneration. This technique could also be used in numerous other applications such as chemical and biochemical protection in defense and security, solar cells and fuel cells in sustainability,

membranes and filters in environmental engineering, biotechnology, and nanoscience and nanotechnology.

4.5. CONCLUSION

In summary, the shape of the void in the new collector plate partially affected the fiber alignment. By manipulating the deposit volume of polymer solution and the size of void in the new collector plate, the pore size (about 10 μm to 350 μm) of the fibers was controllable to be able to meet the optimized pore size for cell behavior study. The distribution of gelatin on single PCL/gelatin fiber and the stability of PCL/gelatin fiber was sufficent to confirm the *in vitro* single cell behavior study on 3D nanofiber using mamalian cells in serum free media. The shape and area of single cell attached on 3D fiber varied and the shape depended on the configuration of the fibers, not the period of the cell culutre. In addition, the *in vitro* cell behavior model on 3D nanofibers with controllable pore size will have a great potential for use in other cell behavior studies using various materials and cells.

4.6. REFERENCES

1. Ingber, D.E., et al., *Tissue engineering and developmental biology: going biomimetic.* Tissue Eng, 2006. **12**(12): p. 3265-83.
2. Derda, R., et al., *Paper-supported 3D cell culture for tissue-based bioassays.* Proceedings of the National Academy of Sciences, 2009. **106**(44): p. 18457-18462.

3. Miller, J.S., et al., *Bioactive hydrogels made from step-growth derived PEG-peptide macromers.* Biomaterials, 2010. **31**(13): p. 3736-3743.

4. Chen, C.S., et al., *Geometric Control of Cell Life and Death.* Science, 1997. **276**(5317): p. 1425-1428.

5. Fletcher, D.A. and R.D. Mullins, *Cell mechanics and the cytoskeleton.* Nature, 2010. **463**(7280): p. 485-492.

6. Lutolf, M.P., P.M. Gilbert, and H.M. Blau, *Designing materials to direct stem-cell fate.* Nature, 2009. **462**(7272): p. 433-441.

7. Huang, Y., M. Siewe, and S.V. Madihally, *Effect of spatial architecture on cellular colonization.* Biotechnol Bioeng, 2006. **93**(1): p. 64-75.

8. Lutolf, M.P. and J.A. Hubbell, *Synthetic biomaterials as instructive extracellular microenvironments for morphogenesis in tissue engineering.* Nat Biotechnol, 2005. **23**(1): p. 47-55.

9. Stevens, M.M. and J.H. George, *Exploring and Engineering the Cell Surface Interface.* Science, 2005. **310**(5751): p. 1135-1138.

10. Derda, R., et al., *Paper-supported 3D cell culture for tissue-based bioassays.* Proc Natl Acad Sci U S A, 2009. **106**(44): p. 18457-62.

11. Lowery, J.L., N. Datta, and G.C. Rutledge, *Effect of fiber diameter, pore size and seeding method on growth of human dermal fibroblasts in electrospun poly([var epsilon]-caprolactone) fibrous mats.* Biomaterials, 2010. **31**(3): p. 491-504.

12. Nerurkar, N.L., et al., *Nanofibrous biologic laminates replicate the form and function of the annulus fibrosus.* Nat Mater, 2009. **8**(12): p. 986-992.

13. Krogman, K.C., et al., *Spraying asymmetry into functional membranes layer-by-layer.* Nat Mater, 2009. **8**(6): p. 512-518.

14. Xia, Y., *Nanomaterials at work in biomedical research.* Nat Mater, 2008. **7**(10): p. 758-760.

15. Li, X., et al., *Nanofiber Scaffolds with Gradations in Mineral Content for Mimicking the Tendon-to-Bone Insertion Site.* Nano Letters, 2009. **9**(7): p. 2763-2768.

16. Nisbet, D.R., et al., *Review Paper: A Review of the Cellular Response on Electrospun Nanofibers for Tissue Engineering.* J Biomater Appl, 2008: p. 0885328208099086.

17. Sill, T.J. and H.A. von Recum, *Electrospinning: Applications in drug delivery and tissue engineering.* Biomaterials, 2008. **29**(13): p. 1989-2006.

18. Hong, J.K. and S.V. Madihally, *3D Scaffold of Electrosprayed Fibers with Large Pore Size for Tissue Regeneration.* Acta Biomaterialia, 2010. accepted pending revision.

19. van der Valk, J., et al., *Optimization of chemically defined cell culture media - Replacing fetal bovine serum in mammalian in vitro methods.* Toxicology in Vitro, 2010. **24**(4): p. 1053-1063.

20. Hartman, O., et al., *Biofunctionalization of electrospun PCL-based scaffolds with perlecan domain IV peptide to create a 3-D pharmacokinetic cancer model.* Biomaterials. In Press, Corrected Proof.

21. Woodruff, M.A. and D.W. Hutmacher, *The return of a forgotten polymer - Polycaprolactone in the 21st century.* Progress in Polymer Science. In Press, Accepted Manuscript.

22. Oh, S.H., et al., *In vitro and in vivo characteristics of PCL scaffolds with pore size gradient fabricated by a centrifugation method.* Biomaterials, 2007. **28**(9): p. 1664-1671.

23. Zhang, Y., et al., *The effects of Runx2 immobilization on poly ([var epsilon]-caprolactone) on osteoblast differentiation of bone marrow stromal cells in vitro.* Biomaterials, 2010. **31**(12): p. 3231-3236.

24. Lu, H., et al., *Cartilage tissue engineering using funnel-like collagen sponges prepared with embossing ice particulate templates.* Biomaterials. In Press, Corrected Proof.

25. Zhang, X., et al., *An in vitro regenerated functional human endothelium on a nanofibrous electrospun scaffold.* Biomaterials, 2010. **31**(15): p. 4376-4381.

26. Ghasemi-Mobarakeh, L., et al., *Electrospun poly([var epsilon]-caprolactone)/gelatin nanofibrous scaffolds for nerve tissue engineering.* Biomaterials, 2008. **29**(34): p. 4532-4539.

27. Zhang, Y.Z., et al., *Fabrication of porous electrospun nanofibres.* Nanotechnology, 2006. **17**.

28. Mondalek, F.G., et al., *The incorporation of poly(lactic-co-glycolic) acid nanoparticles into porcine small intestinal submucosa biomaterials.* Biomaterials, 2008. **29**(9): p. 1159-66.

29. O'Brien, F.J., et al., *Influence of freezing rate on pore structure in freeze-dried collagen-GAG scaffolds.* Biomaterials, 2004. **25**(6): p. 1077-1086.

30. O'Brien, F.J., et al., *The effect of pore size on cell adhesion in collagen-GAG scaffolds.* Biomaterials, 2005. **26**(4): p. 433-441.

31. Nehrer, S., et al., *Matrix collagen type and pore size influence behaviour of seeded canine chondrocytes.* Biomaterials, 1997. **18**(11): p. 769-776.

32. Corin, K.A. and L.J. Gibson, *Cell contraction forces in scaffolds with varying pore size and cell density.* Biomaterials, 2010. **31**(18): p. 4835-4845.

33. Yannas, I.V., et al., *Synthesis and characterization of a model extracellular matrix that induces partial regeneration of adult mammalian skin.* Proc Natl Acad Sci U S A, 1989. **86**(3): p. 933-7.

34. Yannas, I.V., et al., *Synthesis and characterization of a model extracellular matrix that induces partial regeneration of adult mammalian skin.* Proc Natl Acad Sci U S A, 1989. **86**(3): p. 933-7.

35. Zeltinger, J., et al., *Effect of pore size and void fraction on cellular adhesion, proliferation, and matrix deposition.* Tissue Engineering, 2001. **7**(5): p. 557-572.

36. Salem, A.K., et al., *Interactions of 3T3 fibroblasts and endothelial cells with defined pore features.* J Biomed Mater Res, 2002. **61**(2): p. 212-7.

37. Ng, K.W., H.L. Khor, and D.W. Hutmacher, *In vitro characterization of natural and synthetic dermal matrices cultured with human dermal fibroblasts.* Biomaterials, 2004. **25**(14): p. 2807-18.

38. Wang, Y.C. and C.C. Ho, *Micropatterning of proteins and mammalian cells on biomaterials.* Faseb J, 2004. **18**(3): p. 525-7. Epub 2004 Jan 8.

39. Li, D., et al., *Collecting Electrospun Nanofibers with Patterned Electrodes.* Nano Letters, 2005. **5**(5): p. 913-916.

40. Li, D., Y. Wang, and Y. Xia, *Electrospinning of Polymeric and Ceramic Nanofibers as Uniaxially Aligned Arrays.* Nano Letters, 2003. **3**(8): p. 1167-1171.

41. Huang, Y., et al., *In vitro characterization of chitosan-gelatin scaffolds for tissue engineering.* Biomaterials, 2005. **26**(36): p. 7616-27.

42. Wang, Y.C. and C.C. Ho, *Micropatterning of proteins and mammalian cells on biomaterials.* Faseb J, 2004. **8**: p. 8.

43. Tien, J., C.M. Nelson, and C.S. Chen, *Fabrication of aligned microstructures with a single elastomeric stamp.* Proc Natl Acad Sci U S A, 2002. **99**(4): p. 1758-62.

44. Ushiki, T., *Collagen Fibers, Reticular Fibers and Elastic Fibers. A Comprehensive Understanding from a Morphological Viewpoint.* Archives of Histology and Cytology, 2002. **65**(No. 2): p. 109-126.

45. Pengcheng Zhao, H.J., Hui Pan, Kangjie Zhu, Weiliam Chen,, *Biodegradable fibrous scaffolds composed of gelatin coated poly(ε-caprolactone) prepared by coaxial electrospinning.* Journal of Biomedical Materials Research Part A, 2007. **83A**(2): p. 372-382.

CHAPTER V

DEGRADATION OF PCL ELECTROSPRAYED FIBERS WITH DIFFERENT MOLECULAR WEIGHTS

5.1. INTRODUCTION

During tissue regeneration using the approach of tissue engineering, the typical process comprises harvesting cells from the donor, *in vitro* proliferation, scaffold fabrication, cell seeding on scaffold, and implantation of the cell colonized scaffold into the body to cure disordered organs and tissues. While cells become a tissue, the structure of 3D scaffold made of biodegradable polymers fades into the human body. The challenge is designing a scaffold to mimic natural extracellular matrix (ECM), which regulate cell behaviors such as cell migration, cell proliferation, and cell differentiation. Recently, electrospraying process has been extensively studied for fabricating micro and nanosize fibers in tissue engineering due to the possibility of mimicking ECM characteristics [1-6]. When electrosprayed fibers are used, the pore size between the fibers (less than 20 μm) is smaller than mammalian cells, restricting cells to growing on the top surface of the scaffold only.

To fabricate the proper structure of 3D scaffold, I reported a novel technique which allows the large pore size of fibers suitable for cell infiltration into 3D scaffold of electrosprayed fibers. Thirty day cell culture study demonstrated that cells attached on polycaprolactone (PCL) fibers in serum media, and distributed between the fibers horizontally and vertically. The colonized cells glued three layers of fibers, merging into one stable 3D scaffold.

Typically, high molecular weight PCL is used to generate electrosprayed fibers. Even though electrosprayed fibers made of high molecular weight PCL have various merits, the clinical usage is limited due to the long period of degradation *in vitro* and *in vivo* study (6 month to 4 years) [7-8]. However, the electrosprayed fibers with low molecular weight of PCL are seldom fabricated due to processing difficulty such as the low viscosity. In this study, I demonstrated the fabrication of PCL fibers mixed with different molecular weights (high, medium, and low) of PCL to overcome the limitation of PCL fiber with low molecular weight and their degradation studies under physiological conditions.

5.2. MATERIALS AND METHOD

5.2.1. Materials

Polycaprolactones (PCL80K, Mn=80,000 and PCL10K, Mw=14,000) were purchased from Sigma (St, Louis, MO) and PCL45K (Mw=43,000-50,000) was obtained from Polysciences (Warrington, PA). Chloroform and methanol were purchased from Pharmco (Brookfield, CT).

5.2.2. Fabrication of electrosprayed fiber with different molecular weight

Electrospraying apparatus consisted of a syringe pump (74900 series, Cole-Parmer Instrument Company, Vernon Hills, IL), BD 10 mL syringe (Luer-Lok Tip; Becton Dickinson and Company, Franklin Lakes, NJ), needle tip, high voltage power supply (ES30P-5W/DAM, Gamma high Voltage Research, Ormond Beach, FL), earth grounding, and different shape and size of collector plate. The fabrication conditions were kept the same for all processes except the different mixing ratio of polymer solution. Flow rate, needle size, high voltage supply and distance between the needle tip and the collector were10 ml/hr, 20 G, 10 kV, and 9 cm with the novel collector plate (diameter, 1.9 cm and depth 1.2 cm) in a wooden frame (3 cm × 10 cm × 2 cm) wrapped with aluminum foil. The polymer solution with different concentration of PCL80K, 43K, and 10K ranging from 5.1 to 24 % were dissolved in a mixture solvent of chloroform and methanol (mixing ratio 9 to 1) (**Table 5.1**).

5.2.3. Degradation test of PCL fibers with low molecular weight

Three fiber compositions with the same concentration but different mixing ratio of PLC80K/43K/10K (22:0:0, 11:11:0, or 9:9:4 respectively) were selected from **Table 5.1.** Fibers were formed under the same conditions described above and incubated in Krebs Henseleit buffer solution (pH 7.4) at CO_2 incubator at 37 °C for 4 weeks. The morphology of single fiber before and after the degradation was confirmed by using SEM.

Table 5.1. PCL fiber with different mixing ratio of molecular weight 80K, 43K, and 10K

Number of Mixing components	Total concentration (w/v %)	PCL 80K (w/v %)	43K (w/v%)	10K (w/v%)	Fiber
1	22	22			OK
1	20	20	-	-	OK
1	20	-	20	-	OK
1	20	-	-	20	DNW
2	22	11	11		OK
2	20	10	10	-	OK
2	20	10	-	10	DNW
2	20	-	10	10	DNW
3	20.1	6.7	6.7	6.7	DNW
2	18	9	9	-	OK
3	20	9	9	2	OK
3	22	9	9	4	OK
3	24	9	9	6	DNW
3	26	9	9	8	DNW
2	10	5	5	-	DNW
2	10	-	5	5	DNW
2	10	5	-	5	DNW
3	5.1	1.7	1.7	1.7	DNW
3	9.9	3.3	3.3	3.3	DNW
3	15	5	5	5	DNW

OK means the fiber was fabricated on the gap of the new collector plate under the fixed condition. For all the fibers, flow rate, needle size, high voltage supply and distance between the needle tip and the collector were10 ml/hr, 20 G, 10 kV, and 9 cm with the novel collector plate (diameter, 1.9 cm and depth 1.2 cm) in a wooden frame (3cm × 10cm × 2 cm) wrapped with aluminum foil. DNW means that the fiber was not collected under the above condition of the fibers.

5.2.4. Statistical analysis

Statistical analysis was carried out using single-factor analysis of variance (ANOVA). A value of $p \leq 0.05$ was considered statistically significant.

5.3. RESULTS

5.3.1. Limitation of PCL fabrication with low molecular weight

To overcome the low viscosity of low molecular weight of PCL and fabricate proper period of degradation under the physiological condition, I prepared PCL solution with different molecular weight such as PCL80K, 43K, and 10K in the mixed solvent system of chloroform and methanol (9 to 1) (**Table 5.1**). PCL fibers were generated under the same condition of solution (concentration of solution) and process parameters (flow rate, needle size, distance between the needle tip and the collector, and high voltage supply) using the novel and the conventional collector plates. First, I fabricated fibers with one molecular weight and fabricated the fibers on both the novel and conventional collector plates using 20 % of PCL80K or 43K (**Figure 5.1**), but more than 22 % of PCL80K solution began to form beads and fibers on both the collector plates. Overall, 20 % PCL80K/43K (10:10) allowed fiber formation on both collector plates but 20 % PCL10K, 20% PCL80K/10K (10:10), 20 % PCL43K/10K (10:10), and 20.1 % PCL80K/43K/10K (6.7:6.7:6.7) formed droplets of the solution at the needle tip instead of flying to the collector plates. Thus, I increased the fiber concentration of PCL83K/43K/10K (9:9:0) and added 10K from 0 % up to 8 % under the fixed concentration of PCL80K/43K. Fibers were collected on the novel and conventional collector plates using 9/9/0, 9/9/2, and 9/9/4 mixing ratios. When mixing ratio of

PCL10K increased to more than 5 %, the fiber formation decreased in both the void and flat collector surfaces, with the formation of solution droplets at the needle tip instead of flying to the collector plates when high voltage was applied into the system. Thus, fiber fabrication was limited by the low molecular weight of PCL, not the geometry of collector plate.

5.3.2. Fiber characteristics

Collected fibers were evaluated under scanning electron microscope and digital images were obtained from random regions. Quantification study of scanning electron micrographs revealed that the collector plate configuration does not influence the fiber size and the shape of the pores in the scaffold (**Figure 5.1** and **5.2**). Average fiber sizes on both collector plates were approximately 2 μm and both shape factors were approximately 0.50. Even when the concentration and mixing ratio of polymer solution was changed, no significant difference of fiber size or shape of pore was obtained under the same processing conditions. Compared to the pore size of fibers on conventional fibers, the pore size of the fiber made using various mixing ratios on novel collector plate showed significant increase due to the decreased density of fibers deposited in the void [2]. Average pore size of conventional fiber was less than 10 μm and approximately 150 μm. These large pore sizes are similar to our previous results and are suitable for cell infiltration and cell colonization.

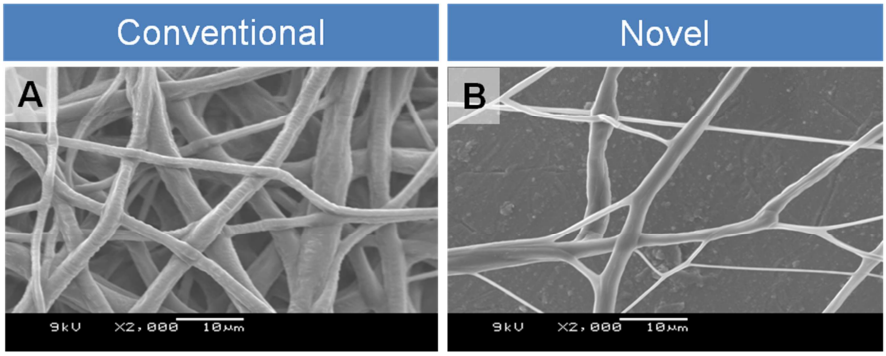

Figure 5.1. The scanning electron micrograph of the fibers fabricated by (A) conventional and (B) novel collector plates.

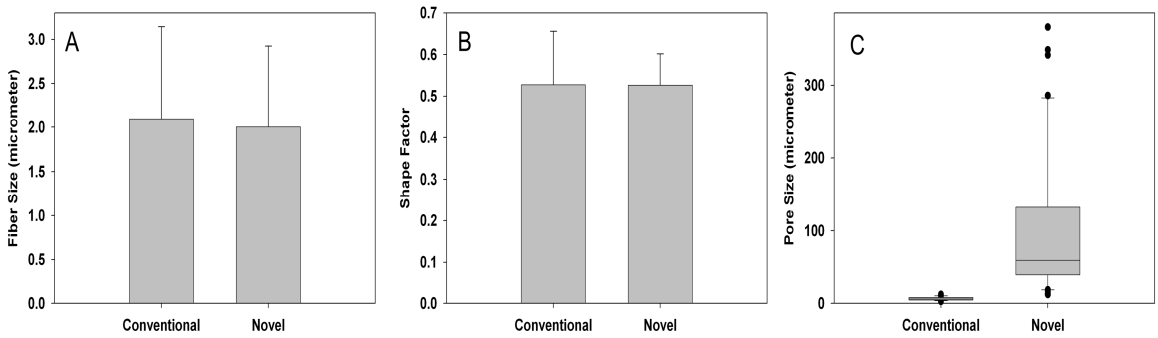

Figure 5.2. Fiber characteristics. (A) Fiber diameters. **(B)** Shape factor. **(C)** Pore size. The error bars correspond to the standard deviation (n = 50).

5.3.3. Degradation of single fibers with low molecular weight

The space distribution of fibers allows the charaterization of single fibers without interference from adjacent fibers. To understand the effect of blending on degradation of the fibrous network, PCL80K fibers mixed with low molecular weight (PCL43K and PCL10K) were incubated in Krebs Henseleit buffer solution (pH 7.4) at CO_2 incubator at 37°C for 2 weeks for 30 days. **Figure 5.3** shows SEM morphology of the fibers before and after the degradation test. The fibers made of PCL80K (22:0:0), PCL80K/43K (11:11:0), and PCL80K/43K/10K (9:9:4) were fabricated under the same condition. Thus, the fiber size and morphology were similar to these conditions. The average single fiber sizes were approximately 2 μm and the morphology of single fibers shows that the all fibers have the tiny grooves on their surface (**Figure 5.3A-5.3C**). In majority of the fibers, the surface morphology of the fibers after 30 day degradation was similar to those before the incubation. However, at some parts of the fibers made of PCL80K, PCL80K/43K, and PCL80K/43K/10K surface morphology had changed with the appearance of cracks. The degree of the surface damage increased in the fibers fabricated with PCL 80K/43K/10K compared to those made of PCL 80K or PCL 80K/43K. The few cracked points existed on the surface with a vertical groove, suggesting that PCL 80K or PCL 80K/43K were partially attached from the fibers during degradation test. However, the PCL80K/43K/10K fibers was cut thus two part of the fibers exists (**Figure 5.3D-5.3F**). These results demonstrate that the presence of 10 K PCL, promotes disintegration of the fibers.

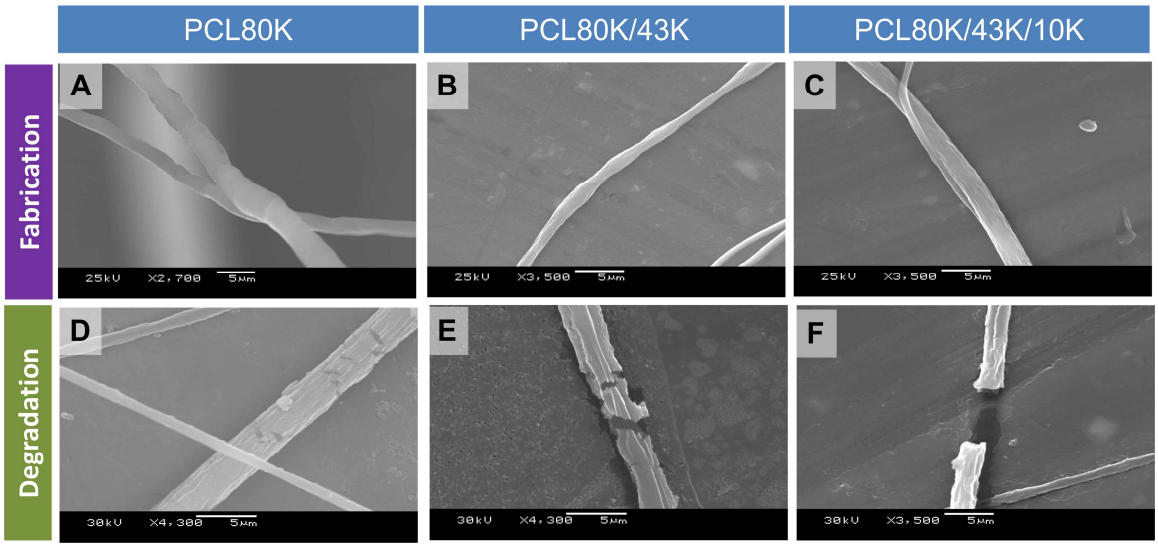

Figure 5.3. Effect of blending different PCL molecular weights on degradation of fibers. (A-C) The polymeric structure of the single fibers made of PCL80K, PCL80K/43K, and PCL80K/43K/10K after the degradation test under the physiological condition for 30 days.

5.4. DISCUSSION

To fabricate the electrosprayed fiber, I mainly used different molecular weight of PCL, a semi-crystaline, bioresorbable polymer belonging to the aliphatic polyester family [9]. PCL degradation is dependent on molecular weight. As the molecular weight increases, degradation time increases (PCL10K for 2 month, PCL43K for 6 months, and PCL80K for 2 years) [10-11]. I have published on the formation of fibers using PCL80K and PCL43K in the novel collector plate previously. However, PCL10K alone has limited use in electrospraying process due to the low viscosity of the solution; the lower molecular weight forms droplets at the needle tip.

One major concerns of a scaffold is its degradability. Different tissue and organs need different periods of degradation. In this study, I fabricated PCL80K fibers in combination with low molecular weight (PCL43K and PCL10K), and compared the fibrous structures with different molecular weight under the same conditions. In addition, I formed scaffolds using the novel and conventional collector plate and evaluated the single fiber morphology under the *in vitro* physiological conditions. I showed that the mixing ratio of polymer solution with different molecular weight is independent of the polymeric structure of fibers. The fiber diameter, shape factor of fibers, and the pore size of fibers were almost the same under the same conditions of process parameters (needle size, flow rate, distance between the needle tip and the collector plate) when mixing ratio of different molecular weights of PCL was changed in chloroform and methanol. Although I fabricated hybrid fibers with PCL 80K/43K/10K, the fiber fabrication with different molecular weight was also limited to mixing ratio from 9:9:0 to 9:9:4.

However, the fiber fabrication was limited mixing ratio from 9:9:5 under the condition. Thus, the molecular weight of PCL affects the fiber fabrication.

The pore size of fibers significantly changed when the collector plate was changed from the conventional flat collector plate to the one with voids. The void in the new collector plate allows the large pore size of polymeric structure due to the low deposit volume of polymer between the air insulated areas. However, shape factor and pore size were the same when the collector plate changed. Even after changing process parameters and solution parameters, the shape factor of the pores did not change, probably due to the random distribution of the fibers on the collector plate. However, the fiber diameters significant changed when formed by changing the solution and process parameters. In particular, the fiber size significantly changed when the distance between the needle tip and the collector plate was changed.

Making use of our innovation to study single fiber characteristics, formed fibers were evaluated for degradation analysis under physiological conditions. Before the degradation test, the fiber morphologies with different molecular weight were identical. However, presence of different molecular weight of PCL altered the surface morphology of the single fibers after 30 days of incubation. Degradation of PCL consists of two steps [12]. In the first step, water diffusion into the amorphous regions and hydrolysis randomly cut the ester bonds in amorphous regions, reducing the molecular weight of the polymer but weight loss of the polymer was restricted. The second step consists of degradation of the amorphous regions, hydrolysis of the crystalline domain and accelerated weight loss [13]. In this study, the surface morphology was observed from 0 to 4 week. The entire fibrous structure was stable during the degradation period but the

surfaces of the single fibers were partially damaged with small amount of the polymer observable in the aqueous media. Thus, all PCL fibers up to 4 weeks belong to the first stage of degradation. Weight loss of the structures could not be determined during the degradation time, primarily due to the problems encountered in errors introduced during sample collection and processing to determine dry weight. Nevertheless, the fibers with low molecular weight showed more damaged area on the surface, suggesting that PCL80K fibers with PCL43K and PCL10K were more degradable than PCL80K fibers. Further, the low molecular weight PCL is more crystalline than high molecular weight, which could contribute to the accelerated degradation and the weight loss of the PCL fibers [13]. In summary, I can alter the degradability of the single PCL fibers by adding the low molecular weight of PCL for tissue regeneration. Since, no other chemical reaction is necessary, there is no change in the functional groups within the porous structure. Use of this technique in various applications such as tissue regeneration and controlled drug release needs further investigation.

5.5. CONCLUSION

The limitation of the fiber fabrication with low molecular weight of PCL can be overcome by mixing the high molecular weight of PCL with large and middle molecular weight. The characteristics of fibers (pore size, shape factor, and fiber diameter) were independent of the concentration of PCL with different molecular weight and different mixing ratios of PCL under the same process parameters of electrospinning. The different molecular weight of PCL accelerated fiber detachment in single fiber under

physiological condition. Thus, the mixing with medium and low molecular weight of fibers is suitable for controlling the degradation of PCL fibers.

5.6. REFERENCES

1. Chung, S., et al., *Bioresorbable elastomeric vascular tissue engineering scaffolds via melt spinning and electrospinning.* Acta Biomaterialia, 2010. 6(6): p. 1958-1967.
2. Hong, J.K. and S.V. Madihally, *Three-dimensional scaffold of electrosprayed fibers with large pore size for tissue regeneration.* Acta Biomaterialia, 2010. 6(12): p. 4734-4742.
3. Metter, R.B., et al., *Biodegradable fibrous scaffolds with diverse properties by electrospinning candidates from a combinatorial macromer library.* Acta Biomaterialia, 2010. 6(4): p. 1219-1226.
4. Soliman, S., et al., *Multiscale three-dimensional scaffolds for soft tissue engineering via multimodal electrospinning.* Acta Biomaterialia, 2010. 6(4): p. 1227-1237.
5. Bottino, M.C., V. Thomas, and G.M. Janowski, *A novel spatially designed and functionally graded electrospun membrane for periodontal regeneration.* Acta Biomaterialia, 2011. 7(1): p. 216-224.
6. Jha, B.S., et al., *Two pole air gap electrospinning: Fabrication of highly aligned, three-dimensional scaffolds for nerve reconstruction.* Acta Biomaterialia, 2011. 7(1): p. 203-215.
7. Munir, M.M., et al., *Scaling law on particle-to-fiber formation during*

electrospinning. Polymer, 2009. 50(20): p. 4935-4943.

8. Koski, A., K. Yim, and S. Shivkumar, *Effect of molecular weight on fibrous PVA produced by electrospinning.* Materials Letters, 2004. 58(3-4): p. 493-497.

9. Cottam, E., et al., *Effect of sterilisation by gamma irradiation on the ability of polycaprolactone (PCL) to act as a scaffold material.* Medical Engineering & Physics, 2009. 31(2): p. 221-226.

10. Chan-Chan, L.H., et al., *Degradation studies on segmented polyurethanes prepared with HMDI, PCL and different chain extenders.* Acta Biomaterialia, 2010. 6(6): p. 2035-2044.

11. Christopher, X.F.L. and et al., *Dynamics of in vitro polymer degradation of polycaprolactone-based scaffolds: accelerated versus simulated physiological conditions.* Biomedical Materials, 2008. 3(3): p. 034108.

12. Hartman, O., et al., *Biofunctionalization of electrospun PCL-based scaffolds with perlecan domain IV peptide to create a 3-D pharmacokinetic cancer model.* Biomaterials, 2010. 31(21): p. 5700-5718.

13. Jones, D.S., et al., *Poly([var epsilon]-caprolactone) and poly([var epsilon]-caprolactone)-polyvinylpyrrolidone-iodine blends as ureteral biomaterials: characterisation of mechanical and surface properties, degradation and resistance to encrustation in vitro.* Biomaterials, 2002. 23(23): p. 4449-4458.

CHAPTER VI

CONCLUSIONS AND RECOMMENDATIONS

6.1. CONCLUSIONS

This research focused on the influence of structural architecture in 3D scaffold of the innovative electrosprayed fibers with large and controllable pore size on cell behavior for tissue regeneration (**Table 6.1**). Micro and nanofibers were manufactured using electrospraying technique and the innovative collector plate allowed the formation of fibers with large pore size in 3D scaffolds. The large pore size allowed the characterization of single fibers-cell interactions. The pore sizes in the 3D scaffolds were controllable by manipulating the deposit volume of the polymer solution and the diameter of the void in the novel collector plate. Findings from the study are summarized in **Table 6.1**, according to the three specific aims described in Chapter 1and basic components in each specific aim, following the pattern shown in Figure 1.1. Detailed descriptions are given below.

Table 6.1.The research summary

	Specific Aim 1	Specific Aim 2	Specific Aim 3
New process	The design of the novel collector	The control of pore size by manipulating the deposit volume	The aligning of the fiber by designing different shape of collector plate
Collector plate	Novel/conventional	Novel/conventional	Novel
Materials	PCL/gelatin Type A	PCL/gelatin Type A	PCL/gelatin Type A
PCL molecular weight	80K/40K	80K	80K/40K/10K
Solvent	CF/MeOH or MeOH/H_2O	HFP	CF/MeOH or HFP
Fiber size	Micro/nanofibers	Nanofibers	Micro/nanofibers
Fibers	Large pore size	Controllable pore size/ Aligned fibers	Hybrid fiber with different molecular weight
Fiber characteristics	Comparison of new and conventional fibers	Comparison of new and conventional fibers	Influence of different molecular weight on surface morphology
	Mechanical test (load-extension curve)	Gelatin distribution in single fiber	Acceleration of PCL fiber degradation by mixing low molecular weight
		Stability of PCL/gelatin fiber	
Cell study system	PCL microfibers	PCL/gelatin nanofibers	
Number of layers	Single/Three or Multiple	Single	
Cell line	HFF-1 cells	HFF-1	
Media	15% serum added media	Serum free media	
Period of cell culture	In vitro from 1 to 30 day	In vitro from 3 to 24 hr	
In vitro cell study (all cell study completed with HFF-1 if not mentioned)	The large pore size of fibers allow cell infiltration (S/M)	The configuration of fibers affect the fiber shape of cell attachment not the period of the time (S)	
	Cell on fiber grow not only horizontally but also vertically (S/M)		
	The cells on 3D scaffold to colonize by themselves (S/M)		
	The cell act as a glue to attach each layer and , become stable cell-glued 3D scaffold (M)		

PCL, polycaprolactone; 80K, 80000; 40K, 40000; 10K, 10000; CF, chloroform; MeOH, methanol; H_2O, distilled water; HFF-1, human foreskin fibroblast; S, single layer; M, multiple layer; HFP, hexafluoro-2-propanol.

6.1.1. *The first specific aim is* to develop thin layers of PCL electrosprayed fibers with large pore size and evaluate its application in developing thick 3D scaffold (Chapter 3).

New process: I successfully designed a novel collector plate (having four circles in a wooden frame wrapped with aluminum foil) to fabricate thin layers of electrosprayed fibers with large pore sizes. The size of the void could be as large as 10 cm and in different shapes. The thin layer of electrosprayed fibers can be easily handled without mechanical damage because of the supporting structure. This novel collector plate is also versatile enough to be associated with existing electrospinning techniques to manipulate mechanical and biological properties of fibers. The novel collector plate was also utilized in dual injection system (sequential and simultaneous injections) of PCL and gelatin.

Characteristics: The diameters of the fibers made of synthetic (PCL), natural (gelatin) and complex (PCL/gelatin) polymers using chloroform/methanol(10 nm to 5 μm) were the same in the novel collector plate to that in the conventional plate when fabricated under the same process and solution conditions. The pore size of fibers produced with the novel collector plate were larger than those produced with the conventional collector plate due to the decreased density of fibers. The load-extension curves of bulk PCL fibers showed that the elongation of fibers from the novel collector plate was two times longer than that of the conventional plate but the load carrying capacity decreased by half. The effect of hydration on single fibers of PCL and gelatin structures showed dissolution of gelatin due to the absence of a stabilization reaction.

Cell behavior: Single layers were successfully used in hydrated conditions to evaluate the interactions of human foreskin fibroblasts. Thin layers were placed serially to

develop thick 3D structures by adapting layer-by-layer assembly. Long term (30 days) cell culture showed that the cells colonized the layer-by-layer assembly and generated a single thick tissue. Cells distributed throughout the scaffold in vertical and horizontal directions. Formed structures were tailorable.

6.1.2. *The second specific aim is t*o develop thin layers of PCL/gelatin electrosprayed fibers with controllable pore size and evaluate its utility to study single cell behavior in 3D configuration (Chapter 4).

New process: The pore size (about 10 μm to 350 μm) of the fibers was controllable to meet the optimized pore size for cell behavior study by manipulating the deposit volume of polymer solution and the size of void in the novel collector plate. The large and controllable pore sizes were fabricated when the deposit volume of the polymer solution was manipulated in microscale. As the injection volume increases, the pore sizes decreased since the deposit volume of polymer increased among the holes. When the size of the void in the novel collector plate increased from 9 mm to 19 mm, the pore size increased from 10 μm -60 μm). Furthermore, the shape of the hole such as a circle, triangle, and square affects the fiber structure, in particular; few fibers were aligned in a triangular collector plate and fibers in rectangular system also seemed to have aligned perpendicular to the long side in macroscale but the fibers were distributed random in microscale.

Characteristics: The fiber diameters were not affected by change in the void size or the shape of the void compared to the conventional plates. The PCL/gelatin fibers formed

using hexafluoro-2-propanol showed uniform distribution of gelatin when analyzed using CFDA-SE. Further, gelatin was stable for two weeks under the physiological conditions.

Cell behavior: *In vitro* cell culture study also showed that single cells were attaching to the nanofibers and hugged around the 3D nanofiber even though the cell size (20 μm) was at least 20 times bigger than that of the fiber size (700 nm), single cell attached on the single nanofiber. The cell shapes were different when they lodged in one or two single electrosprayed fibers. Cell shapes were elliptical, triangular, and quadrangular on single fiber, nearby intersection of two single fibers, and on the intersection of two single fibers, respectively. However, shape did not regulate the cell spreading area.

6.1.3. *The third specific aim* to develop hybrid PCL fibers with different molecular weight and evaluate its degradation under physiological condition (Chapter 5).

New process: The limitation of the fiber fabrication with low (10K) molecular weight of PCL can be overcome by mixing with high (80K) molecular weight of PCL with large and middle molecular weight.

Characteristics: The characteristics of fibers (pore size, shape factor, and fiber diameter) were independent on the concentration of PCL with different molecular weight and different mixing ratio of PCL under the same conditions of process parameters of electrospinning. The different molecular weight (80K/40K/10K) of PCL accelerated fiber detachment in single fiber under the physiological condition. Thus, the mixing with medium (40K) and low (10K) molecular weight of fibers are suitable for controlling the degradation of PCL fibers.

6.2. RECOMMENDATIONS

6.2.1. Nanoscale characterization of single fibers

The new process of electrospraying technique allowed the controllable large pore size of fibers similar to ECM. Nanostructure of the 3D scaffold influences cell behavior such as cell infiltration, cell adhesion, cell growth, and cell colonization. However, the process need to be explored for other fiber configurations by modifying the apparatus, especially the injection system and the collector plates since nanostructure [1] of fibers with stiffness, pore orientation and topography in microscale such as surface roughness, groove, and edge affect cell behavior on single nanofibers. For better understanding of these interactions, single fibers needs to be characterized in nanoscale using techniques such as nanoindentation and nano-tensile test. The shape and size of holes affect the alignment and pore size of fibers as the distribution of the external electrical field becomes more complex [2]. Thus, further study is necessary to understand electrical field changes in the void to understand the rationale for fiber alignment.

6.2.2. Development of the new fiber with various biomaterials

In this study, I used PCL and gelatin to form porous structures and evaluated cellular interactions direct the growth of cells in vitro culture. However, tissue regeneration requires that cells be given more specific instructions. Inside the body, the cells that repair damaged areas receive different signals both from the wounded tissues and healthy surrounding sites. Cells are sensitive to their surroundings. Between 10 and 100 μm, cells interact with environmental features at all length scales from the macro to the molecular. The ideal scaffold structure is one in which the scaffold consists of

biomaterials that can selectively react with the specific adhesion and growth factor receptors from healthy cells in normal surrounding tissue. Scaffolds guide migration of the healthy target cells to the wounded sites and stimulate their growth and functionality such as differentiation [3]. 3D Scaffold mimics ECM, which have various formulations in different tissues and at different developmental stages. Variety arises from the molecular interactions between many isoforms, ratios, and geometrical configuration of collagen, elastins, proteoglycans, and adhesive proteins such as fibronectins [1]. Thus, various materials have to be explored apart from PCL and gelatin for the new scaffold to include hybrid multifunctional materials such as growth factor immobilized PCL/Chitosan/gelatin fibers with various cells.

6.2.3. Development of bioreactor

The proper micro and macroscopic architecture of the tissue is necessary for proper function of the tissue. For instance, connective tissue cells cultured on 3D scaffolds in vitro secrete ECM molecules but fail to acquire the appropriate tissue architecture. The solution may depend on applying appropriate external stress during in vitro cell culture by using bioreactors such as simply pumping media through the cell containing porous structures or waving the reactor [4-5]. Thus, the development of thick tissues (more than 300 μm) using the thin layer of fibers also requires a design of an appropriate bioreactor to accelerate tissue growth and improve functionality. For instance, the cell glued 3D scaffolds of three layers demonstrated that cells in three layers were well distributed, colonized, and merged each layers to one stable 3D scaffold. However, a thicker 3D scaffold study using four or more layers needs to clarify the

limitation of media diffusion. Further, a new bioreactor design that allows cells to colonize in thicker 3D scaffolds needs to be explored [5-6].

6.2.4. Tissue engineering model

In vitro cell culture study of human fibroblasts for 30 days confirmed the new fibers have a significant potential developing thick 3D scaffold and to be able to expand its use in various tissues such as blood vessels, bone, neural and tendons/ligaments. One of the current drawbacks in regenerating tissues using in vitro cell culture is the lack of their own blood supply systems. Thus, the distance of oxygen diffusion is limited to a few hundred micrometers at most. When implanted, colonized cells in 3D scaffold start to consume oxygen in a few hours, however, it will take a few days to grow the new vessels. If vascular system with artificial tissues or organs can be fabricated using in vitro tissue engineering, this tissue can be used as a model for many different fields such as pharmaceutical and cosmetic industries.

6.2.5. Clinical applications

Tissue regeneration involves the cell culture from a donor or human body, in vitro cell culture, cell seeding, colonization of cells on 3D scaffold, and finally the colonized scaffold is implanted into the human body or the patient to cure and regenerate damaged organs and tissue [7]. Before the implant, the in vivo animal culture is essential to confirm the clinical use of the scaffold. In vivo result will also provide information on improving the architecture of 3D scaffold followed by another animal study. Repeating this process will facilitate fabrication of an optimum 3D scaffold. Consequently, the

clinical test is the ideal goal of this innovative system to apply to various tissue regenerations with different cells and fine-tuned structure of 3D scaffold made of various biomaterials. Thus, the innovative fibers with large pore size open a new window using biomimetic 3D scaffold in clinical medicine.

6.2.6. Other applications

Several recent advanced technology of electrospraying process is a near-field electrospinning process to deposit solid nanofibers in a direct, continuous, and controllable manner [8], fiber alignment and the patterns of fiber deposit on insulated gaps on the collector plate (gold/quartz systems) [2, 9]. Due to the controllable pore size of nano and microsize fibers from few decade to few hundred micrometers, my new electrospraying process can be utilized in many fields: nanoscience and nanotechnology, drug delivery system, gene delivery system, protein delivery system, environmental engineering, sustainability such as fuel cell, polymer science and engineering, pharmaceutical science and engineering, biomedical science and engineering, mechanical engineering, electrical engineering, textile engineering, bioengineering, clinical medicine, biology, biochemistry, organic chemistry and chemical engineering.

6.3. REFERENCES

1. Stevens, M.M. and J.H. George, *Exploring and Engineering the Cell Surface Interface.* Science, 2005. **310**(5751): p. 1135-1138.

2. Li, D., Y. Wang, and Y. Xia, *Electrospinning of Polymeric and Ceramic Nanofibers as Uniaxially Aligned Arrays.* Nano Letters, 2003. **3**(8): p. 1167-1171.

3. Hubbell, J.A., *Bioactive biomaterials.* Current Opinion in Biotechnology, 1999. **10**(2): p. 123-129.

4. Griffith, L.G. and G. Naughton, *Tissue Engineering--Current Challenges and Expanding Opportunities.* Science, 2002. **295**(5557): p. 1009-1014.

5. Grodzinsky, A.J., et al., *CARTILAGE TISSUE REMODELING IN RESPONSE TO MECHANICAL FORCES.* Annual Review of Biomedical Engineering, 2000. **2**(1): p. 691-713.

6. Hong, J.K. and S.V. Madihally, *Three-dimensional scaffold of electrosprayed fibers with large pore size for tissue regeneration.* Acta Biomaterialia. In Press, Corrected Proof.

7. Langer, R. and J. Vacanti, *Tissue engineering.* Science, 1993. **260**(5110): p. 920-926.

8. Sun, D., et al., *Near-Field Electrospinning.* Nano Letters, 2006. **6**(4): p. 839-842.

9. Li, D., et al., *Collecting Electrospun Nanofibers with Patterned Electrodes.* Nano Letters, 2005. **5**(5): p. 913-916.

APPENDICE

THE PARAMETER OF ELECTROSPINNG FOR CONTROLLING FIBER SIZE

Appendices consist of two tables: **Table A1** and **Table A2** where various solution and process parameters of electrospraying to fibers to fabricate various fiber sizes. The abbreviations in table are as follows; molecular weight (MW), concentration (CON.), solvent (SOL.), flow rate (FR), syringe volume (SV), needle gauge (NG), distance between needle tip and collector plate (DIS.). The all materials are related to Polycaprolactone (PCL). The abbreviations of polymers, solvents, and ingredients stand as follows: Poly(lactic-co-glycolic acid) (PLGA); poly(2-dimethylamino)ethyl methacrylate (PDMAEMA); Cloisite 25A (CL25A), organically modified montmorilonite, ; Poly(l-lactide-co-caprolactone) (PLCL); Polyurethane (PU); β-tricalcium phosphate conjugated PCL (PCL-β-TCP); TCPPCLEEP; polyethylene glycol (PEO); Dichloromethane (DCM); Dimethlyformamide (DMF); Hexafluoropropylene (HFP); Tetrafluoroethylene (TFE); Methanol (MeOH); Chloroform (CF); drug delivery system (DDS). The superscripts of numbers after materials are the number of the citation to show in **Chapter 2.6**. **REFFERENCES**.

Table A1. Parameters of electrospinning to control fiber sizes (I)

Materials	MW (g/mol)	CON. (w/v %)	SOL.	FR ml/h	SV (ml)// NG	DIS. (cm)	Strength of Voltage (kV)	Diameter (nm)	Others
PCL [73] (2009)	-	20	DCM/ DMF (8:2)	0.2-0.3	-/23	7.6-14	-	250	-
PCL [74] (2008)	80000	8-12	TFE	1.5	-/-	15	12	100-500	Calcium phosphate coating
PCL [75] (2008)	80,000	-	Acetone DMF/ CF	-	-	5-50	5-20	250-2500	-
PCL/ C [76] (2009)	-	-	HFP	3	-/18.5	10	20	-	-
PCL based SMPU [77] (2008)	180,000	3-12	DMF	-	5/-	15	12-25	50-700	-
PCL [78] (2008)	69,000	7-11	DMF	1.84	5 /-	15		615-4000	Conical nozzle
PCL [79] (2008)	-	3-10	HFP	3	5/18	10	20	582-637	-
PCL [80] (2008)	60,000	16	CF/ MeOH (8:2)	3 4	-/-	5	7	2026	-
PCL [81] (2007)	-	8	DMF/ MeOH (7:3)	2.5	10/-	15		1400-11900	Three electrodes
PCL [82] (2007)	40,000	0-15	CTAB	5	10/-	30	20	180–220	-
PCL [83] (2007)	80,000	0.14	DMF/ THF	-	-/-	20	15	438-519	-
PCL [84] (2007)	40,000	9	Acetone	-	-/-	-	-	691	-
PCL [85] (2007)	65,000	12	Acetone	24	-/-	30	24	-	Carbon dioxide
PCL [86] (2006)	-	15	-	5	-/-	20	20	-	Ion intensity
PCL [87] (2006)	80,000	8	CF/ MeOH (7:3)	0.5	-/-	10	0.8 (kV/cm)	550-810	Heparin

Table A2. Parameters of electrospinning to control fiber sizes (II)

Materials	MW (g/mol)	CON. (w/v %)	SOL.	FR ml/h	SV (ml)// NG	DIS. (cm)	Strength of Voltage (kV)	Diameter (nm)	Others
PCL/ PLGA [88] (2008)	-	-	-	1-16	-/-	-	-	1500-2750	-
PCL/ PDMAEMA [78] (2008)	69,000	10.5-15	DCM	1.84	5 /-	15	15	390-850	Conical nozzle
PCL/ CL25A [89] (2008)	80,000	-	DCM	0.38	10/18	7	7.5-20	250-600	-
PLCL/ Gelatin [90] (2008)	-	2 -3	HFIP	1-2	-/22	15	15-18	200-1400	-
PCL/ PU [91] (2008)	2000	8 (w/w)	DMF, THF (7/3; w/w)	0.3	-/-	15	14	350-560	DDS
PCL/ Gelatin [92] (2008)	10,000–20,000	1-10	HFP	-	-/-	15	-	640-880	-
PCL-β-TCP [93] (2008)	80,000	12	DCM	0.6	-/-	7.5	5	200-2000	-
PCL/ Collagen [94] (2008)	-	5	HFP	3	5/18.5	-	20	275-334	Different rotating rate
PCL/ PEG [95] (2008)	80,000	10	THF/ DMF	2.5	20/18	15	13	-	Dual polymer
PCL/ Collagen [96] (2007)	67,000	9	HFP	0.5	-/20	20	20	541±164	Dual collector
PCL PCLEEEP [97] (2007)	65,000 70,760	12 21.5	CF/ MEOH (4:1) Acetone	1.0 0.3	-/27	-	10	246-790	-
PCL/ PEO [98] (2007)	65,000	10–15	CF	1.2	5/22	12	15	1020	-
PCL/ Gelatin [99] (2007)	80,000	10	TFE	0.7	10/-	21.5	10.5	300–600	-

VITA

JONG KYU HONG

Candidate for the Degree of

Doctor of Philosophy

Thesis: ELECTROPSRAYED FIBER WITH CONTROLLABLE PORE SIZE FOR TIUSSE REGENERATION

Major Field: Chemical Engineering

Biographical:

Personal Data: Born in Pusan, Republic of Korea on October 2, 1972.

Education
Completed the requirements for the Doctor of Philosophy in Chemical Engineering at Oklahoma State University, Stillwater, Oklahoma in 2010.
Completed the requirements for the Master of Engineering in Materials Science and Engineering, The University of Tokyo, Tokyo, Japan in 2003. Thesis: A Novel Carrier for MRI Contrast Agent of Polyion Complex Micelle with PEG-PLL and Gd-DTPA.
Completed the requirements for the Bachelor of Engineering in Chemical Engineering at Dongguk University, Seoul, Korea in 1999. Thesis: Computer-Based Database on Chemical Engineering in Korea.

Experience:
Employed by Biomaterials Research Laboratory (National Laboratory), Korea Institute of Science Technology (KIST), Seoul, Korea as a research employee in 2001; researched at Kataoka Laboratory, The University of Tokyo, Tokyo, Japan as a research assistant fully supported by Japanese Government (Monbusho) fellowship from 2001-2003; worked as a graduate assistant at Oklahoma State University from 2007-2010.

Professional Memberships:
American Institute of Chemical Engineering (AIChE)
Materials Research Society (MRS)
American Chemical Society (ACS)
The Polymer Society of Korea
The Korean Society for Biomaterials
Korean Tissue Engineering and Regenerative Medicine Society (KTERMS)

Name: JONG KYU HONG Date of Degree: December, 2010

Institution: Oklahoma State University Location: Stillwater, Oklahoma

Title of Study: ELECTROSPRYAED FIBER WITH CONTROLLABLE PORE SIZE FOR TISSUE REGENERATION

Pages in Study: 137 Candidate for the Degree of Doctor of Philosophy

Major Field: Chemical Engineering

Scope and Method of Study: Architecture of 3D scaffold is closely related to cell behaviors such as cell infiltration, cell attachment, cell growing and cell colonization in 3D scaffold. The influence of 3D scaffold on the cell behavior is very important to understand the nature of cells in artificial 3D structure and to design better 3D scaffold. Thus, the thin layer of nano or microsize fibers made of synthetic (polycaprolactone or PCL) and natural (gelatin) polymer are fabricated using novel electrospraying process. I designed the innovative collector plate with void gaps and developed novel process with the collector plate to fabricate large and controllable pore size. Physical (pore diameter, shape factor, and pore size), mechanical (load-extension curve), chemical (gelatin distribution on single fiber, stability test of single fiber under physiological condition) were evaluated. Using human fibroblast and the thin layers of the large and controllable new fibers, the cell cultures study was carried out in serum free media or in serum media. The multilayer of cell culture was developed using layer-by-layer assembly methods. The cell morphology was confirmed by using confocal and light microscope, SEM. The cells were stained with Alexa Fluor 546, DAPI, and CFDA-SE for morphology study and H & E staining for cell histology. The cell glued 3D scaffold with multilayer was confirmed by tailoring random area of the scaffold.

Findings and Conclusions: The novel collector plate allowed the new fiber with large pore size and the pore size to be controllable by manipulating the deposit volume and the size of the circular void gap in the collector plate. The fiber diameter is independent of the new collector plate and they are related to the electrospraying parameters such as the distance between the needle tip and the collector plate. The shape of the void gap affects the alignment of the fiber on the edge of the triangular shape but in circular and rectangular shape of the void gap, fibers were randomly oriented. While 30 day cell culture using PCL fibers and serum added media, some cells were infiltrating through large pore and other cells are attaching on the fiber, growing on or between the fibers not only horizontally but also vertically, colonizing each other, and merging three layers of the fibers into one stable 3D scaffold, finally becoming cell-glued thick 3D scaffold even after tailoring the aluminum frame since cell acts as a glue. The shape of single cell on PCL/gelatin single nanofibers in serum free media was regulated by the configuration of single fibers, not the period of cell culture from 3hr to 24 hr.

ADVISER'S APPROVAL: Dr. Sundararajan V. Madihally